2009

Photoluminescence spectroscopy of bioconjugated quantum dots and their application for early cancer detection

Ganna Chornokur
University of South Florida

Photoluminescence Spectroscopy Of Bioconjugated Quantum Dots And Their Application For Early Cancer Detection

by

Ganna Chornokur

A dissertation submitted in partial fulfillment
of the requirements for the degree of
Doctor of Philosophy
Department of Chemical & Biomedical
College of Engineering
University of South Florida

Co-Major Professor: Sergei Ostapenko, Ph.D.
Co-Major Professor: John T. Wolan, Ph.D.
William E. Lee, Ph.D.
Mark Jaroszeski, Ph.D.
Catherine Phelan, Ph.D.

Date of Approval:
March 19, 2009

Keywords: spectral shift, biomarkers, prostate specific antigen, ELISA, agarose gel electrophoresis

Acknowledgments

I would like to thank my major professor Dr. Sergei Ostapenko for his help, guidance and patience during my research work that led to this PhD, and for all other support that I have received. I am very grateful to my co-major professor Dr John T Wolan for helping me to cope with the organization of the academic part of my PhD work - classes, schedules, forms and deadlines. I would like to thank Dr. Catherine Phelan, who was of a great help and shared her biology expertise and provided other support for the majority of my experiments. I wanted to thank the many others who have lent their support during my course work period, especially Dr. William E. Lee and Dr Mark Jaroszeski for the organization help and friendly, cheerful conversations which motivated me to work harder and obtain better study result. Many fruitful discussions with Professor Nadia Korsunkaya contributed a great deal to this work and I want to thank her in this letter as well. The TEM analysis would not be possible without the kind help of Dr Yusuf Emirov, who spent hours and applied all his expertise trying to get the best shots for me - many thanks, Dr Emirov! And last but certainly not least, I would like to thank Dr. Maciek Dybiec. He had the patience to work and aid me in many aspects of the photoluminescence segment of this work.

Table of Contents

List of Tables

List of Figures

Photoluminescence Spectroscopy of Bioconjugated Quantum Dots and their Application for Early Cancer Detection

Ganna Chornokur

ABSTRACT

Most of the bio-applications of semiconductor quantum dots (QDs) show and utilize their superior optical properties over organic fluorophores. An estimated 3–35% of all cancer deaths could be avoided through early detection, therefore, there is a critical need to develop sensitive probes.

The objectives of this work are:

Research the phenomena of “blue” photoluminescence (PL) spectral shift on the dried bioconjugated QDs and develop the relevant mechanism;

Develop a methodology that will allow successful confirmation of the bioconjugation reaction between biomolecules and QDs;

Propose a modification of an existent method or approach to employ the “blue” spectral shift of bioconjugated QDs for early cancer detection.

Results indicated that the “blue” spectral shift, observed for dried on the silicon substrates bioconjugated QDs, is increased with the time of storage and reaches 30-40nm in 14 days. It is accelerated at elevated temperatures and slowed down at lower temperatures. Larger size QDs generate spectral shifts of larger magnitudes, and the spectral shift is positively correlated with the biomolecule’s size/weight. This

phenomenon is explained by elastic and compression stress due to nonhomogenious drying of the QD droplet and the reaction with the solid surface.

Agarose gel electrophoresis technique, optimized with organic dye fluorescamine, is suitable for bioconjugation verification. The optimal running parameters were found to be 2% agarose gel, 1.5V working voltage, 0.5X TBE as a running buffer, and about 120 mins running time.

The spectral shift was implemented for improving the sensitivity of Prostate Specific Antigen (PSA) Enzyme-Linked ImmunoSorbent Assay (ELISA). It was found that QD ELISA could be as much, as 100 times more sensitive than the regular commercial ELISA, based on the enzymatic detection.

The results of this work show that QDs may be very useful for early detection of several types of cancers, including prostate cancer in men and breast/ovarian/uterine cancers in women.

1. Introduction

1.1 Scope and motivation

Cancer is a major cause of illness and death in the United States, second after heart diseases in 2004 [1]; approximately, half a million people die because of cancer in the United States alone every year. An estimated 3–35% of all cancer deaths could be avoided through early detection [2]. Clinical outcome of cancer is strongly related to the stage at which malignancy is detected, especially for breast cancer in women and prostate cancer in men [3]. Most solid tumors, however, are detectable with standard diagnostic methods during a late phase of disease when it may have already metastasized. Therefore, there is a critical need to develop sensitive probes for early cancer detection. Quantum dots (QDs) represent state-of-the-art nano-scale devices that exhibit promising results toward the development of a sensitive probe for screening cancer markers. Currently, QDs are successfully used for *in vitro* and *in vivo* imaging of tumors [4, 5], immunochemistry [6, 7], DNA hybridization [8–10], cell imaging [11–16] and potential photodynamic therapy [17]. QDs possess inherent advantages over organic fluorophores [18], such as SYPRO protein stains [19] or fluorescamine [20, 21], and are a possible replacement in biomedical imaging applications [22, 23].

There are several reasons why QD's have advantages over organic fluorophores [18, 22, 23]. The first of these is that QD's can absorb a wide band of light for their

excitation, but they emit in a very narrow spectral interval. In contrast, most molecular dyes can absorb only a very narrow band of wavelength, so most of the illuminating light is not used. This is illustrated in Figure 1.1.

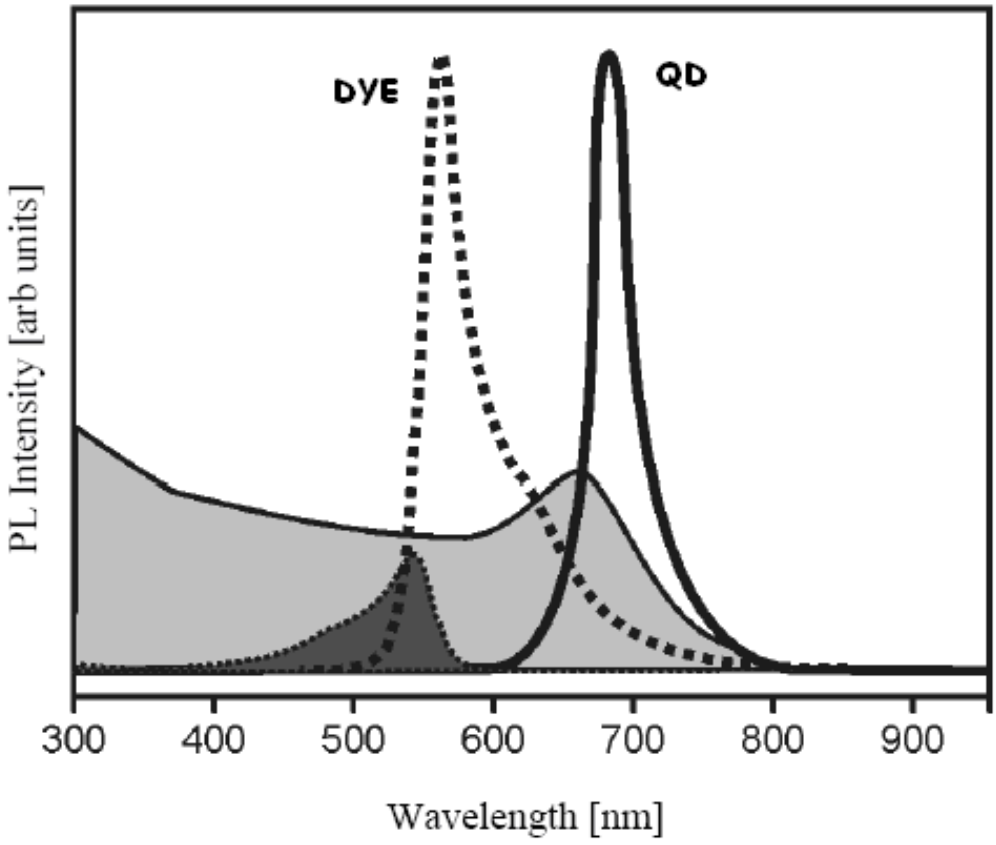

Figure 1.1 Comparison of the emission and absorption spectra of QD (continuous line) and organic dye (dotted line) (curves with the shaded area are the absorption spectra) [18]

Also, dye molecules emit in a much wider band of wavelengths compared to QD's. As a result, to distinguish separate features one needs to use very different molecular dyes, each with its own required excitation wavelengths. In the case of QD's the emission wavelength depends on the size. So, QD's made of the same semiconductor material, but of different sizes, can all be excited by the same light source (provided above band-gap energy is used), but then they emit distinctly different wavelengths.

Emission is very efficient in Quantum Dots and doesn't decrease so rapidly with time under UV illumination as in organic tags [24]. Quantum dots have large molar extinction coefficient value [25], typically on the order of 0.5-5 x 10-6 M-1cm-1 [26] which means that quantum dots are capable of absorbing excitation photons very efficiently; the absorption rate of QD's is approximately 10-50 times faster than organic dyes [27]. The higher rate of absorption is directly correlated to the quantum dot brightness and it has been found that QD's are 10-20 times brighter than organic dyes [24, 25, 28], allowing highly sensitive luminescence imaging. Their photo stability over long periods of time is one of the key factors that put them as the best fluorophores so far. In comparison to organic dyes that bleach after a couple of minutes under a standard confocal microscope, QD's can last for several hours under same illumination conditions [29]. Another feature of QD's that makes them a preferable candidate for tagging purposes is that their tagging property is controllable. With proper chemistry these objects can be attached to specific biomolecules that perform specific tasks, such as anti-gene and antibody recognition, for example. This is in contrast to traditionally used molecular tags that have well defined binding characteristics. As a result a particular fluorophore tag may or may not bind with a given molecule or surface of interest. QD's have a surface that can bind with a variety of molecules, they can be prepared (functionalized) so as to attach to well defined targets.

Enzyme Linked Immuno-Sorbent Assay (ELISA) is a powerful technique for detection and quantitation of biological substances such as proteins, peptides, antibodies, and hormones. By combining the specificity of antibodies with the sensitivity of simple enzyme assay, ELISA can provide a quick and useful measurement of the concentration of an unknown antigen or antibody. The "sandwich" technique is so called because the

antigen being assayed is held between two different antibodies. The secondary antibodies, also called captured antibodies, are usually linked to either a substrate for certain enzyme, or the organic dye which emits light and is used for visualization. The sensitivity of this method is low, for instance the threshold of PSA AG detection for "sandwich"-ELISA with organic dyes, is about 0.1 ng/ml [30], which is usually low enough for most cancer detections. However, lowering the threshold for PSA AG detection may be very useful in forensic analysis, dealing with sexual assaults. In this case, forensic scientists may deal with the smallest traces of semen liquids which require extremely sensitive methods of PSA detection [31-32].

The recent scientific works [33-39] have indicated that the PSA is not an exquisitely a male molecule. It is produced in female organisms as well, but at much lower concentrations (usually in the range of 0.01-1.1 ng/ml [33-39]), and its concentrations are being associated with breast, ovarian and uterine cancers. Therefore, the need for a sandwich ELISA modification, which lowers its threshold for antigen detection, is evident.

One of the current problems in QD usage for biomedical applications is that bioconjugation reactions may be incomplete and result in residual non-conjugated QDs in the same bio-conjugated solution. Therefore, the need for a reliable spectroscopic feature which allows to confirm the bioconjugation reaction, is also evident. In this work, both issues were successfully addressed.

1.2 The need for earlier cancer detection

Cancer is a major cause of illness and death in the US, occupying the second place after the diseases of the heart in 2004 [1] (Figure 1.2); approximately half a million people die of cancer in the United States alone every year.

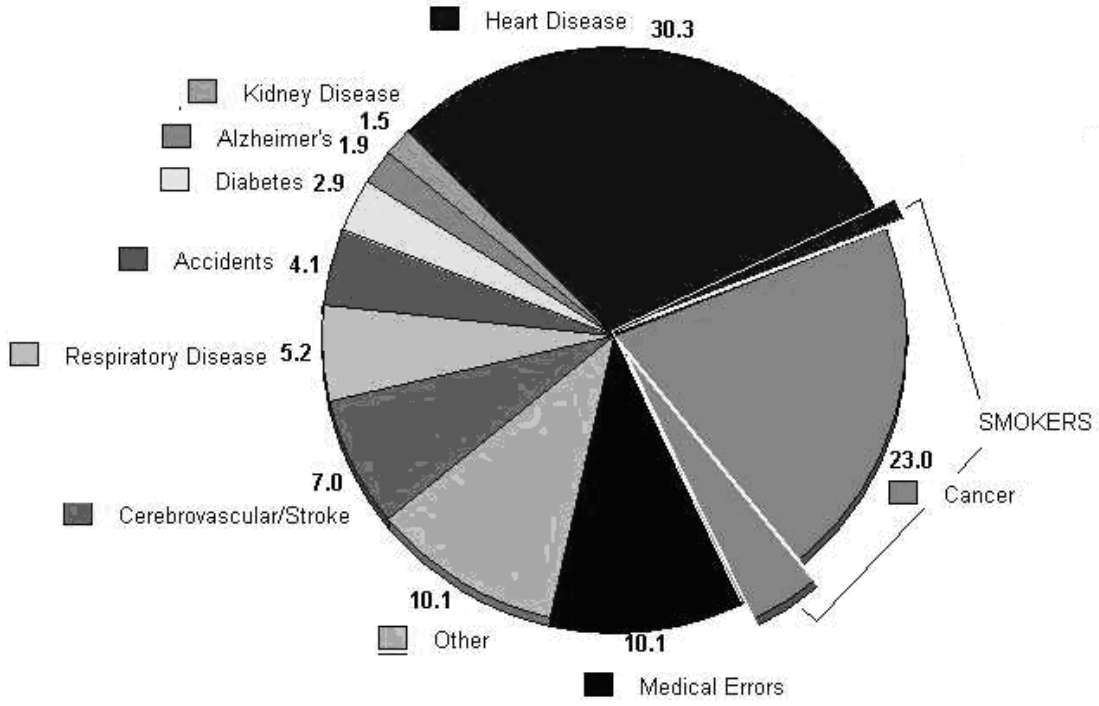

Figure 1.2 Ten leading causes of death in the USA [40]

An estimated 3 to 35 percent of all cancer deaths could be avoided through early detection [2]. Clinical outcome of cancer is strongly related to the stage, at which the malignancy is detected, especially for breast cancer in women and prostate cancer in men [3]. In order for an outcome to be successful, the solid tumor must be detected until it reaches 1cm in diameter. However, most solid tumors are detectable with standard diagnostic methods during a late phase of disease when it may have already metastasized. Therefore, there is a critical need to develop sensitive probes for early cancer detection.

1.3. Research plan

This research is divided into two major parts which are strongly interconnected. The first part describes experimental data of a short-wavelength "blue" spectral shift in photoluminescence (PL) spectra of bioconjugated QDs, while the second part employs this spectroscopic effect for the sake of early cancer detection via the ELISA molecular tool modification.

The "blue" PL spectral shift of QDs bioconjugated to different Abs is being investigated. For this, the bioconjugation was performed with different cancer specific antibodies followed by and PL spectroscopic analysis of samples dried on solid substrates of both bioconjugated and pure QDs. The PL spectroscopy and PL spectroscopic mapping at room temperature was performed in the effort to accurately record and evaluate the spectral properties of the QD luminescence, such as full-width-at-half-maximum (FWHM), spectral peak position and intensity. The effects of physical conditions (temperature, vacuum, moisture, gases, light and ultrasonic agitation) on the dried sample has been investigated. The TEM experiments were performed in order to reveal the shape and size of both pure and bioconjugated QDs The different substrate chemistry was also analyzed and correlated with the "blue" spectral shift magnitude. The quality of bioconjugation reaction was verified with the agarose gel electrophoresis technique, improved with the organic dye fluorescamine to detect free (unconjugated) antibodies. This technique was also optimized to better fit the needs to detect bioconjugation. The result provided a phenomenological model of the "blue" spectral shift mechanism on bioconjugated QDs, dried on the solid substrate (silicon chip).

The second part is focused on the employing the described above "blue" spectral shift of bioconjugated QDs to improve accuracy of early cancer detection. To achieve this goal, the modification of the sandwich-ELISA method has been proposed so that bioconjugated QDs are employed instead of commonly used organic dyes or the enzymatic substrate to detect target biomolecules. It was documented that sandwich-ELISA employing QDs is by two orders of magnitude more sensitive than the regular ELISA technique. A possibility of detecting antigen molecules at smaller concentrations evidently benefits the earlier detection of cancer and can be used in forensic science. The biomolecule, for which sandwich-ELISA with QDs was used, was Prostate Specific Antigen (PSA) which is a well known, and so far only one well established prostate cancer biomarker. It was shown that QD ELISA may be as much, as 100, or at least 20 times more sensitive, than commercial PSA ELISA. The negative dependence of the "blue" spectral shift VS the PSA concentration was found, which may become the fingerprint of the bioconjugation reaction and serve as an additional variable (together with the intensity) in the cancer detection. It is suggested that the results of this work could be employed both in research and clinics for cancer screening and detection. There is a possibility to use the improved ELISA technique in forensic science.

In the process of this work, several papers in the pier-reviewed journals were published (see pages 121-122 for details), as well as it was presented at several interdisciplinary conferences, including Material Research Society Meeting in San-Francisco, CA (March 2008), Nano-science Conference (Paris, 2007) and The 9th International Workshop on Beam Injection Assessment of Microstructures in Semiconductors (*BIAMS 2008*), Barcelona, Spain. The spectroscopic part of this work

was performed at the College of Engineering at USF, while the bioconjugation, agarose gel electrophoresis and ELISA were done at H. Lee Moffitt Cancer Center and Research Institute.

1.4 Summary

Unique optical properties of quantum dots structures in colloidal solutions make them suitable for medical applications as fluorescent markers. CdSe/ZnS and CdSeTe/ZnS QDs have been studied for photoluminescence (PL) signatures of possible biomolecules attachment (bioconjugation). The "blue" spectral shift of the dried bioconjugated QD sample can increase the sensitivity of any nowadays applicable cancer tests which is very desirable and motivation for this type research is clear. The sensitivity of sandwich-ELISA method, which is widely used for detection of almost any biomolecules, benefits from the implication of bioconjugated QDs instead of organic dyes. The author believes that the results of this work could be used in:

1. Science – as a base for further research of physical, chemical and biological particularities of bioconjugated QDs;
2. Medicine - to benefit early cancer detection;
3. Forensic science - to detect trace amounts of biomolecules, such as PSA.

The objectives of the research are:

1. Research the phenomena of "blue" PL spectral shift on the dried bioconjugated QDs and develop the relevant mechanism;
2. Develop a methodology that will allow successful confirmation of the bioconjugation reaction between biomolecules and QDs;

3. Propose a modification of an existent method or approach to employ the “blue” spectral shift of bioconjugated QDs for early cancer detection

2. Bioconjugated Quantum Dots

2.1 Introduction

Quantum dots are colloidal nanocrystalline semi-conductors that, as a result of their unique light emitting properties, are starting to attract considerable attention as a novel luminescent probes. Quantum dots in a spherical shape have diameters between 1 and 12 nm, with each dot containing a relatively small number of atoms in a discrete cluster [41]. Semiconductor nanocrystals can also be produced with other shapes such as rods and tetrapods [42], but spherical QDs are the most widely used for biological Applications [23, 27].One of the most intriguing features of QDs is that the particle size determines many of the QD optical properties, most importantly the wavelength of luminescence emission (Fig.2.1).By altering the QD size and its chemical composition, luminescence emission may be tuned from the near ultraviolet, throughout the visible, and into the near-infrared spectrum, spanning a broad wavelength range of 400–2000 nm [10–14]. Currently, scientists and engineers are utilizing these unique optical properties to create useful nanoscale devices. Give n the fact that the QD photoluminescence emission maximum can be manipulated by changing the particle size, their use as fluorescent labels for biological macromolecules has attracted considerable attention.

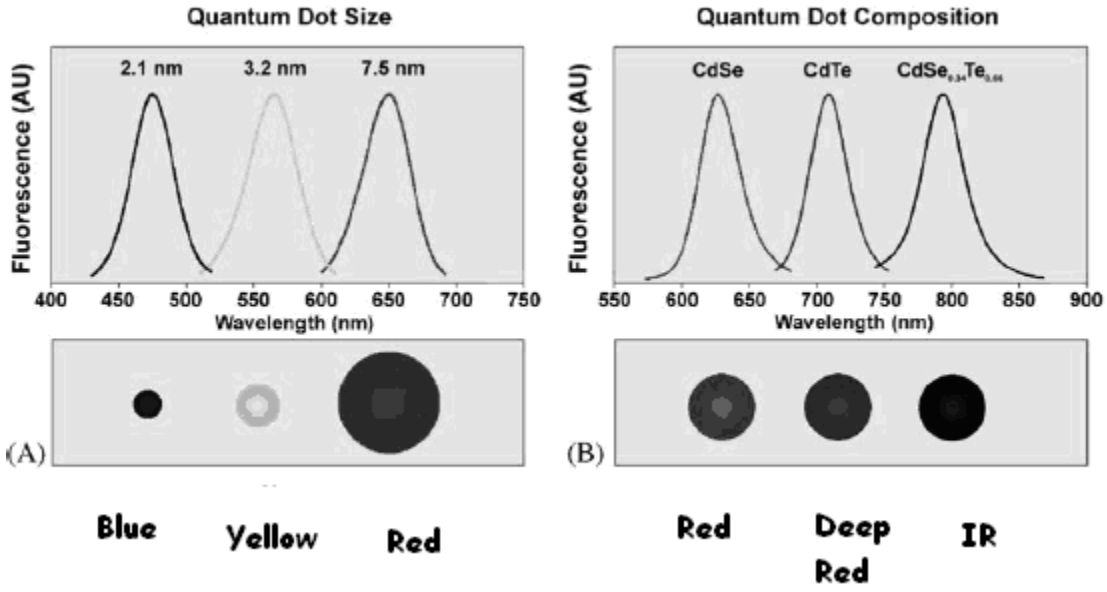

Fig.2.1 Tuning the QD emission wavelength by changing the nanoparticle size or composition.(A) The emission of a CdSe QD may be adjusted to anywhere within the visible spectrum (450–650 nm) by selecting a nanoparticle diameter between 2 and 7.5 nm. The relative sizes of these particles of constant composition are shown schematically below the luminescence spectrum.(B) While keeping the nanoparticle size constant (5nm diameter) and varying the composition of the ternary alloy CdSexTe1_x, the emission maximum may be tuned to any wavelength between 610 and 800 nm.The emission wavelength of this alloy is longer than that of both of the binary alloys due to a nonlinear relationship between the bandgap energy and the composition [41].

2.2 Photoluminescence and Quantum Dots

Luminescence (also known as fluorescence) spectroscopy is a widely used tool in physics, engineering, chemistry as well as in biology. The urgent need to measure more biological indicators simultaneously places new demands on the fluorescent probes used in these experiments. For example, an eight-color, three-laser system has been used to measure a total of 10 parameters on cellular antigens with flow cytometry [43], and in cytogenetics, combinatorial labeling has been used to generate 24 falsely colored probes for spectral karyotyping [44]. Ideal probes for multicolor experiments should emit at

spectrally resolvable energies and have a narrow, symmetric emission spectrum, and the whole group of probes should be excitable at a single wavelength [24].

Photoluminescence (PL) is a process in which a chemical compound absorbs a photon with a wavelength in the range of visible or UV electromagnetic radiation, thus transitioning to a higher electronic energy state, and then radiates a photon back out, returning to a lower energy state. The period between absorption and emission is typically extremely short, of the order of 10 nanoseconds. Under special circumstances, however, this period can be extended into minutes or hours [45]. Ultimately, available chemical energy states and allowed transitions between states (and therefore wavelengths of light preferentially absorbed and emitted) are determined by the rules of quantum mechanics. A basic understanding of the principles involved can be gained by studying the electron configurations and molecular orbitals of simple atoms and molecules. More complicated molecules and advanced substrates are treated in the field of computational chemistry**.**

The simplest PL processes are resonant radiations, in which a photon of a particular wavelength is absorbed and an equivalent photon is immediately emitted. This process involves no significant internal energy transitions of the chemical substrate between absorption and emission and is extremely fast, on the order of 10 nanoseconds. More interesting processes occur when the chemical substrate undergoes internal energy transitions before re-emitting the energy from the absorption event. The most familiar such effect is a non-radiative transition, which is also a fast process when part of the absorbed energy is dissipated in heat (phonons) so that the emitted light is of lower energy than that absorbed.

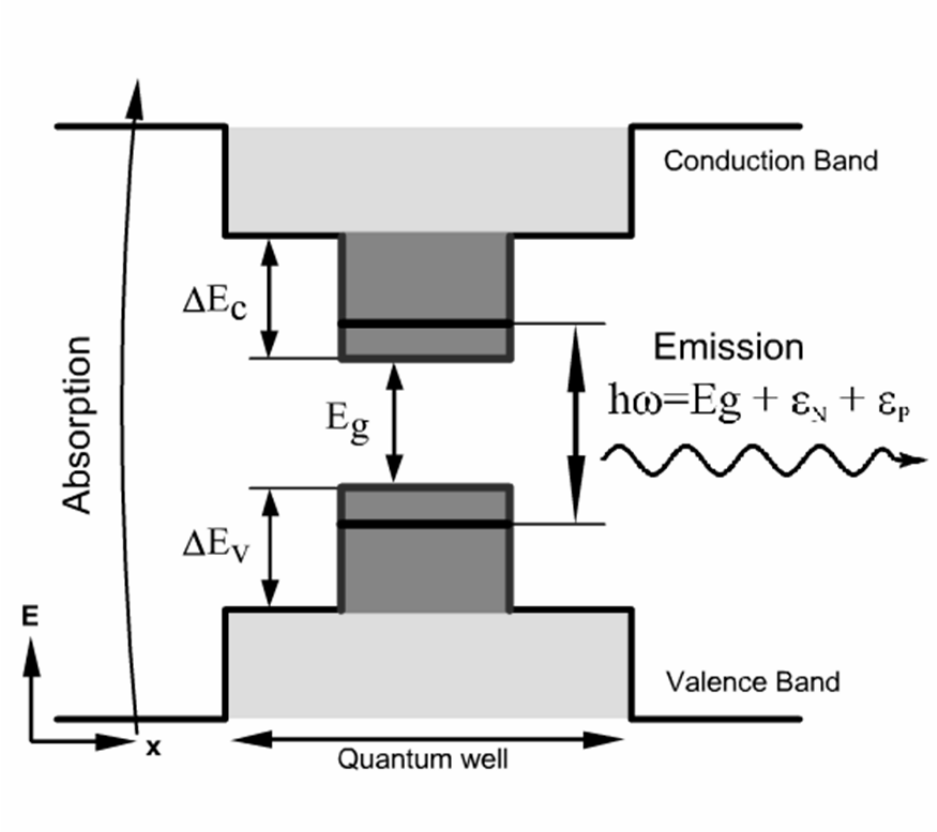

Figure 2.2 Schematic representations of the basic photoluminescence mechanisms for Quantum Dots [46]

Photoluminescence in QD is governed by the same mechanisms as in the bulk materials, however major difference is that all the energy levels inside the quantum dots are strongly quantized due to small dimensions of QD. Direct consequences of this quantization are very sharp emission spectral lines (δ function – like for a single QD), that are in general broadened only by the QD size distribution (Figure 2.2). A typical core-shell nanoparticle used for bio-tagging is shown on Figure 2.3. This figure represents the scheme with the highest quantum efficiency design, in some cases the core is protected only by single-layer shell [22]. Structurally, QDs consist of a metalloid crystalline core and a "cap" or "shell" that shields the core and renders the QD bioavailable (Figure 2.3). QD cores consist of a variety of metal complexes such as semiconductors, noble metals, and magnetic transition metals. For instance, group III-V

series QDs are composed of indium phosphate (InP), indium arsenate (InAs), gallium arsenate (GaAs) and gallium nitride (GaN) metalloid cores, and group II-IV series QDs, of zinc sulfide (ZnS), zinc-selenium (ZnSe), cadmium-selenium (CdSe), and cadmium-tellurium (CdTe) cores (28, 47). For biological tagging applications CdSe/CdTe (core) nanocrystals are the most popular. They are covered with a wide-gap ZnS or CdS (shell) capping layer providing a barrier for quantum confinement and also improved quantum yield and photo stability [Fig 2.3].

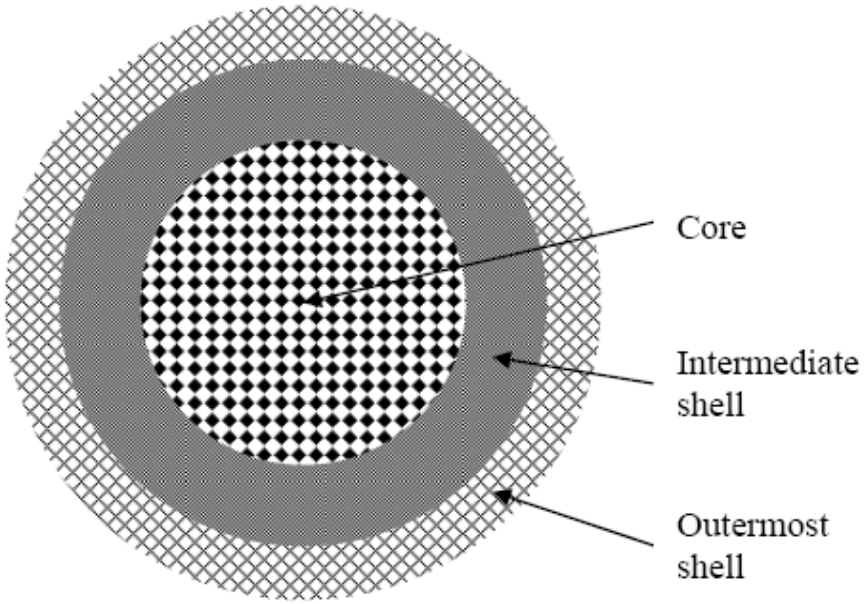

Figure 2.3 Schematic diagram of a typical core-shell nanoparticle used for bio-tagging. This figure represents the scheme with the highest quantum efficiency design, in some cases the core is protected only by single-layer shell [22]

It is possible to assign the biocompatible coatings and/or functional groups to the QD which gives them a desired bioactivity. Newly synthesized QDs are usually hydrophobic in nature and not useful for usage in biological sustems, because a hydrophobic cap forms on the metalloid core during the QD synthesis in organic solvents. To make QDs biologically compatible and active, newly synthesized QDs are

"functionalized," or given secondary coatings, which improves water solubility, QD core durability, and suspension characteristics and renders them a desired bioactivity. For instance, QD cores can be coated with hydrophilic polyethylene glycol (PEG) groups which makes them biocompatible and water soluble, and enables further conjugation with bioactive molecules to target specific biologic cellular structural features (Figure 2.4). Hence, bonding various molecular entities to the QD core functionalizes QDs for specific diagnostic or therapeutic purposes. Functionalization may be achieved via electrostatic interactions, adsorption, multivalent chelation, or covalent bonding, important physicochemical features when considering QD durability/stability and *in vivo* reactivity. In the literature, QD physicochemical characteristics are typically referred to as "core-shell-conjugate" or vice versa. CdSe/ZnS, for example, would refer to a QD with a CdSe core and ZnS shell, and a CdSe/ZnS QD conjugated with sheep serum albumin (SSA) would be referred to as CdSe/ZnS-SSA. Controlling the physicochemical properties during synthesis, which can be done with high precision, allows tailoring QDs for specific functions/uses. [48-49, 88]

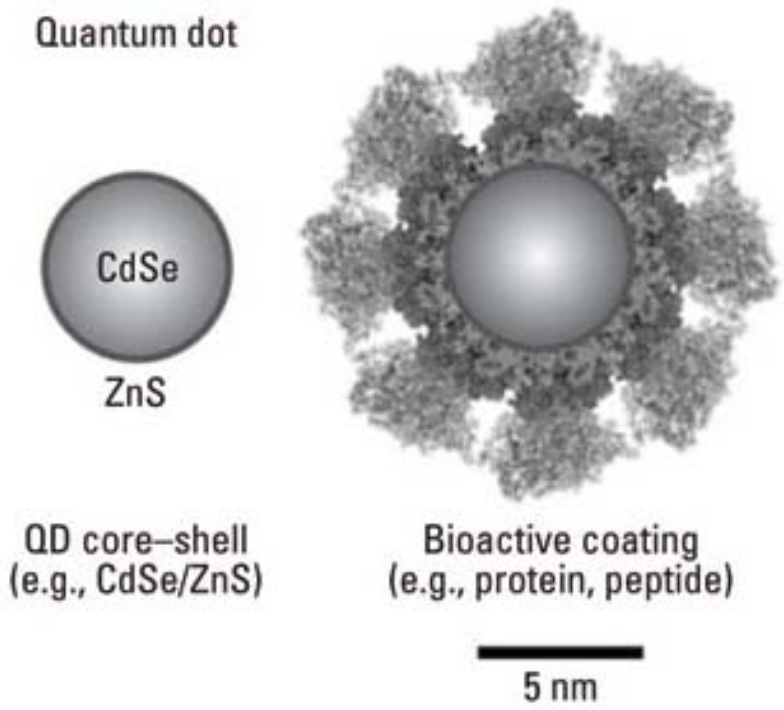

Figure 2.4 Biofunctionalized CdSe/ZnS Quantum Dot [48]

2.2.1. TEM visualization of QDs

Transmission electron microscopy (TEM) is a widely used microscopy technique. It's principle is based on a beam of electrons is transmitted through a very thin specimen, interacting with the specimen as they pass through [50]. An image is formed from the interaction of the electrons transmitted through the specimen, which is magnified and focused onto an imaging device, such as a fluorescent screen, as is common in most TEMs, on a layer of photographic film, or to be detected by a sensor such as a CCD camera (Figure 2.5).

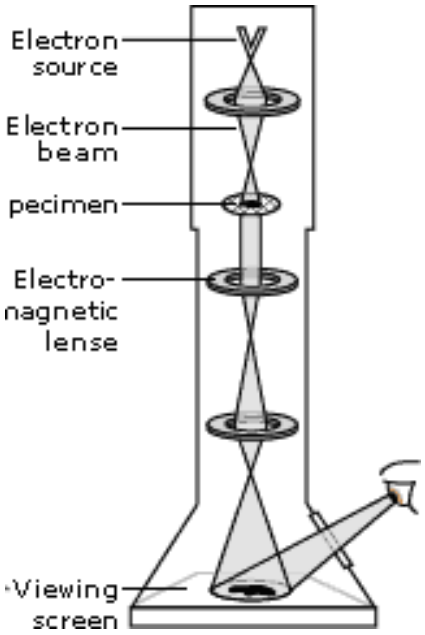

Figure 2.5 TEM basic schematic [51]

TEMs are capable of imaging at a significantly higher resolution than light microscopes, owing to the small de Broglie wavelength of electrons. This enable the instrument to be able to examine fine detail -- even as small as a single column of atoms, which is tens of thousands times smaller than the smallest resolvable object in a light microscope. TEM forms a major analysis method in a range of scientific fields, in both physical and biological sciences [52].

2.3. Biofunctionalization of QDs and bioconjugation, general information

Bioconjugation is the process of coupling two biomolecules together in a covalent linkage. As was described in the Section 2.2 of this work, the typical QD used for bioconjugation experiments, has a CdSe or CdSeTe core, which is responsible for PL, but the core is unstable, so it is capped with the inorganic shell – ZnS, in our case. The third

layer, organic coating, provides water solubility and functional groups for conjugation [figure 2.6]. The process of this layer addition to the QD is called biofunctionalization.

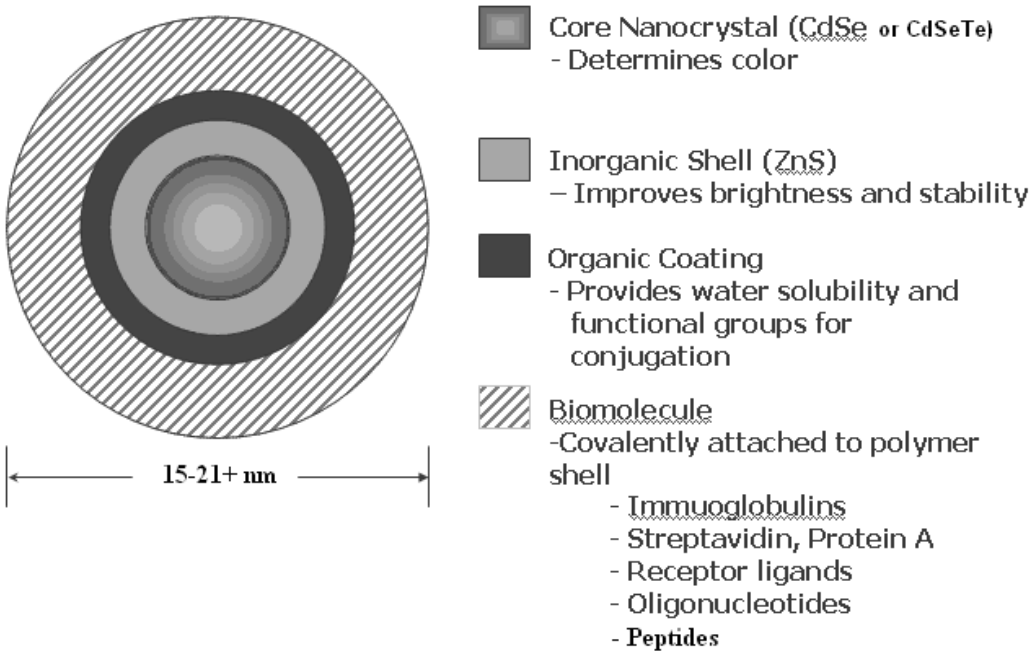

Figure 2.6 Invitrogen Quantum Dot schematic [26]

In order to add functionality (organic coating) to the QD surface, a ligand-exchange process is required.

For this purpose, we need a ligand with two functional groups:

1. one group should have high affinity for the QD surface (e.g., thiol, carbonyl or amine); and,

2. the other must be a polar group (e.g., carboxylate) to make the NPs soluble in aqueous media.

The most commonly used ligands include, but are not limited to: thiol, cystein, citrate, surfactants, purine, and nitroxide groups [53]. The adding ligand strategies can be

divided into two fundamentally different ways solving this problem via functional polymers. One approach completely replaces the surface bound ligands remaining from synthesis; the other only caps the present ligands on the QDs with suitable amphiphilic polymers [54] (Fig. 2.7).

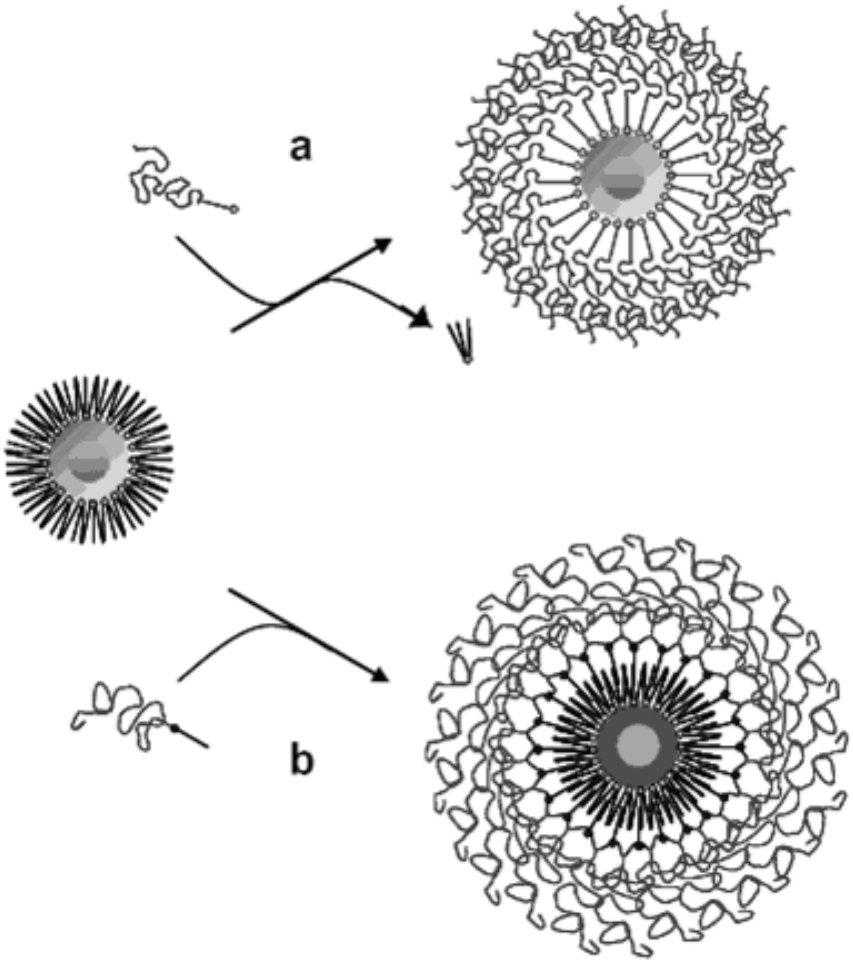

Figure 2.7 Scheme of the (a) ligand exchange and (b) the ligand capping Strategy [54].

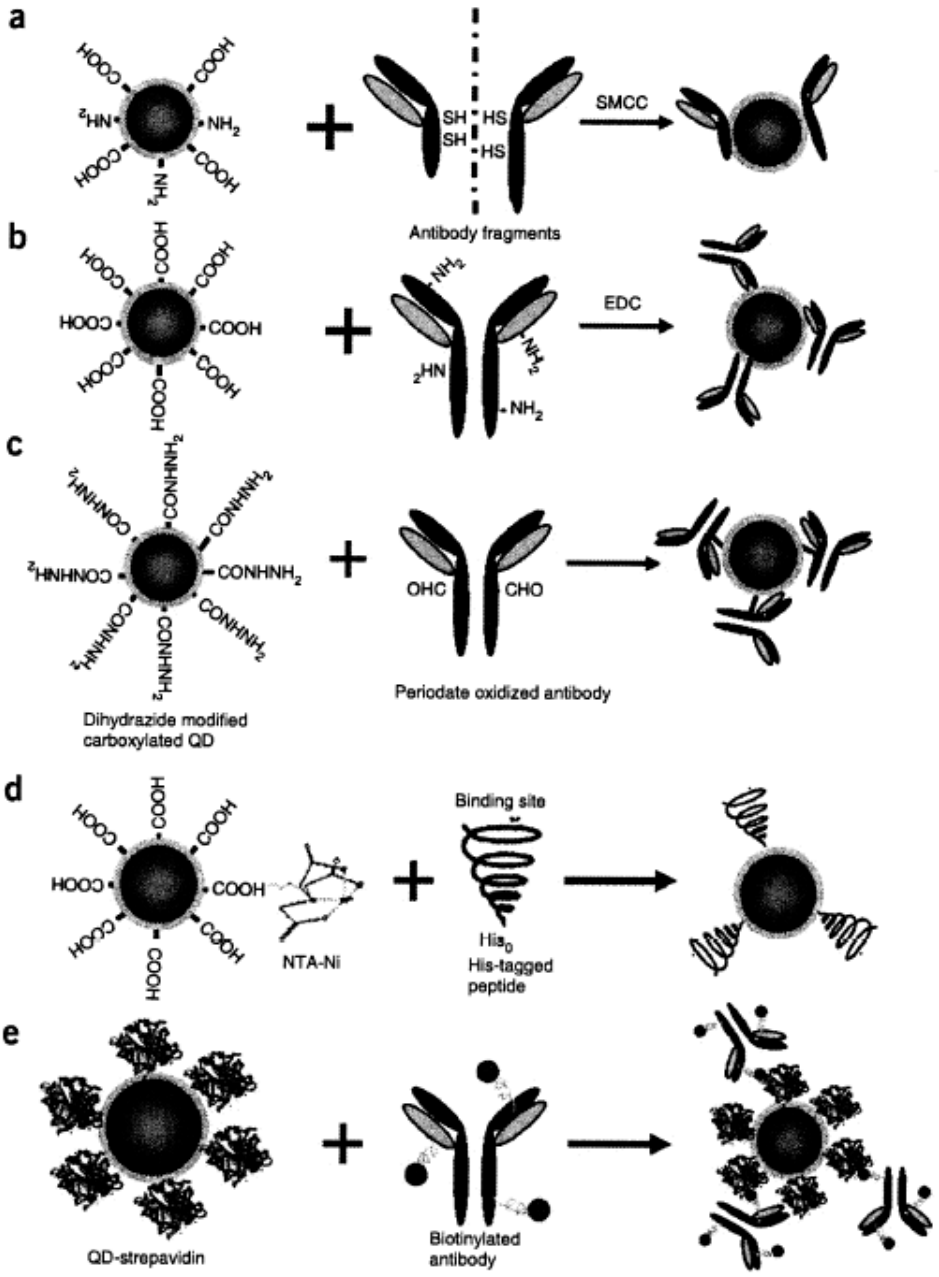

Figure 2.8 Schematic diagram showing various methods for QD-antibody (QD-Ab) bioconjugation. A. QD conjugation to antibody fragments via disulphide reduction and sulfhydryl-amino coupling; B. covalent coupling between carboxylic acid (-COOH) coated QDs and primary amines (-NH2) on intact antibodies usind EDAC as a catalyst; C. site-directed conjugation via oxidized carbohydrate groups on the antibody Fc portion and covalent reactions with hydrazide-modified QDs; D. conjugation of histidine-tagged peptides or antibodies to Ni-NTA modified QDs; E. noncovalent conjugation of streptavidin-coated to biotinylated antibodies [6]

Now, when the biofunctionalized QD is ready for conjugation with different biomolecules, several approaches may be used at this stage [Figure 2.8] The first approach, QD conjugation to antibody fragments via disulphide reduction and sulfhydryl-amino coupling, is being the most used for cancer diagnostics.

2.3.1. Bioconjugation, procedure

Development or substantial improvement of a conjugation procedure, however, is not proposed in the scope of this work. Therefore a commercially available Qdot® Antibody Conjugation Kit, made by Invitrogen was utilized. In this procedure [26], Qdot® 705 nanocrystals (Figure 2.6) are used, which are composed of CdSeTe/ZnS core/shell, covered with a thick layer of polymer and PEG molecules to facilitate solubility and prevent aggregation [26]. These QDs also have protein molecules on the surface as conjugation linkers, but the exact surface chemistry is proprietary information of the vendor. The core is not stable alone; it is very reactive. It can collect counterions different impurities and then no longer fluoresce. The shell protects the core, but is water-insoluble. The organic coating is an amphiphilic polymer (inner portion hydrophobic, outer portion hydrophilic, bound non-covalently to the shell) to make the final Qdot® nanocrystal product water-soluble and provide sites for conjugation. PEG (polyethylene glycol) is provided on the various products to minimize stickiness.
The conjugation procedure is described step by step in the Qdot® 705 Antibody Conjugation Kit , made by Invitrogen, and is shown on Fig 2.9 [26].

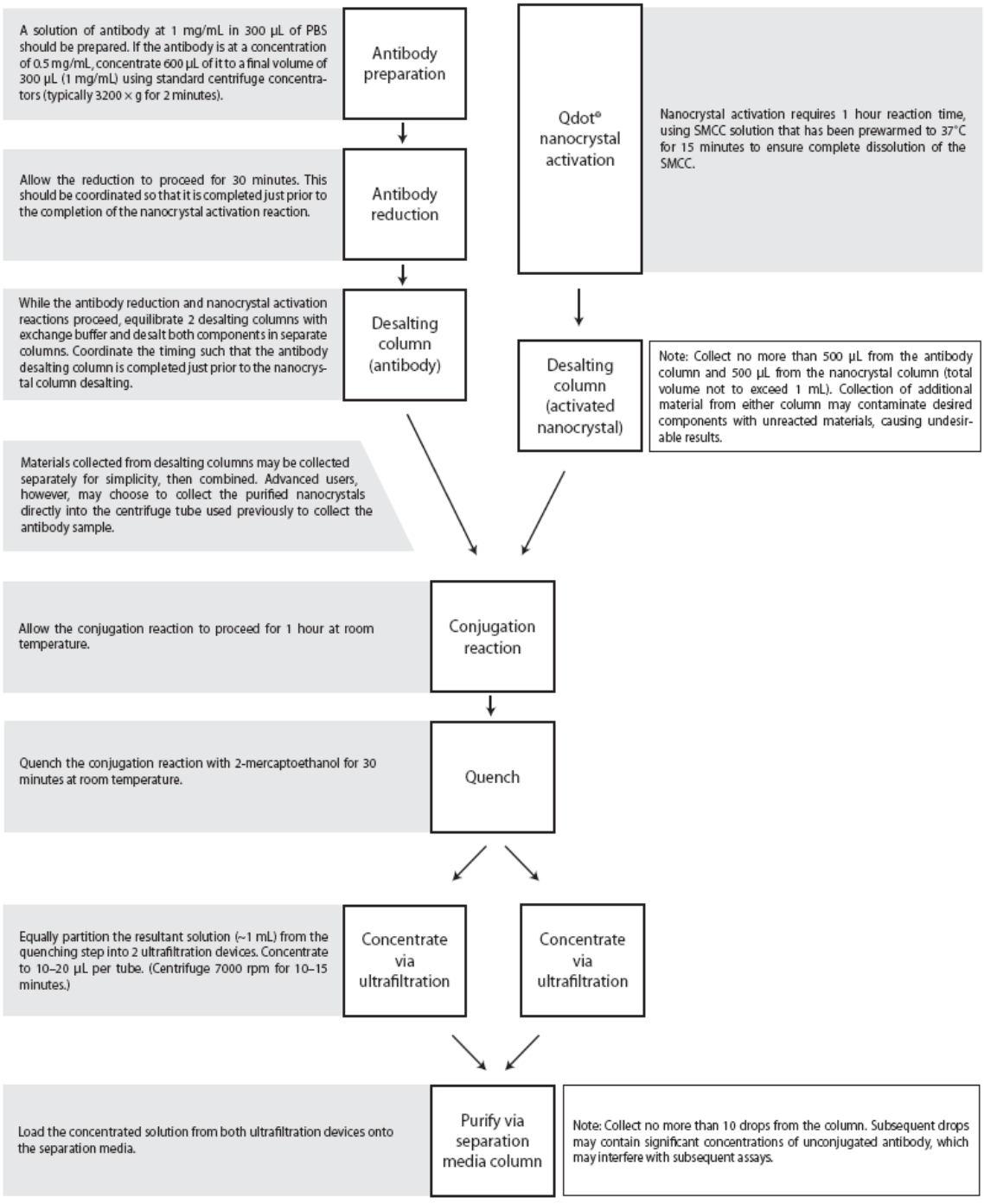

Figure 2.9 Workflow diagram of the Qdot® antibody conjugation procedure [26].

2.3.2. Confirming bioconjugation, general information

Confirmation of the QD-AB conjugation is a very important stage in the proposed study. According to our understanding and experience, it must follow any newly beginned conjugation procedure to be sure we actually have a quality conjugate.

Bioconjugated quantum dots are characterized with increased size/volume/weight due to attached biomolecules which makes possible to employ different separation techniques for bioconjugation verification [Figure 2.10].

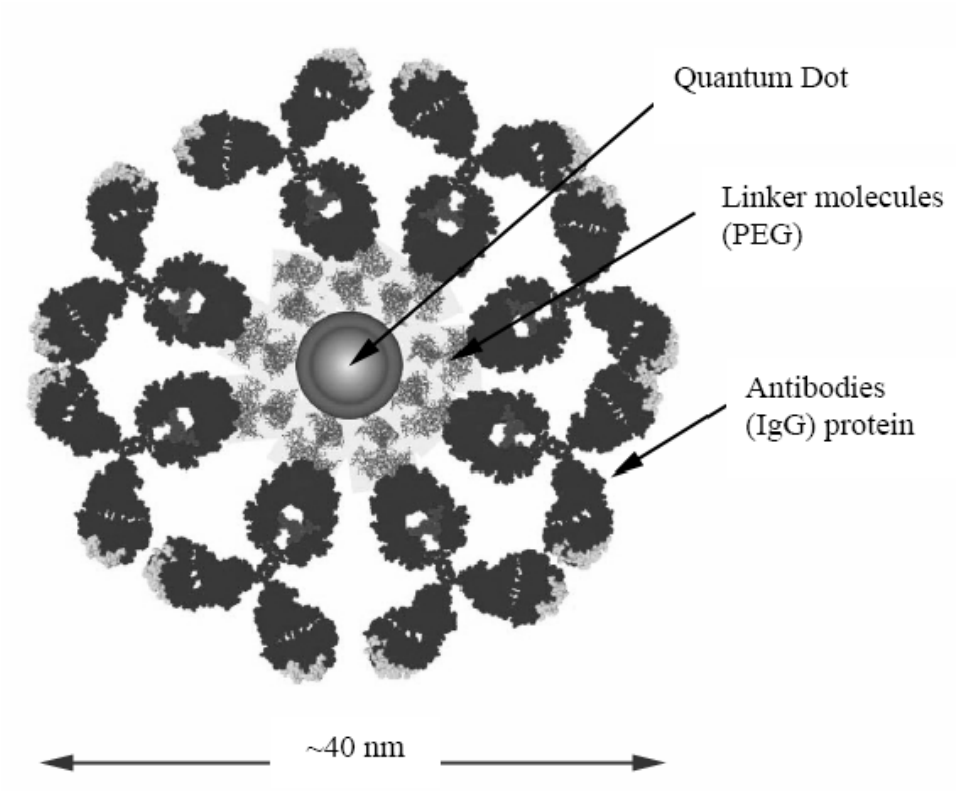

Figure 2.10 Schematic representation of the QD bound to a biomarker (molecules are drawn to scale) – after Jaiswal [55]. Note that a single QD size is usually up to 12nm.

According to the scientific publications, several bioconjugation verification methods/procedures are currently available, however, the different variations of gel

electrophoresis are the most popular [4, 56-60]. The other two most widely used methods are variations of capillary electrophoresis [61] and protein microarrays [62].

Gel electrophoresis is a simple method to separate the substances by size and charge in the electric field. In this case, the separation is happening in gel media. The researchers [4] used this method to successfully confirm bioconjugation of CdSe/ZnS QDs to Luc-8 antibodies. The conjugated band performed retarded mobility in a gel when the electric field was applied (Fig 2.11) [4]

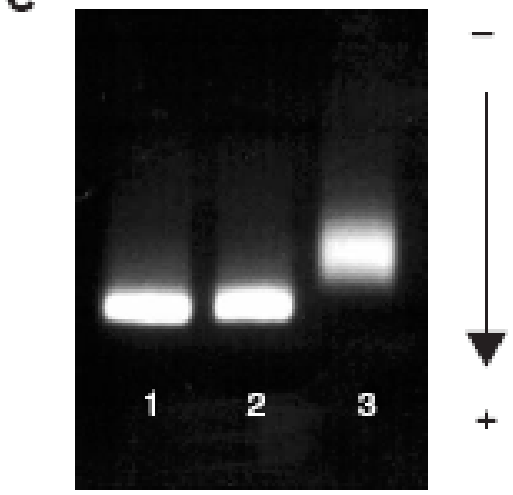

Figure 2.11 Gel electrophoresis analysis of the conjugation of Luc8 to QD655: (1) unconjugated QD655, (2) the mixture of QD655 and the coupling reagent EDC and (3) purified QD655-Luc8 conjugates [4].

Capillary electrophoresis is a technique which can be used to separate ionic species by their charge and frictional forces [20]. The separation takes place interior of a small capillary filled with an electrolyte, and the detection is based on the photoluminescence of QDs, under the laser excitation. The researchers [61] have successfully used this method to both verify bioconjugation and separate the

bioconjugated by the ratio of conjugated QDs. In Fig 2.12 A are shown three cases of 54.9% bioconjugated fraction of QDs, B – 82.1%, and C – 98.2%.

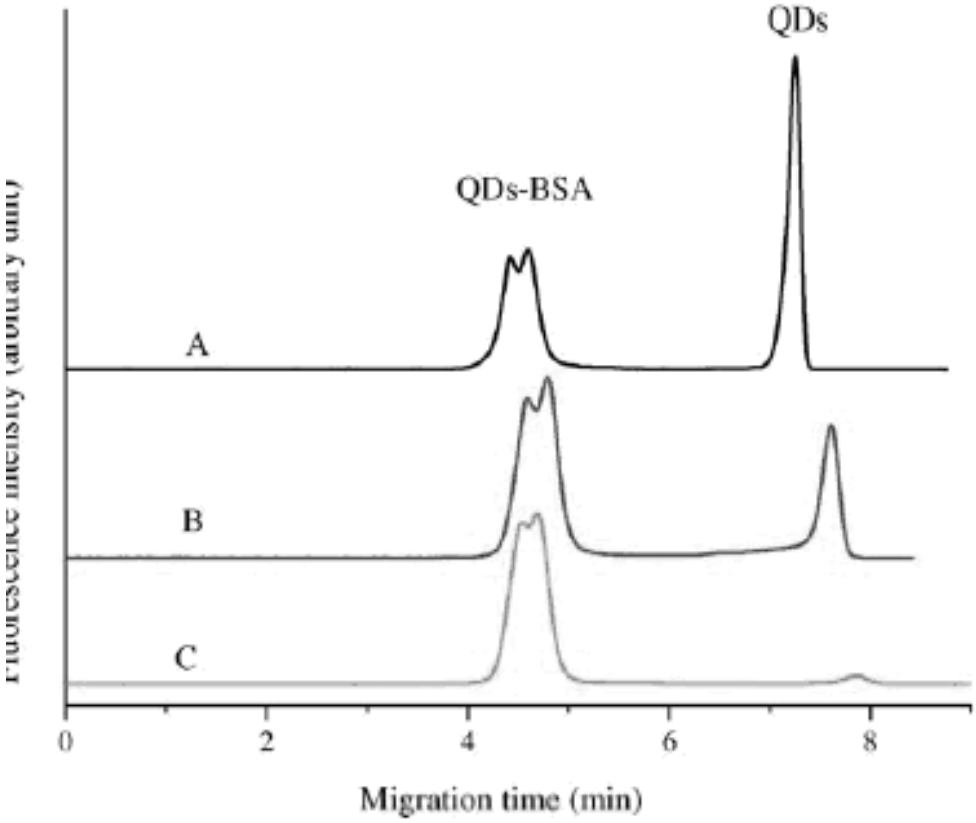

Figure 2.12 Analysis of QD–BSA conjugates by capillary electrophoresis with LIF Detection [61].

Protein microarrays are mostly used to employ bioconjugates for the antigen detection [63], but results have been reported that this method is successfully used to confirm bioconjugation [64]. For example, on Fig 2.13 the microarray assay for the different concentrations of IL10 antigen is shown. Brighter spots correspond to the increased antigen concentrations which gives a rationale to conclude that bioconjugation was successful.

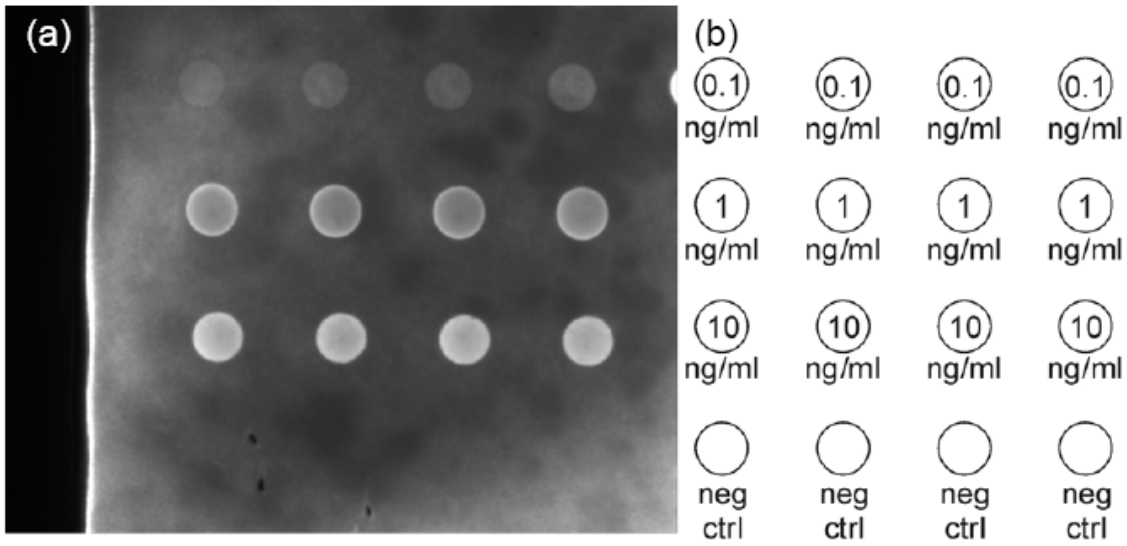

Figure 2.13 Example of fluorescent microscope image (mag. 2.5x) of the small part of an array printed from micro array printer (QD655 + IL10 complex) with 100 μm spot diameter (a), spots description (b) [64]

2.3.3. Confirming bioconjugation, agarose gel electrophoresis with fluorescamine

Although the gel electrophoresis technique is widely used for bioconjugation confirmation, it has several weak points which should be addressed. First of all, it does not allow the visualization of pure antibodies, used for bioconjugation, which together with pure QDs may serve as an important control. Also, the fraction of nonconjugated antibodies is expected to be present in each bioconjugate, so it may be useful to visualize it. And lastly, the important running parameters, such as running time and voltage, and gel thickness should be tested and optimized for the best separation.

The author of the current work upgraded this methodic with the use of organic dye Fluorescamine (4-phenylspiro[furan-2(3*H*),1'-phthalan]-3,3'-dione, [65], which is a very well known protein dye and widely used since 1970 [65-66]. It reacts with primary amino groups found in terminal amino acids and the e amine of lysine to form fluorescent pyrrolinone type moieties [67].Several factors make fluorescamine suitable for labeling

primary amines, including amino acids, peptides, and proteins. Reaction with primary amines proceeds at room temperature, with a half time of a fraction of **a** second, and it is active in a wide pH range (4-10). Excess reagent is concomitantly destroyed with a half-time of several seconds. The competing reactions are shown in Fig. 2.14. Fluorescamine, as well as its hydrolysis products, is nonfluorescent. Studies with small peptides have shown that the reaction goes to near completion (about 88 to 95 percent of theoretical yield) even when fluorescamine is not present in large excess. The resulting luminescence is proportional to the amine concentration and the fluorophors are stable over several hours.

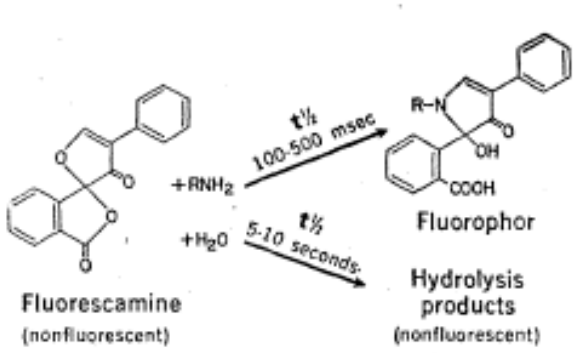

Figure 2.14 Reaction of fluorescamine with primary amines and hydrolysis of the reagent [68]

This dye has an excitation wavelength at 390nm and emission at 480nm [69], which makes it appropriate for visualization under either a UV lamp (365 nm) or UV laser excitation (325nm). The emission at 480nm (green light) allows to distinguish the QD emission (which in this work was red with maxima usually at 705nm) from the dye emission. This dye also does not luminescence, only the protein-fluorescamine complex fluoresces and the resultant PL spectra could be recorded [69]. This is very advantageous and convenient for our use in the agarose gel electrophoresis. Fluorescamine gives us an

opportunity to visualize the pure, unconjugated ABs under UV light and therefore compare the band of pure proteins and conjugated proteins in the agarose gel.

In this work, the agarose gel electrophoresis technique was performed using genetic analysis grade agarose and Tris-Borate-EDTA buffer (TBE) 10X stock solution, purchased from Fisher Scientific. A horizontal electrophoresis batch purchased from Owl Separation Systems Inc, rated as 0-150V, 0-100mA, was used to run the gel with X0.5 EDTA as a running buffer. The running buffer was prepared from stock EDTA solution by dilution with distilled water. The organic dye fluorescamine was purchased from Invitrogen Inc. The fluorescamine bulk 1% solution was prepared by diluting the fluorescamine powder in acetone, and stored at 4^0C in the dark. To make a sample, 5µl of AB solution was mixed with 5µl TBE buffer at pH 7.4, followed by the addition of 2µl 1% solution of fluorescamine in acetone, and mixed for 30 seconds [66]. The sample was then left exposed to air for approximately 30 minutes to let the acetone evaporate. To prevent the protein from denaturing under the influence of acetone, the samples were stored continuously on ice (~2-4^0C) until the gel procedure was started. Non-conjugated QDs were tracked in the electrophoresis study using their own luminescence emission without adding fluorescamine.

2.4. Bioconjugated QD applications in biology and medicine

The development of high-sensitivity and high-specificity probes that lack the intrinsic limitations of organic dyes and fluorescent proteins is of considerable interest in many areas of research, from molecular and cellular biology to molecular imaging and

medical diagnostics. QDs are believed to overcome these limitations [70]. The Figure 2.15 shows the main applications of bioconjugated QDs in biology and medicine.

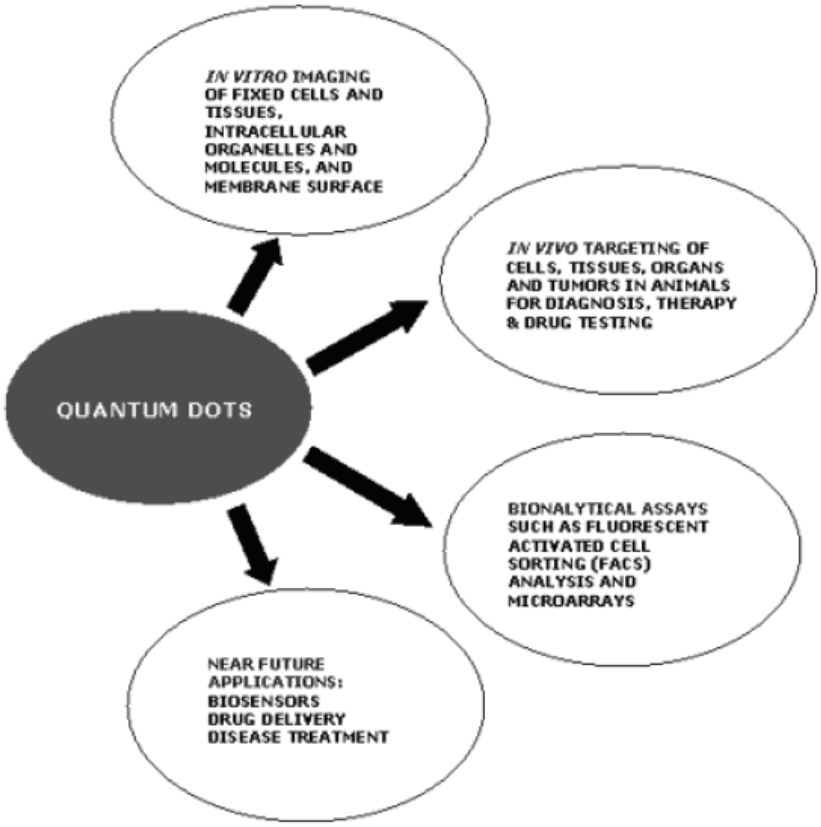

Figure 2.15 Applications of quantum dots [70]

In vivo targeting: Most recently, QDs have been used as stable fluorescent tracers for nonspecific uptake studies and lymph node mapping in living animals [71-72]. Antibody-conjugated QDs have allowed real-time imaging and tracking of single receptor molecules on the surface of living cells with improved sensitivity and resolution [14].

The group [73] reported the development of bioconjugated QD probes suitable for *in vivo* targeting and imaging of human prostate cancer cells growing in mice. They were able to get an image of the prostate tumor using bioconjugated QDs targeting Prostate-Specific Membrane Antigen which is a a cell surface marker for both prostate epithelial

cells and neovascular endothelial cells. Figure 2.16 shows excellent visualization of the tumor in mice.

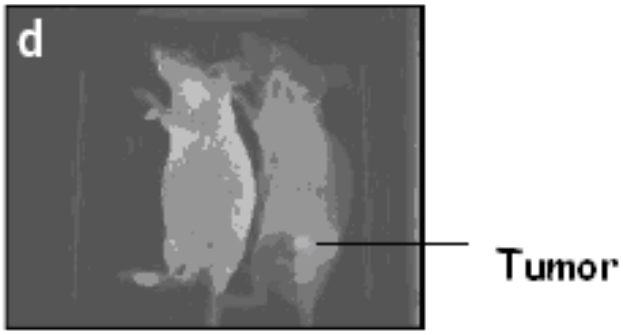

Figure 2.16 Spectral imaging of QD-PSMA Ab conjugates in live animals harboring C4-2 tumor xenografts. Orange-red fluorescence signals indicate a prostate tumor growing in a live mouse [73].

The similar work was successfully performed to target different tumors/cells etc in animals by other groups [4, 14, 74,].

Drug delivery is another possible in vivo application of QDs. The same group (73) modified the original CdSe QD with an impermeable coating of polymer that prevented the leaking out of highly toxic cadmium ions from the QD conjugate and provided a means to chemically attach tumor-targeting molecules and drug delivery functionality to the QD conjugate.

It was reported by [75] that QDs can be successfully used for the in vitro imaging of cells and tissues. For instance, SiHa cell culture, overexpressing epidermal growth factor receptor (EGFR) was successfully labeled with QDs, conjugated to anti-EGFR. EGFR targeting is of a great importance, because it is overexpressed in many cancers, including cervical cancer. The results are evident from Figure 2.17 : Images of the SiHa with the specific targeting due to anti-EGFR antibody showed significantly stronger intensity than the controls with non-specific IgG antibody

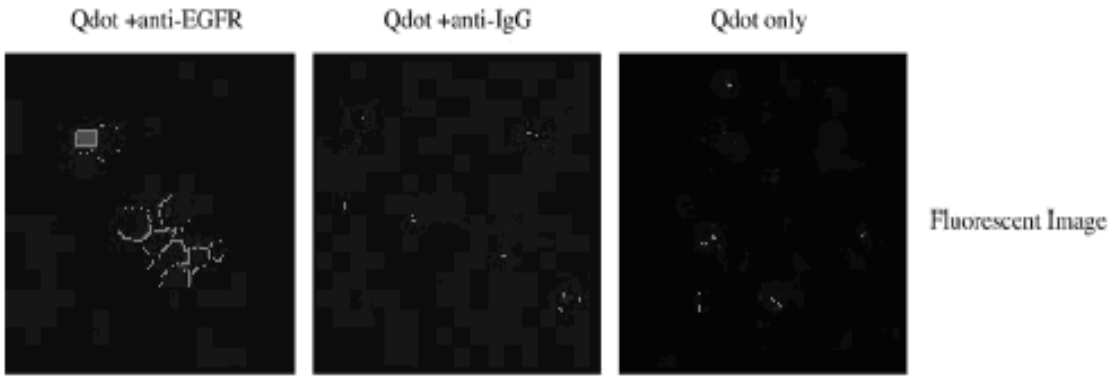

Figure 2.17 Confocal fluorescence images of SiHa cervical cells labeled with 30 nM anti-EGFR quantum dots [75]

There are other publications reporting similar QD in vitro targeting of different cells/cultures [76, 77].

QDs are also suitable for use in the bioanalytical assays. The in vitro analysis of extracted cellular proteins may give a wealth of information on their expression level, modification, degradation, complex formation, activity, and localization. One of such analyses is the high-throughput measurement allowed by patterning the protein in a microarray format [78-79]. The proteins can be covalently linked to or immobilized by high-capacity absorption on a substrate surface, then detected with immunochemistry. This method, although is widely used for years, has one main challenge: their level of detection permits a lower detection threshold in the picomolar range. Therefore, there is an urgent need to develop detection techniques that do not rely on organic dyes.

The group [59] performed assays on the reversed phase protein lysate arrays using both the conventional method and novel streptavidin–Qdot-based method. The relative luminescence unit data obtained through the Qdot method has shown a close linear

correlation with relative protein concentration on a logarithmic scale. This suggests that Qdots can be used for protein quantification in high-density microarray format (Figure 2.18).

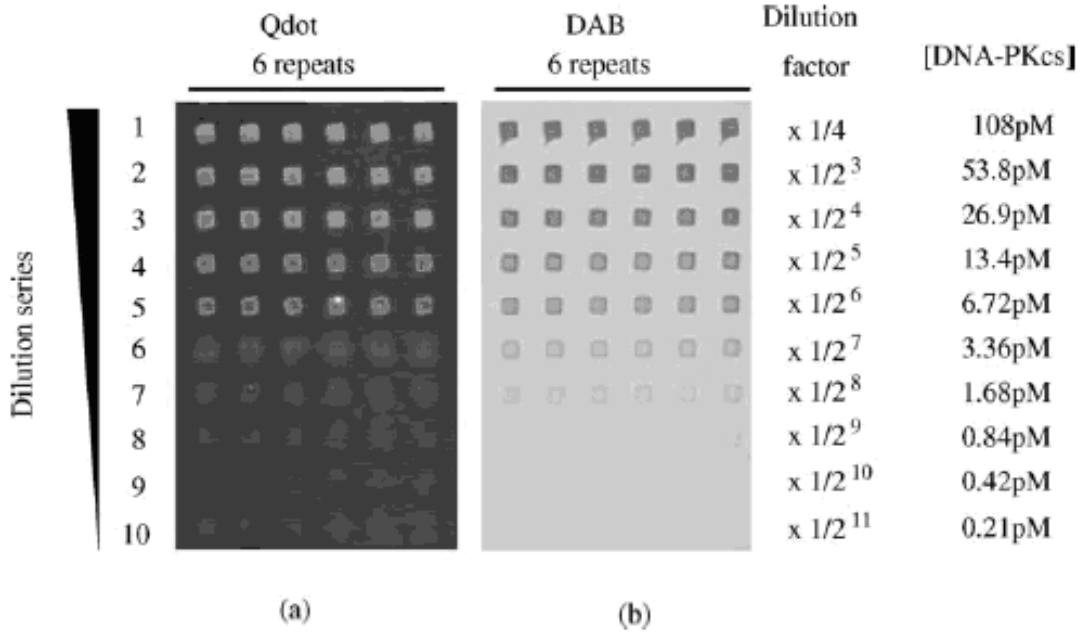

Figure 2.18 Spot image of reverse phase protein microarray. Each column consists of 10 two-fold dilutions of protein DNA-dependent protein kinase catalytic subunit spiked lysate of M059J cells. There are six repeats at each dilution point. (a) Qdot staining. (b) DAB staining [59]

There is a number of other publication on in vitro bioanalytical QD assays available, which assumes this field is gaining growing attention [80, 81, 82].

QDs are used as labels in immunoassays, immunohistochemical staining, and cellular imaging. The fact that multiple QDs may be excited by a single light makes them amenable for multiplex diagnostics [83, 84]. Figure 2.19 depicts, how different targets (biomolecules) can be detected in the solution using multicolored QDs, covered with different functional groups. The spectral analysis then reveals the spectra with different intensity and peak positions, which corresponds to the fractions of detecting

biomolecules. Goldman et al. [7] developed a multiplex immunoassay for the simultaneous detection of cholera toxin, ricin, shiga-like toxin 1, and staphylococcal enterotoxin B using the relevant antibodies conjugated to QDs of different sizes (different emission colors). The lowest detectable concentrations were 10 ng/ml (cholera toxin), 30 ng/ml (ricin), 300 ng/ml (shiga-like toxin 1), and 3 ng/ ml (staphylococcal enterotoxin B).

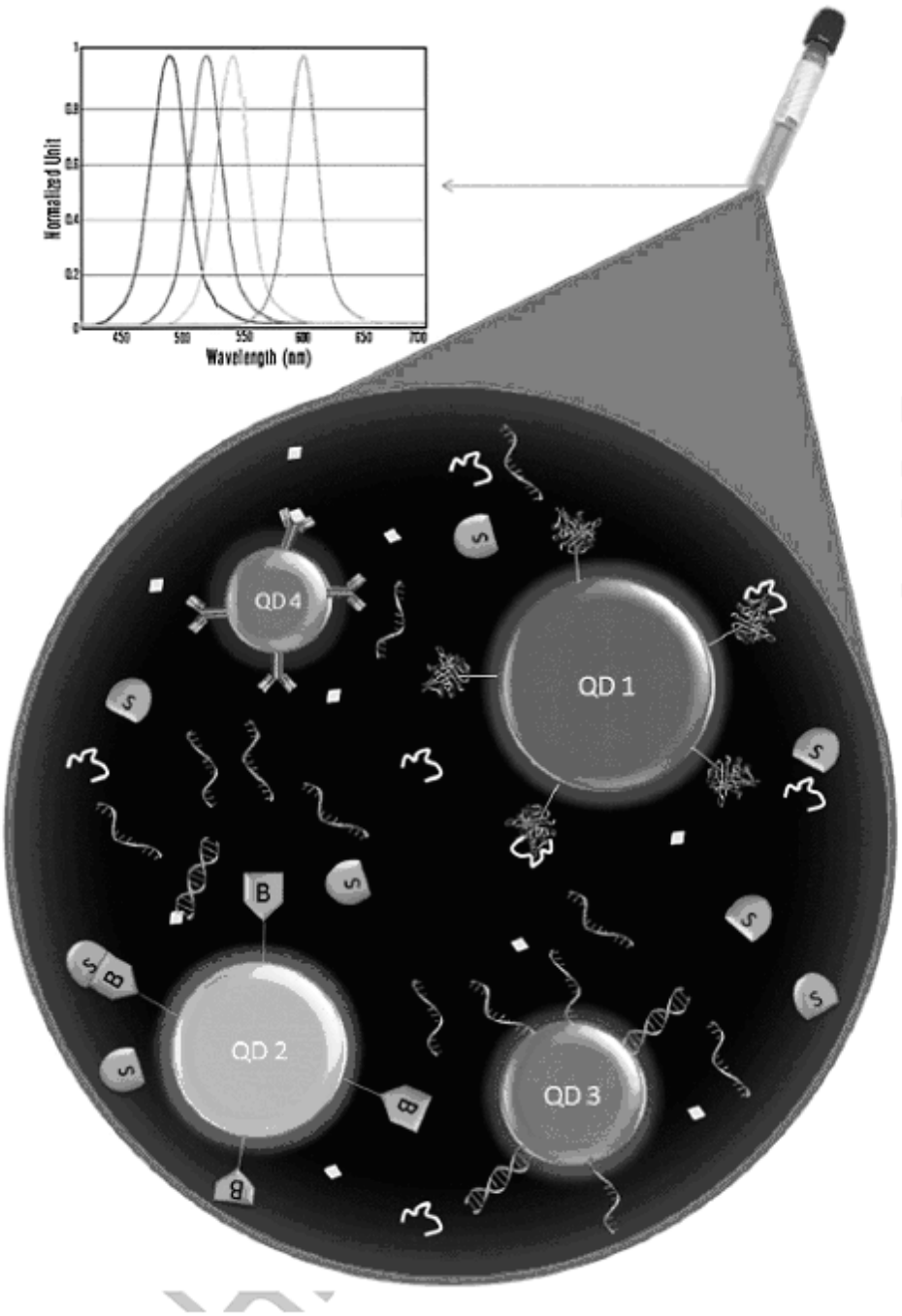

Figure 2.19. Schematic diagram for simultaneous detection of different targets in a serum sample using QDs of different sizes, functionalized with different recognition moieties: peptide/ protein (QD1), biotin (QD2), oligonucleotide (QD3), or antibodies (QD4). Abbreviations: B (biotin), S (streptavidin). Emission spectra of different sized-QDs (1–4) are shown in the upper left corner [85].

2.4.1. Challenges and limitations of bioconjugated QDs applications

Although the case for using QD-based fluorescent labels is compelling, it should be noted that QDs are not likely to replace organic dyes in all biological applications. Some of the challenges that have yet to be overcome include economic factors: QDs are expensive in comparison to organic dyes, and there is an initial investment required for researchers and instrument suppliers to produce systems optimized for use with QDs. Also, probe size and steric hindrance must be examined when assessing the suitability of a QDbased approach to fluorescent labeling of molecules. Since QDs are an order of magnitude larger than organic dyes, the extent to which their presence perturbs the biological process being observed must be determined. This is particularly important when multicolor experiments are desired, since labeling several biomolecules with QDs of different sizes could result in varying degrees of perturbation due to the large differences in the QD sizes. In contrast, most organic dyes are of similar size in spite of their large differences in absorption/ emission characteristics. [86]

Although QDs were considered to be safe for living organisms, the question about QD's toxicity has been rising by many groups. QDs have been found to cause vascular thrombosis in the pulmonary circulation [87], could induce apoptosis and cell death [88], and may accumulate in the lungs, spleen, liver and kidneys [89]. Therefore, QDs may not be as safe for humans, as previously reported. This factor is especially important for the in vivo QD applications (bioimaging, drug delivery), as in this case, QDs are injected into humans directly. In vitro applications of QDs could also be affected, but at least these issues may be solved with the proper precautious measures (wearing protective equipment, washing hands etc).

To summarize, although QDs may look very promising as novel fluorescent biomarkers, there are still many issues to be overcame for them to be widely used in clinics.

2.4.2. Future QD applications

One of the most exciting bioconjugated QD future applications is for in vivo noninvasive bioimaging in humans and for the drug delivery [90]. Today this powerful methodic was proven to perfectly visualize tumors in mice and other live animals [91-92], but the toxicity of such probes is an open question [87-90]. The issues of better DQ surface biofictionalization must be addressed in order to protect the organism from toxic Cadmium leak, which is a compoment of QD core. Also, the coating must be opitimized in order to allow better excretion of QDs with urine, desirably in 2-3 hours. The small part of injected bioconjugated QDs was found to stay in the area of injection and occasionally other sites [87-88], which must be avoided in humans. All these and other current flaws of QD bioimaging are to be solved in the future. QDs will definitely be one of the components of the envisioned multifunctional nanodevices that can detect diseased tissue, provide treatment and report progress in real time.

2.5 Enzyme-Linked Immuno Assay (ELISA) technique

ELISA is a biomolecular method which allows determination of the concentration of an antigen or antibody in a sample. One of the most well known examples is a HIV-antibody test [93-96]. Proteins from the virus are adsorbed (or chemically bound in some cases) to the walls of a reaction tube (usually 96 such tubes are fused together to form a plate, that simplifies handling). Then a serum sample is added

into the tube and incubated for some time. If that sample contains antibodies against HIV proteins, they will bind. The serum is then discarded and the tube washed a couple of times, to remove all antibodies that did not bind to antigen. Then, the tube is filled with a solution of antibodies directed to the constant part of human antibodies (raised in sheep, horse, donkey or similar animals). This second antibody is chemically linked to an enzyme like alkaline phosphatase or horseraddish peroxidase. If any human antibodies are present, the second antibody will bind to it. After washing away unbound second antibody the amount of bound enzyme is determined by a colour reaction. So you get a kind of sandwich: the enzyme is chemically bound to the second antibody, which is immuno adsorbed to the human antibody, which is immunoabsorbed to the virus protein on the walls of the tube. There are modifications to this principle, but that is the basic form [97].

The advantages of the ELISA are as follows:

1. it employs no radioactivity which is very beneficial and safe
2. it is sensitive
3. it is reasonably specific, and allows to achieve low noise to signal ratios
4. it is fairly cheap, because a large number of samples (usually at least up to 48) can be analyzed simultaneously and small amounts of reagents (usually up to 50 µl are required). [98]

Enzyme Linked Immuno-Sorbent Assay (ELISA) is a powerful technique for detection and quantitation of biological substances such as proteins, peptides, antibodies, and hormones. By combining the specificity of antibodies with the sensitivity of simple enzyme assay, ELISA can provide a quick and useful measurement of the concentration

of an unknown antigen or antibody. Currently, there are three major types of ELISA assays commonly used by researchers [99]. They are: indirect ELISA, typically used for screening antibodies; sandwich ELISA (or antigen capture), for analysis of antigen present; and competitive ELISA, for antigen specificity. Figure 2.20 A depicts a typical 96-well ELISA plate, while Figure 2.20 B shows a sample standard curve for the IL-4 Antigen.

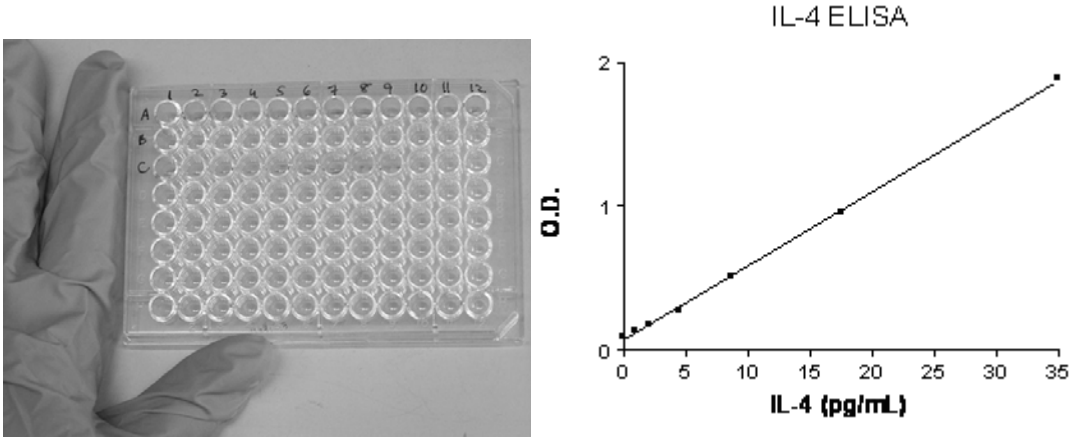

A B

Figure 2.20. A: typical 96-well ELISA plate [100]; B: typical standard curve for an IL-4 antigen [101].

2.5.1. "Sandwich" ELISA technique

The "sandwich" technique is so called because the antigen being assayed is held between two different antibodies. In this method (Figure 2.21): 1. Plate is coated with a capture antibody. 2. Sample is then added, and antigen present binds to capture antibody. 3. The detecting antibody is then added and binds to a different region (epitope) of the antigen. 4. Enzyme linked secondary antibody is added and binds to the detecting antibody. 5. The substrate is then added and the reaction between the substrate and the enzyme produces a color change. The optical density (OD) values can be measured

spectrophotometrically. 6. The signal generated is directly proportional to the amount of antibody bound antigen. Optimizing an ELISA assay requires the careful selection of antibodies and enzyme-substrate reporting system. Once optimized, sandwich ELISA technique is fast and accurate. If a purified antigen standard is available, this method can be used to detect the presence and to determine the quantity of antigen in an unknown sample [98-99].

The sensitivity of the sandwich ELISA is dependent on 3 factors:

1. The number of molecules of the first antibody that are bound to the solid phase, namely, the microtiter plate.
2. The avidity of the antibodies (both capture and detection) for the antigen
3. The specific activity of the detection antibody that is in part dependent on the number and type of labeled moieties it contains. It is important to note that while an ELISA assay is a useful tool to detect the presence and the quantity of an antigen in the sample, it does not provide information concerning the biological activity of the sample. ELISAs are not generally used to discriminate active or non-active forms of a protein. It may also detect degraded proteins that have intact epitopes. [102-103]

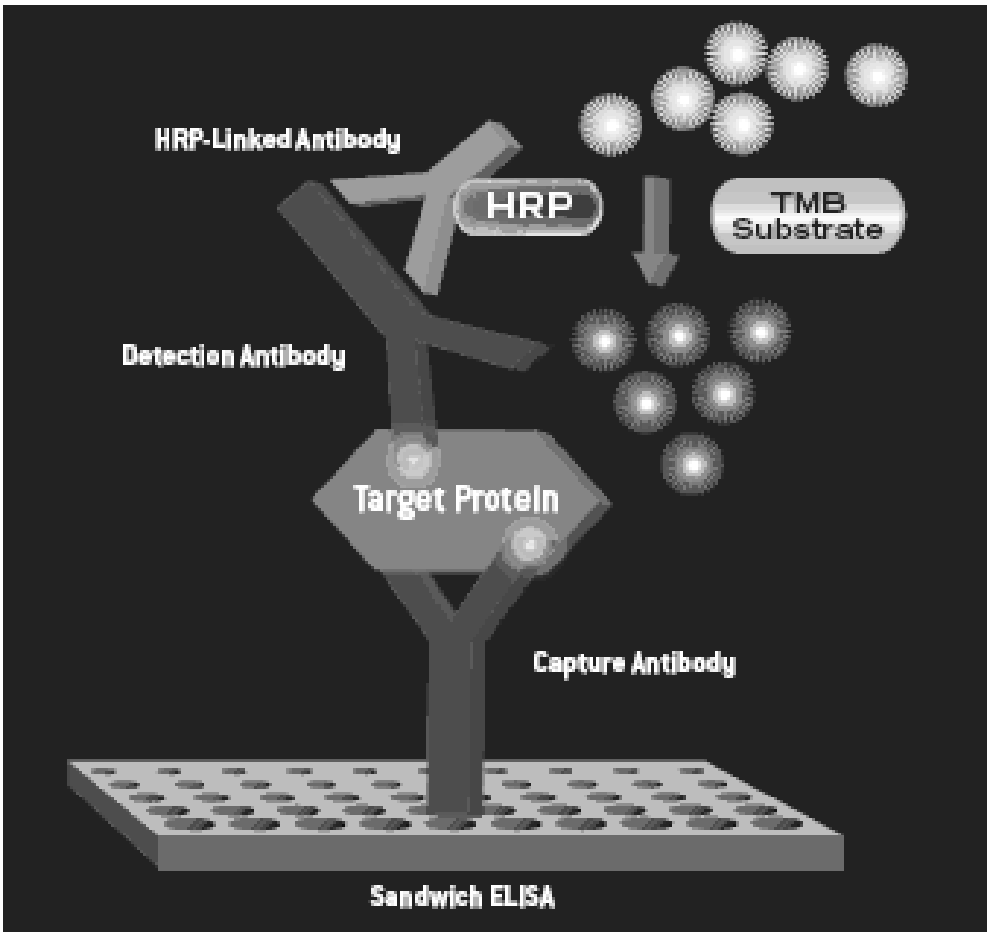

Figure 2.21. An example of a "sandwich" ELISA, which uses the enzymatic reaction for detection [104].

2.6. Prostate Specific Antigen (PSA), general information

PSA is a protein with molecular weight ~ 33-34kDa [105] which is produced mainly by the prostate gland in males, and its highest concentrations are found in prostate cells and seminal fluid [106]. It is now clear, that PSA is found in a variety of both male and female estrogen dependent tissues and biological liquids, including serum, urine, nipple aspirate, breast milk, amniotic fluid etc [33-39]. It is well known that the elevated above 4ng/ml tPSA levels in male serum may serve as an evidence of PSA-dependent prostate cancer [106], therefore, PSA screening is nowadays one of the most reliable

early prostate cancer detection test [107]. A body of publications is now available on the presence of PSA in female tissues/biological fluids, as well as role of tPSA levels in females with cancer [33-39]. It was found that small quantities of PSA are expressed by the breast, ovaries, uterus, and other estrogen and progesterone dependent tissues (Table 2.1) [108]. The elevated levels of PSA were found in the breast aspirate, saliva, serum and urine of pregnant women [33]. PSA concentrations in healthy not pregnant females who do not receive oral contraceptives or other estrogen supplements are so small that the exact numbers remain unclear because of the current detection threshold limits, however, according to the available sources, they usually fall in the range far below 0.1ng/ml [33-39] with the levels of 0.1ng/ml and higher being considered elevated and associated with either taking estrogen supplements, being pregnant or developing a breast tumor. It was reported that about 30% of all breast tumors are PSA positive (accompanied by the elevated PSA levels in female biological liquids, especially nipple aspirate and serum). In addition, a significant advantage in both overall and disease free survival rates were observed for PSA positive tumors, because these tumors tend to be more benign and respond to a selective estrogen receptor modulator treatment because of the over expression of the estrogen receptor [109]. Overexpression of the PSA in breast tumors, therefore, may be a good marker for the estrogen receptor positive (ER+) cancers and a reliable predictor of how well a person will respond to a selective estrogen receptor modulator treatment (the drugs like Tamoxifen, Anastrozole or Raloxifene) [110]. Keeping in mind, that even overexpressed levels of PSA in female's biological fluids may still be around 0.1ng/ml [33], the need of a molecular tool with the lower threshold for PSA detection is evident.

Prostate specific antigen (PSA), a glycoprotein in human serum, has been proved to be the most reliable and specific clinical tool for preoperative diagnosing and monitoring prostate cancer. Normally, prostate cancer is suspected if the total PSA level is higher than 10 ng ml−1 [111]. Therefore, sensitive and specific detection of PSA for early prostate cancer detection is of great significance.

Human prostate-specific antigen (PSA or KLK3) is an important marker for the diagnosis and management of prostate cancer. This is an androgen-regulated glycoprotein of the kallikrein-related protease family secreted by prostatic epithelial cells. Its physiological function is to cleave semenogelins in the seminal coagulum and its enzymatic activity is strongly modulated by zinc ions [112].

Besides cancer detection, the molecular tool with low PSA threshold detection may benefit the forensic science cases, dealing with sexual assaults [113]. Because the ratio of morphologically intact spermatozoa detected in victims' samples is frequently low, the other substances present in seminal fluid are needed to be detected, and PSA is currently one of such molecules [31], as it is always present in seminal fluid in huge concentrations. Because it was proved that PSA is not an exquisitely male's protein [33-39], the control of a female victim's unaffected biological fluid must always be taken, and here the need for a method with lower PSA threshold detection is also evident.

Table 2.1. PSA concentrations in biological fluids

Concentration of PSA in human body fluids	
Fluid	PSA (ng/mL)
semen	200,000 to 5.5 million
amniotic fluid	0.60-8.98
breast milk	0.47-100
saliva	0
female urine	0.12-3.72
female serum	0.01-.53

2.7. Summary

Nanoscience has become an emerging field in the recent 20 years, opening new possibilities in the biology and medicine. Photoluminescence QDs possess several advantages over currently used organic fluorophores, including their reduced tendency to photobleach, and the emission wavelength dependence on their size. In addition, QDs may be excited by a wide range of wavelengths which makes it possible to use one light source for different QDs. This feature is especially useful for multiplexing analysis, ie for labeling and determining several biomolecules with differently sized QDs. CdSe/ZnS QDs are the most used in biomolecular field. It is possible to create a unique surface chemistry by capping different groups on top of QDs, which enables the subsequent bioconjugation of QDs to different biomolecules, including cancer biomarkers.

Bioconjugation is an attachment of the biomolecules to QDs. It may be performed in a number of different ways, and the choice of procedure depends upon the needs bioconjugate will be used for. In this work, conjugation to antibody fragments via disulphide reduction and sulfhydryl-amino coupling was chosen and the commercially available conjugation kit, made by Invitrogen, was used. The conjugation was successfully confirmed with the agarose gel electrophoresis, improved with organic dye fluoprescamine, it was found that bioconjugated QDs have a retarded movement in the gel, because of their increased size. The working conditions of this methods have been optimized to allow better separation of conjugated and pure QDs. TEM analysis of pure 705nm QDs and bioconjugated QDs revealed the ellipsoid shape and approx dimensions 11x6nm +/- 0.5nm. No significant difference in the shape and size was observed between pure and bioconjugated QDs.

ELISA and one of its types, “sandwich” ELISA were described and proved to be useful techniques in cancer detection. These methods can detect most cancer biomarkers in nanomolar concentrations, however, as was proven with the PSA molecule, this sensitivity may not be low enough to detect it in biological fluids. PSA molecule is a standard, and most reliable prostate cancer biomarker in men, and there is a growing body of evidence, that PSA is present in female biological fluids in extremely low concentrations. The presence of PSA in female body may correlate with breast, uterine or ovarian cancers, but the sensitivity of the standard PSA ELISA is not low enough, to detect the concentrations at or below 0.1 ng/ml. This is why QD modification of PSA ELISA will be presented in the last section of this work.

The literature review, described in this section, will serve as a solid base for the further experiments, described in the subsequent sections of this work.

3. Confirming bioconjugation, photoluminescence (PL) measurements and short-wavelength spectral shift of bioconjugated QDs

3.1. Introduction

Quantum dots, attached to different biomolecules, have being investigated for a long period of time, and a number of publications are available on this topic [114-118]. However, due to the nature of bioconjugate further use in biology and medicine, the research is mostly being focused on the liquid bioconjugate [114-118]. To the best of our knowledge, for the first time, it was noticed by our group, that CdSe/ZnS QDs, bioconjugated to IL6 antibodies, perform a short-wavelength, so-called “blue” spectral shift (I may be referring to it as simply “the shift” in future) when dried on the silicon chip substrate at room ambience [119-123]. Figure 3.1 illustrates this effect. This is one of the first recorded evidence of the “blue” spectral shift, which appears on bioconjugated QDs, dried on the silicon substrate, in comparison to pure, non-conjugated QDs of the same type. Both conjugated and pure QDs were used to make a drop approx 3mm in diameter on the silicon substrate, dried for several hours at room ambience, and then up to 80 spectra per spot were generated for both bioconjugated and nonconjugated drops. It allows to generate more than one spectra per spot which allows a more accurate spectroscopic analysis in comparison to just one spectra per spot [123-125]. The Figure

3.1 clearly shows, that conjugated QDs spectra are shifted approx 5nm to the short-wavelength region in comparison to pure QDs.

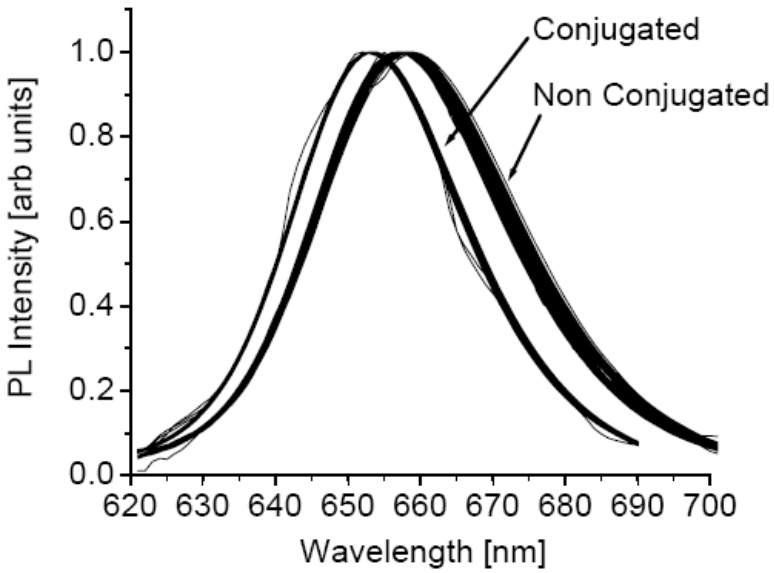

Figure 3.1 Normalized spectra of CdSe/ZnS quantum dots with principal emission maxima around 655 nm (nonconjugated) and same quantum dots after IL10 antibody attachment (conjugated).

Investigation of this short-wavelength "blue" spectral shift of bioconjugated QDs was one of the main tasks of this PhD work. Different QDs, as wells as a number of antibodies, which are known to be important cancer biomarkers (Section 3.4, Table 3.2) have been investigated, as well as the time of dried sample storage and the ambient conditions (temperature, gases, light, vacuum, substrates etc) and their effect on the shift.

At the end of this section (discussion section) several mechanisms which may cause the shift, have been proposed. The author believes the shift may be used in favor of early cancer detection as well as benefit forensic science.

3.2. Hardware description

Two lasers were used as the excitation sources in the PL experiments. In Table 3.1 their specifications are presented:

Table 3.1 Lasers used in the PL experiments

Laser type	Emisson wavelength, nm	Output power, mW	Manufacturer/Model
HeCd (cw)	325	50	Coherent Inc HeCd seires 74
Ar+ (cw)	488	50-100	Coherent inc

The photoluminescence signal was dispersed with a 0.5 m SPEX-500M grating spectrometer possessing a reciprocal dispersion of 3.2 nm/mm (2nd order) with a 600 lines/mm diffraction grating. The dispersed signal was registered in the spectral range of 400 - 800 nm with either a cooled photomultiplier (Electron Tubes) or in the range of 700 – 1700 nm with a liquid nitrogen cooled Ge detector (North Coast Scientific Corp.). A mechanical chopper modulated the excitation light of the CW laser with 82 Hz frequency. AC signal from the detectors was fed to Lock-in amplifier EG&G Model 5209 and collected by a computer. Both ELISA sample and dried QD spots deposited on silicon were used for spectroscopic PL mapping with a smallest step of 0.5mm to produce a set of up to 160 individual PL spectra for each well and spot. The scanning PL spectroscopy was performed at room temperature using a 488 nm Ar laser with power density of 70 W/cm2 as the excitation source. ELISA samples or silicon wafers with deposited QD spots were mounted on a computer-controlled *X*–*Y* moving stage. The typical mapping area was 8mm x 8mm for ELISA wells, and 3.5mm x 3.5mm for dried QD samples. The PL spectrum was dispersed by a SPEX 500M spectrometer and recorded by a cooled

photomultiplier tube coupled with a lock-in amplifier. A schematic of the PL setup is shown on Figure 3.2

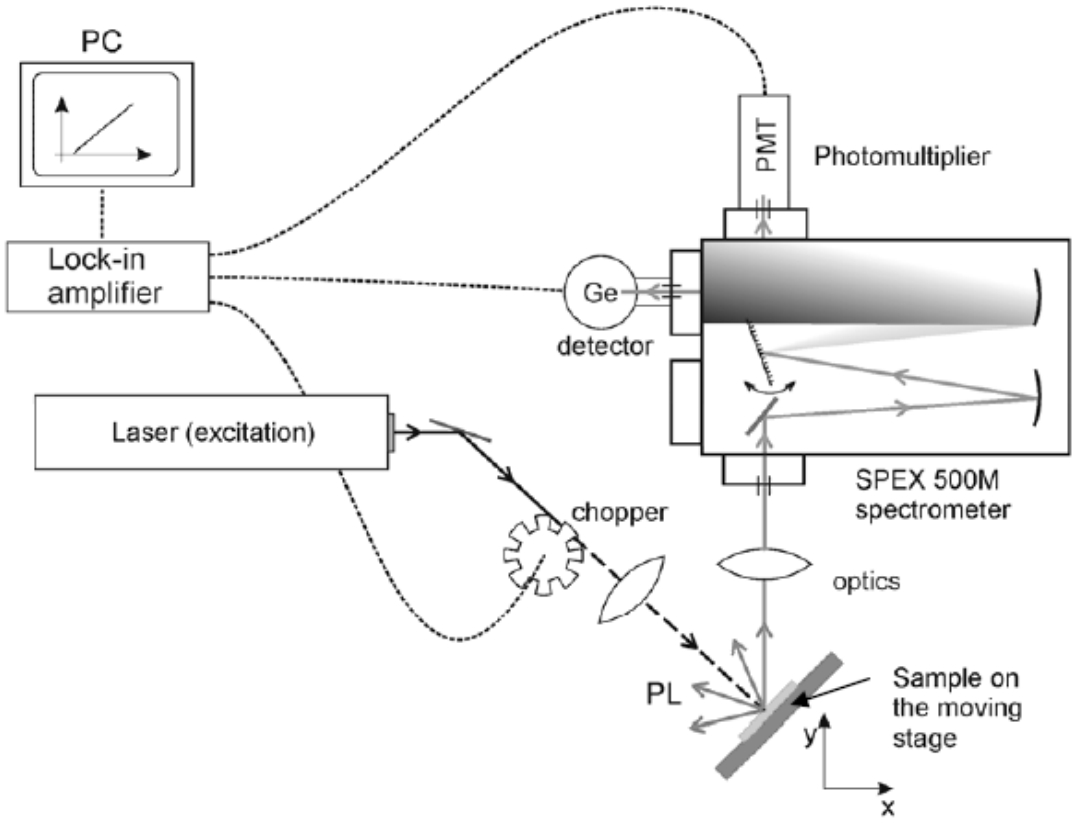

Figure 3.2 Photoluminescence setup for room temp measurements of quantum dots

The PL mapping experiment was done with the use of an X-Y computer controlled moving stage (Velmex 8300) with 10 μm step precision and (Klinger CC 1.2) for 1 μm resolution maps.

3.3 TEM visualization of pure and bioconjugated 705nm QDs

Quantum dots, possessing the size of at most 12nm, are hard to visualize with other techniques, however, with the TEM technique they can successfully be visualized. In this work, Transmission Electron Microscope Tecnai T20 with the line resolution of

1.2 A and electronic images captured using Orius 831 7 MP CCD camera. The TEM analysis of pure and conjugated 705nm QDs was conducted. It revealed an ellipsoid shape approximately 11x6 nm +/- 0.5nm (Fig 3.3).

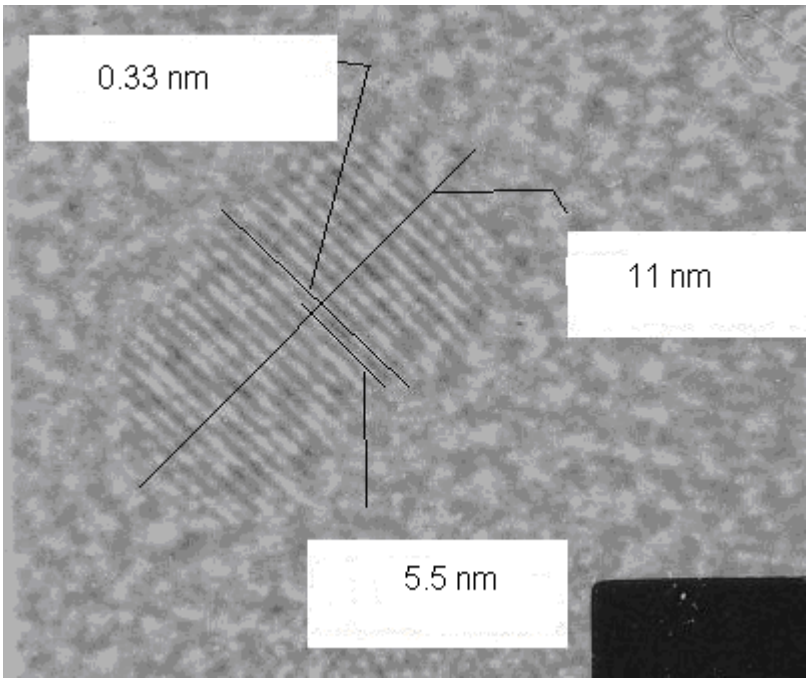

Figure 3.3. TEM image of the individual 705nm CdSeTe/ZnS core/shell quantum dot.

TEM analysis of conjugated to Caveolin-1 (CAV-1) Anribodies was also performed in order to establish any size/shape differences with the pure QDs. The Figure of bioconjugated QDs is shown on Fig 3.4

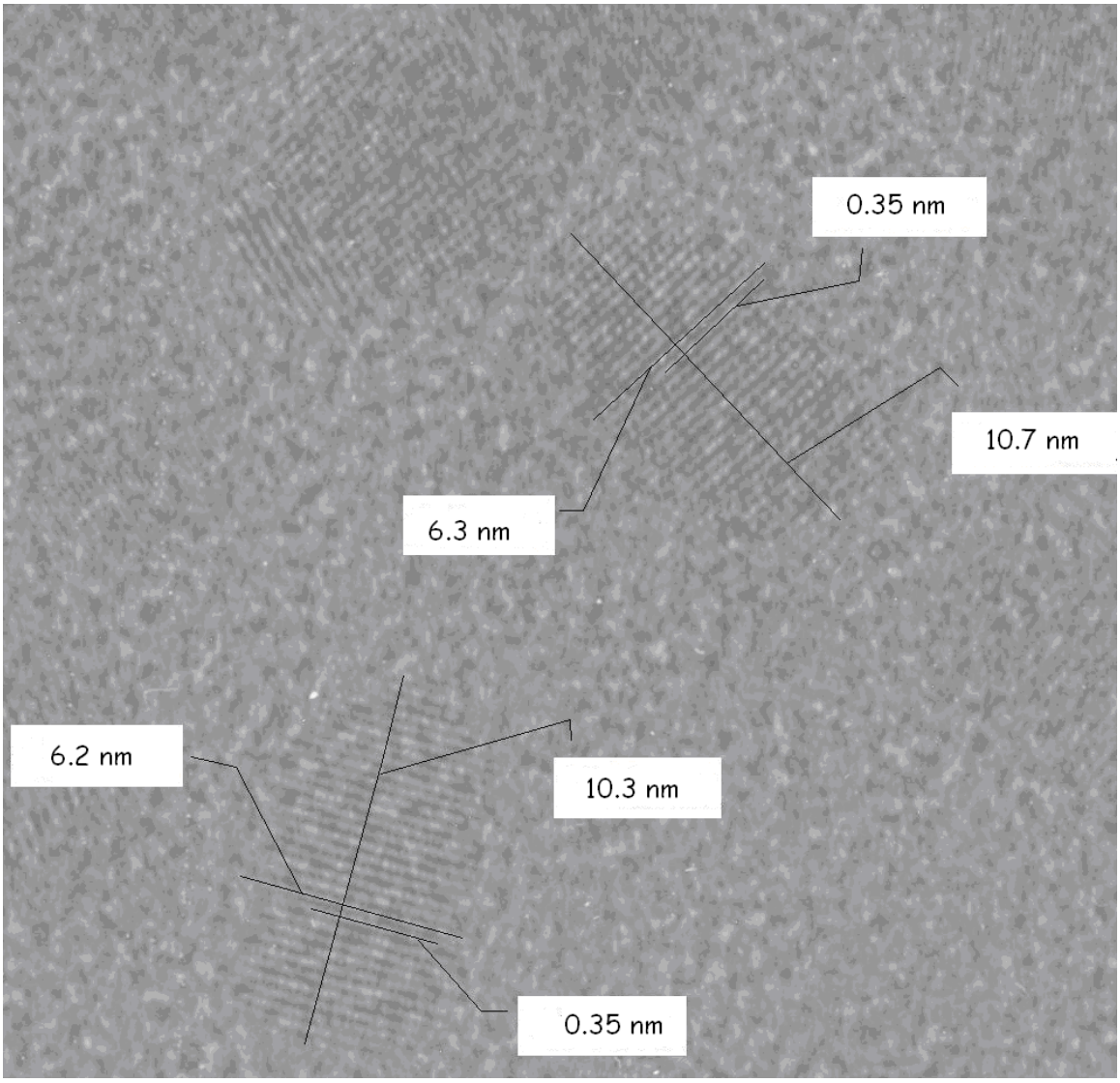

Figure 3.4. 705nm QDs, conjugated to CAV-1 antibodies.

According to the pictures, no significant differences between pure and bioconjugated QDs was found. This analysis, however, provides important data that the short wavelength “Blue” spectral shift of bioconjugated QDs (discussed in the sections 3.6 – 3.11) is not because of the size decrease or shape change resulting from the bioconjugation reaction directly.

There is, however, one remark about this effect which should be taken into account. It is in detail described in the section 3.5 of this dissertation. QD solutions, used

for the TEM analysis, were dried on the copper grits, covered with the amorphous carbon layer [126]. This was done in order to protect QD samples from contact with copper, as copper reacts with the CdSe core and quenches PL [127-128]. As will be shown in the section 3.8, substrate plays an important role in the "blue" shift development, and it was not developed on the soft and porous rubber substrates. Same effect may be observed with the carbon amorphous coating. Additional research in this direction is needed in order to carefully examine the size/shape of bioconjugated QDs.

3.4. Biomolecules, used for bioconjugation

A wide range of biomolecules (antibodies) was used for bioconjugation experiments within the scope of this work. The careful choice of the antibodies was based on the following reason: all of them are known for being cancer biomarkers. Table 3.2 summarizes the list of biomolecules, their molecular weights, and cancers for which these molecules serve as biomarkers.

Table 3.2 The list of biomolecules, their molecular weights, and cancers for which these molecules serve as biomarkers

Antibody	Molecular weight, kDa	Type of cancer	Remarks
Interleukin-6 (IL-6)	28	Prostate cancer	One of the seven biomarkers which predict the risk of recurrence for prostate cancer: all seven elevated – 86.6% [129]
Interleukin-10 (IL-10)	23	Ovarian cancer, lymphoma and myeloma	Elevated levels alone may serve as biomarkers for mentioned cancers [130-132]
Osteoprotegetin OPG	55	myeloma, breast and prostate cancer	Elevated levels serve as tumor cell survival factors by inhibiting apoptosis [133]
Protein 53 (P53)	53	Adenocarcinomas and other cancers	Important tumor suppressor, often altered in cancers, or its levels lowered [134]
kallikrein *14* (KLK14)	31	Breast cancer	KLK14 is overexpressed in breast cancer in comparison to normal breast tissues and is positively associated with conventional parameters of tumour aggressiveness [135]
Prostate Specific Antigen (PSA)	34	Prostate cancer in men, breast/ovarian cancers in women	At least 2/3 of all prostate cancer are characterized by the PSA elevated levels [106-107, 111-113]
(Caveolin1) CAV-1	22-23	Prostate cancer	Involved into predisposition of high aggressive prostate cancer [136]

3.5 Verifying bioconjugation

Agarose gel electrophoresis represents an easy, inexpensive and reliable method to verify the conjugation of QDs to different monoclonal ABs. According to Invitrogen [26], one QD molecule, covered with all layers, has a molecular weight about 750 KDa, which is larger in comparison to AB molecules being in the weight range of 20-55 KDa.

One QD molecule could attach 2-3 AB molecules [26], therefore we should see a difference in the electric field drift and separation of the 750KDa pure QDs and 800-850KDa conjugated QDs This task requires careful optimization of the experimental conditions to improve the separation distance in gel.

Several works are available on agarose electrophoresis, which conclude that for bigger fragments higher agarose concentrations are recommended [137]. Therefore, we used 2% agarose gel, applied voltages up to 1.5V and running time up to 2 hours. In figure 3.5 the agarose gel image is shown after 120 min of running time. Here the retardation in movement between the pure 705nm QDs and conjugated 705nm QDs is evident (compare wells #1 and #2; #5 and #6). In this image pure ABs mixed with Fluorescamine (wells #3 and #7) have already run out of the gel, and only the trace PL from them could be seen in well #3. We observed also that two different ABs, PSA and IL6, move with different velocities in the gel experiment as illustrated in Figure 6 (wells #2 and #6). According to [138], molecular weight of the PSA molecule is 32-33 kDa, while the one for IL6 is 22-28kDa [139]. It is logical to assume that QDs conjugated to IL6 molecule will move faster than these conjugated to PSA, because of the size difference. This hypothesis is confirmed (wells 2 and 6): the PSA movement is retarded in comparison to IL6 movement. Also, the trace of the PSA + Fluorescamine PL is visible in well 3, while no PL could be observed for the Il6 molecule, where there's an IL6 + Fluorescamine mixture. Therefore, the separation capacity of the agarose gel is high enough for this type of application.

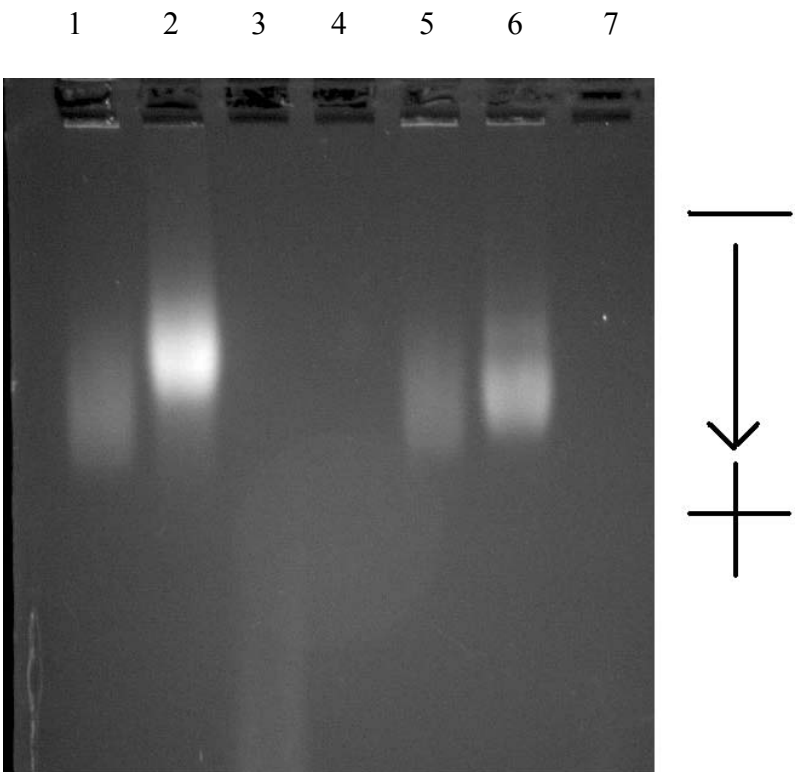

Figure 3.5. Agarose gel electrophoresis photograph, 2% agarose gel, 1.5V, 120 mins running time, 0.5xTBE running buffer. Wells are as follows: (1) non-conjugated 705nm QDs; (2) PSA conjugated to 705nm QDs; (3) PSA pure protein + Fluorescamine, (4) empty, (5) non-conjugated 705nm QDs, (6) IL6 conjugated to 705nm QDs, and (7) IL6 pure protein + Fluorescamine.

In every biological procedure, timing is an important option, and it is highly desirable to minimize the running time. Therefore, the gel which is shown on Figure 3.5, was analyzed 30mins after the run cycle started. The result is shown on Figure 3.6

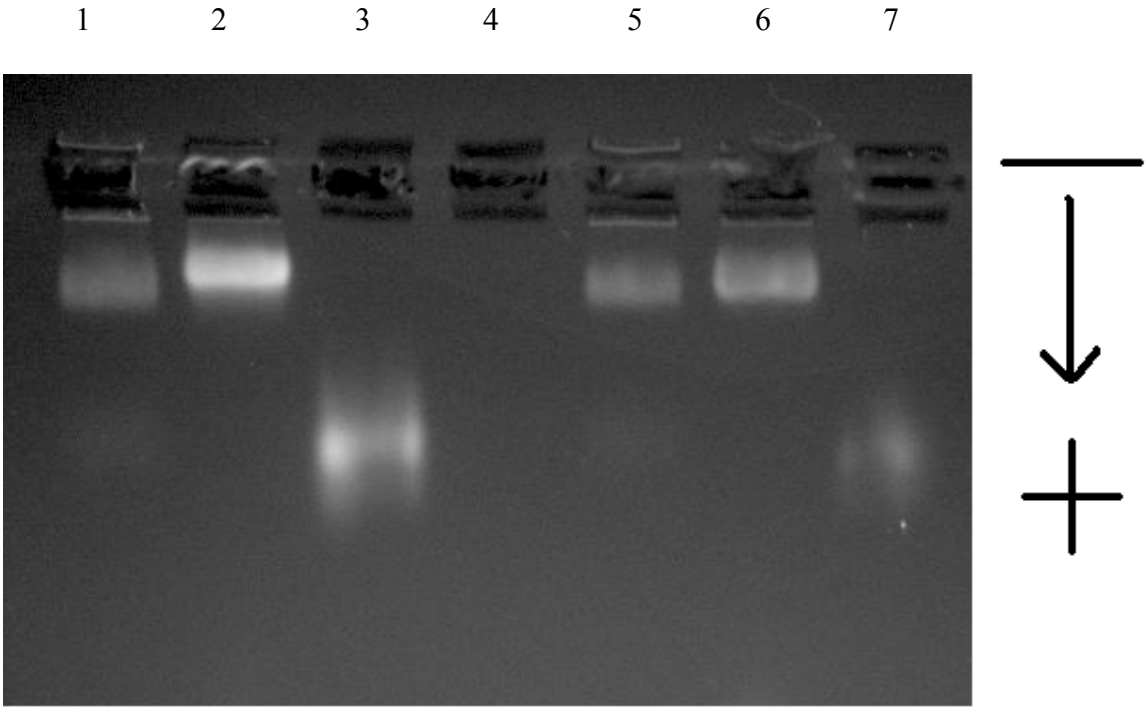

Figure 3.6. Agarose gel electrophoresis photograph, 2% agarose gel, 1.5V, 30 mins running time, 0.5xTBE running buffer. Wells are as follows: (1) non-conjugated 705nm QDs; (2) PSA conjugated to 705nm QDs; (3) PSA pure protein + Fluorescamine, (4) empty, (5) non-conjugated 705nm QDs, (6) IL6 conjugated to 705nm QDs, and (7) IL6 pure protein + Fluorescamine.

By comparing wells # 1 and 2; and # 5 and 6, it is evident that 30mins is not enough for the complete separation of conjugated and nonconjugated QDs. However, the 30mins gel allows the clear visualization of pure PSA (well #3) and IL6 (well #7) antibodies, mixed with fluorescamine. It is evident, that because of their smaller size they run much faster in a gel.

So, the following agarose gel specifications are proposed to be optimum for CdSe/ZnS QDs + various antibodies conjugation verification: 2% agarose gel, 1.5V, 120 mins running time, 0.5xTBE running buffer. The amount of time may be increased 15-30 mins if the satisfactory enough separation is not achieved within the 120 minutes slot.

3.6. QD samples in liquid and in the agarose gel

After the shift of dried bioconjugated samples was discovered, it was necessary to find out, if the pure QD and bioconjugated QD emission spectra are identical in the liquid state. For this purpose, for any new batch of bioconjugated QDs the measurements of liquid samples were conducted. The results showed no or a negligibly small (below 2nm) blue spectral shift of all liquid samples analyzed. In Figure 3.7 one liquid sample measurement is shown: 705nm CdSe/ZnS QDs, conjugated to Prostate Specific Antigen (PSA) antibodies. The measurement was done on the system shown in Fig 3.2 , and the plastic tubes with liquid samples were attached to the moving stage. As could be seen from Figure 3.7B, the blue shift here is ~1nm which is below the precision limit of the PL measurements. Additionally, the storage of the liquid samples in dark and lowered (2-4C) temperature did not influence a position of the PL maximum. Therefore, it was concluded that the blue spectral shift of bioconjugated QDs appears only when the samples are dried.

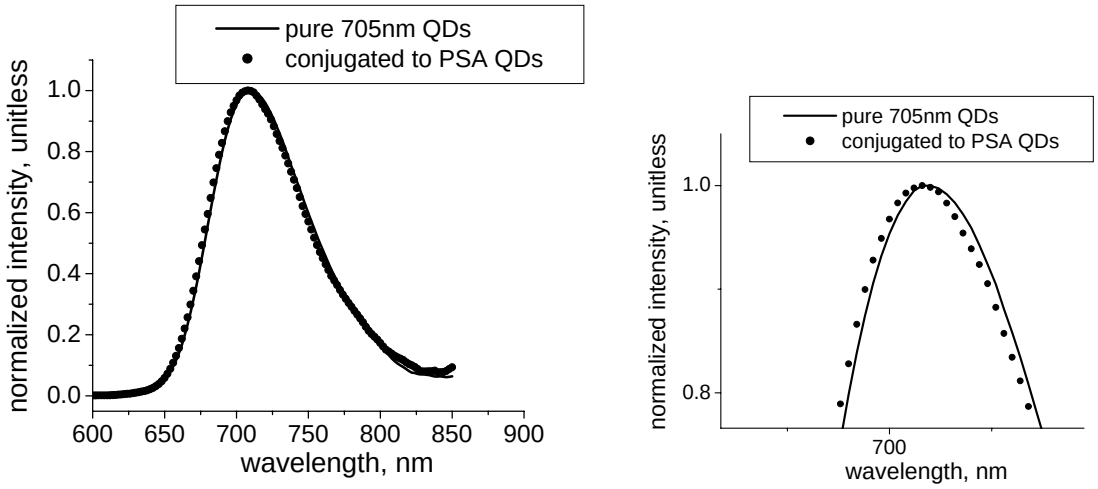

A B

Figure 3.7 Liquid measurements of pure 705nm QDs (line) and 705nm QDs, bioconjugated to PSA antibodies (circles): A – whole spectra; B – magnified center of the plot to better reveal peak positions.

The similar observation was made for the pure and bioconjugated QD solutions, used to run the agarose gel to check conjugation (Figures 3.5 and 3.6). No statistically significant spectral shift was detected for the 705nm QDs, conjugated to PSA antibodies, in comparison with the control pure QD samples (Figure 3.8). The measurement was done in a fresh not dried gel as shown in Figures 3.5 and 3.6, wells #2 and # 1. This data allows us to suggest, that drying is an important factor, which causes the spectral shift of bioconjugated QDs.

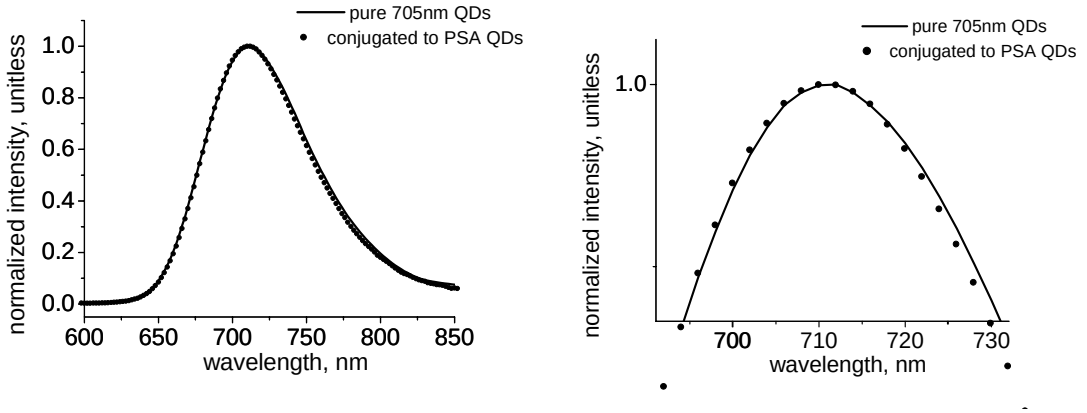

A B

Figure 3.8. Gel measurements of pure 705nm QDs (line) and 705nm QDs, bioconjugated to PSA antibodies (circles): A – whole spectra; B – magnified center of the plot to better reveal peak positions.

3.7. QD samples dried on the silicon substrate

In order to dry the sample on the silicon substrate, the spots of different, but known, volume were placed on the clean silicon chip with the automatic pipette and let dry on air for at least 30 mins before the initial PL spectrum was measurement. For all experiments the nonconjugated fraction of the same size QDs was used as a reference. All samples were clearly marked and dated on the chip to avoid possible confusion. Between the measurements, the samples were stored in clear plastic boxes to minimize contamination, or stored on the oven surface for higher temperature measurements. A typical sample is shown on Fig 3.9

Figure 3.9. 705nm QD samples, dried on silicon chip: "-" is nonconjugated drop; "+" – conjugated to PSA drop. The scale is in centimeters.

The single PL spectrum was recorded from the shown above sample approximately in 30 to 60 mins after the drops deposition. This first measurement of dried samples will be referred further as the "initial measurement". Figure 3.10 illustrates that although the liquid samples did not have a valid "blue" shift (Figure 3.7), the initial shift of the dried samples is 6-7nm. The initial shift depends upon several factors, including the QD size and the biomolecule molecular weight, but in average it is between 4 and 8 nm.

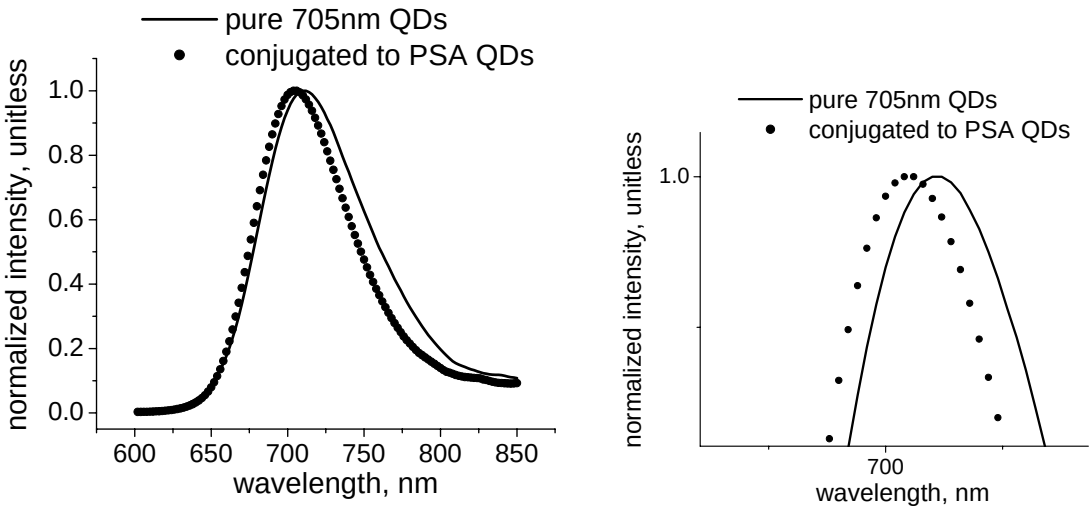

A B

Figure 3.10. Dried measurements of pure 705nm QDs (line) and 705nm QDs, bioconjugated to PSA antibodies (circles): A – whole spectra; B – magnified center of the plot to better reveal peak positions.

3.7.1. Time dependence of the "blue" spectral shift

As soon as the initial shift of bioconjugated QDs was discovered, it was necessary to research, if it changes with the time of storage of the dried sample. To do this, the sample shown in Figure 3.9 was stored in the clear plastic box at room ambience and the spectra were taken once a day to monitor the peak positions. It was discovered that the blue spectral shift of bioconjugated QDs increases with time: the PL spectrum of bio-conjugated spot gradually shifts to the short-wavelength region, while the pure QDs retain the same peak position within 2nm accuracy threshold (Figure 3.11 A). As could be seen from the Figure 3.11 B, for this particular 705nm QDs + PSA sample, the blue shift increased from 6-7nm up to ~27nm in 11 days of storage. This effect was also observed and documented for other QDs and Antibodies as described below. The average spectral shift after 10-13 days of storage at room ambience is usually 22-35nm.

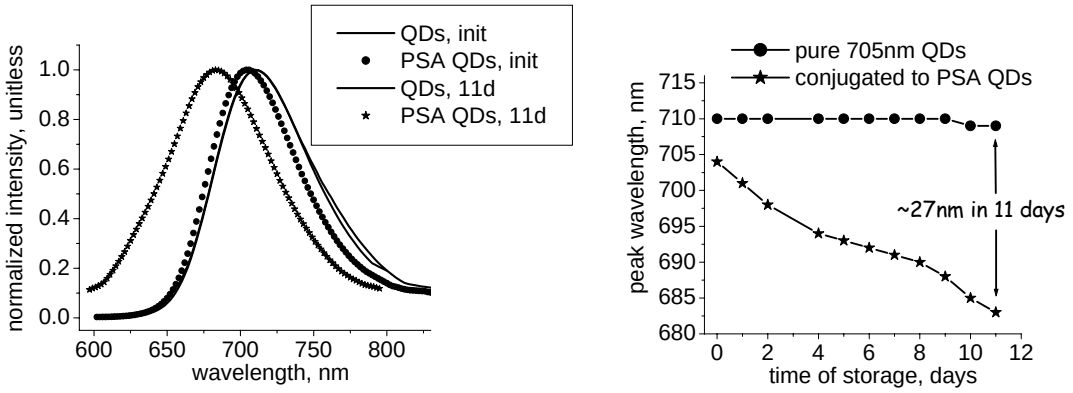

A B

Figure 3.11. The blue shift dependence on the sample storage time at room ambience: A – PL spectra of pure 705nm QDs and conjugated to PSA QDs, initial and after the 11 days of storageas room T; B – PL peak positions on a daily basis for pure 705nm QDs and same 705 nm QDs conjugated to PSA.

3.7.2. The influence of QD size (emission color)

The drying experiments were conducted with different QD sizes in order to research the possible influence of QDs size on this effect.

The shift was also observed for other QD sizes (different emission wavelength maxima) namely 605 (4 nm in diameter) and 705 (7 nm in diameter) [3]. Experiments were carried out in a similar manner as for the 655 QDs. The spots were dried out on a Si surface and mapped with 0.2 mm spatial resolution. Spectra were recorded at each spot and their maxima position and relative shift vs. non conjugated QDs is presented in Figure 3.12.

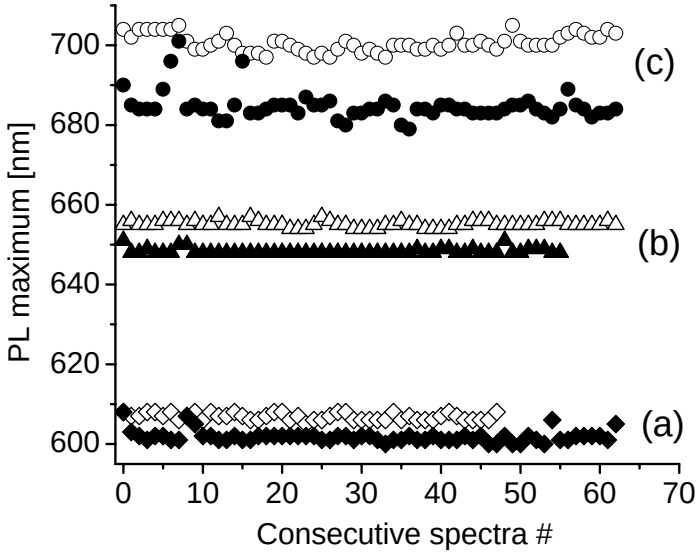

Figure 3.12 Peak position of the PL maximum measured on non-conjugated (open shapes) and conjugated with IL 10 antibody molecule (close shapes) CdSe/ZnS core-shell QDs of three different sizes with maxima at (a) 605nm, (b) 655nm and (c) 705nm. Spectral shift caused by the conjugation was observed for majority of measured PL spectra that were collected for each sample in the PL mapping mode.

From the Figure 3.12 it is clear that larger size QDs exhibit in average larger spectral shift. The possible mechanisms for this effect will be explained in the discussion section of this chapter. Because we are interested in maximization of the blue spectral shift, it was decided to continue the experiments with the 705nm QDs. Therefore, most of the data presented in this work, is for the 705nm QDs.

3.7.3. The influence of drying temperatures

In order to establish the influence of the ambient temperature on the blue shift, two identical dried samples were stored at the room (+22 - +23C) and fridge (+2 - +4C) ambiences for 13 days and the spectra were taken daily. The fridge samples were kept in a fridge for the whole time, except for the measurement which did not exceed 10mins a day. Each sample had a pure 705nm QD drop and bioconjugated to PSA QD drop. The

results are shown on Fig 3.13. It is clear that conjugated sample which was kept in a fridge performs smaller blue shift than the one which was kept in the room ambience, suggesting that lower temperatures slow down the blue shift formation. The relative difference between the shift magnitudes is ~26%.

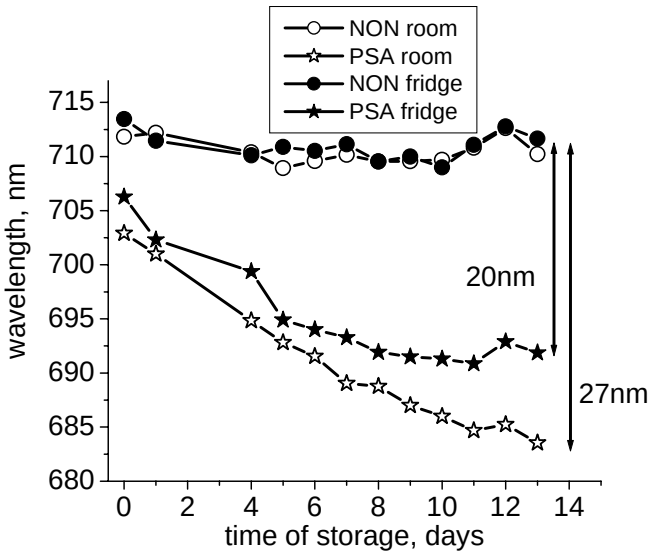

Figure 3.13 The blue shift of the conjugated to PSA sample (stars) in comparison to pure QD sample (rounds) after the 13 days of storage. The average shift of the room conjugated sample (open shapes) is ~ 26% bigger in comparison to the fridge conjugated sample (closed shapes).

Because the lower storage temperatures show a diminishing effect of the shift formation, the assumption was made that the higher temperatures may speed its formation. To test this, conjugated and reference samples were dried in a temperature stabilized oven at air ambient atmosphere at various temperatures up to 245 °C. It is realized that high-temperature processing may produce a decomposition of the protein structure. However, it was used to facilitate PL shift process for exploration purposes.

The kinetics of the annealing process was monitored using PL spectra at room temperature. Figure 3.14 shows the kinetic curves of the PL spectral shift versus

annealing time at different temperatures over a period of 12 h. At annealing temperatures of 140 and 190 °C, the kinetic curves show an exponential growth with saturation of the relative PL spectral shift allowing for an estimate of the time constant of this process at 5 hrs and 8 hrs for 190°C and 140 °C, respectively. The spectral shift rate was much higher for 250 °C drying temperature, while for 115 °C observable shift change does not show full exponential saturation level even after 12 hours of storage.

Apart from the PL spectral shift, we noticed a gradual reduction of the PL intensity. In contrast, the nonconjugated reference QD samples are stable at the same annealing conditions with respect to the peak position, intensity, and FWHM values.

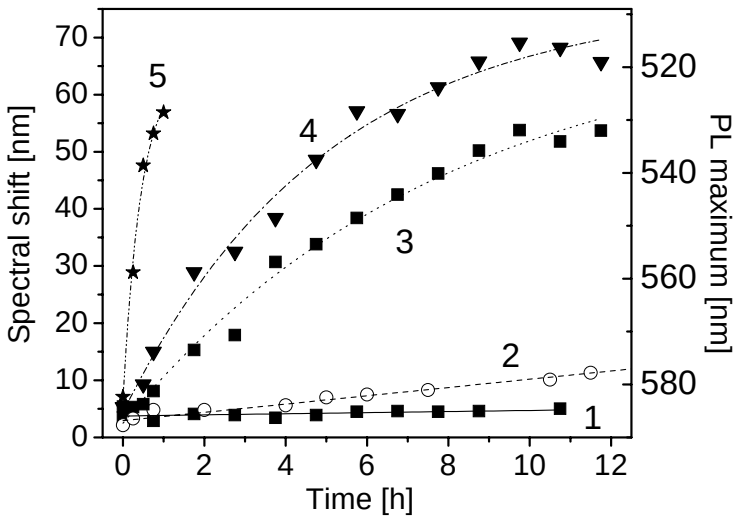

Figure 3.14 Kinetics of the PL spectral shift enhancement in the bio-conjugated sample due to annealing at different temperatures: 1 – room, 2 - 115°C, 3 - 140°C, 4 - 190°C and 5 – 250°C. Non-conjugated QD samples retain a PL band spectral position within experimental accuracy of ~1 nm.

The observed results may be described by the influence of temperatures on the proteins, attached to QDs. At lower temperatures, proteins dry and denature slower, which may reduce the tension on the QD-substrate surface or have the chemical effect of the QD. It will be discussed in detail in the discussion section.

3.7.4. The influence of a biomolecule's molecular weight

We extended this study to other types of cancer related antibodies. In this experiment the identical type and size of QDs with the PL maximum at 705 +/- 2 nm was used. The bioconjugation and subsequent PL spectroscopic analysis was performed on 6 monoclonal ABs, currently being considered as cancer biomarkers. They are: IL-6, IL-10, PSA, P53, OPG and CAV-1. 705nm QDs, conjugated to all ABs, mentioned above, perform "blue" spectral shift of different magnitude with the IL-6 giving the smallest shift, and OPG – the largest approaching 36 nm after 11 days of room temperature sample storage (figure 3.15).

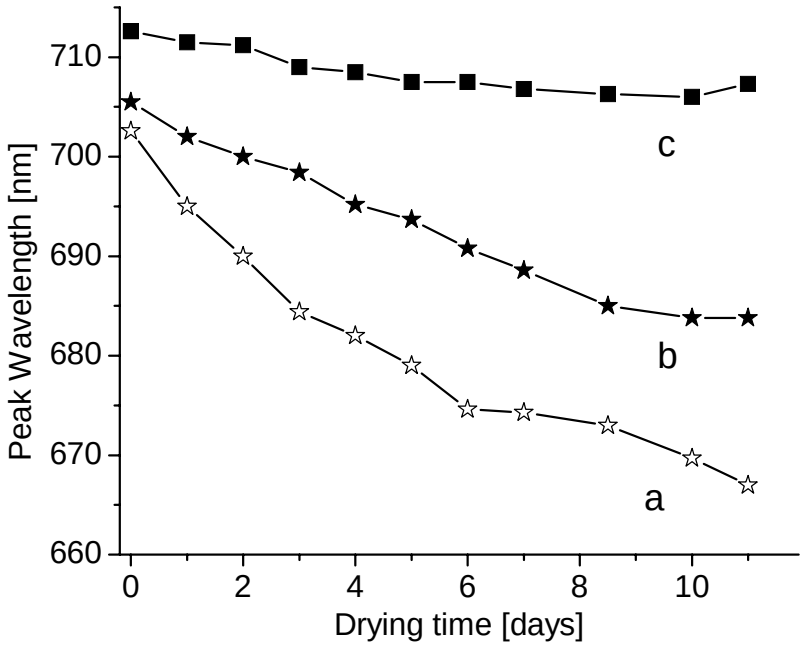

Figure 3.15. "Blue" spectral shift developed during 11 days of sample drying at room temperature. (a) 705nm QDs conjugated to OPG AB; (b) 705nm QDs, conjugated to IL-6 AB and (c) non-conjugated 705 QDs used as a control.

The different magnitude of the blue spectral shift for different ABs, is repeatable and observed in samples dried at room or higher temperatures. For instance, we previously observed an approximately 40 nm spectral shift for IL-10 antibody after 12 days drying at room temperature or after annealing at 140C for 12 hours [123]. In figure 3.16 we present data of the maximum PL spectral shift for different ABs after room-temperature drying and correlated this shift with the AB molecular weight. It occurred that the AB molecules with larger molecular weight show a larger "blue" shift of the conjugated 705 nm QDs. For instance, molecular weight of the IL6 AB molecule is 22-26 kDa [139], while OPG AB molecule weights 48 kDa [140], which corresponds to 27 and 36 nm PL shifts.

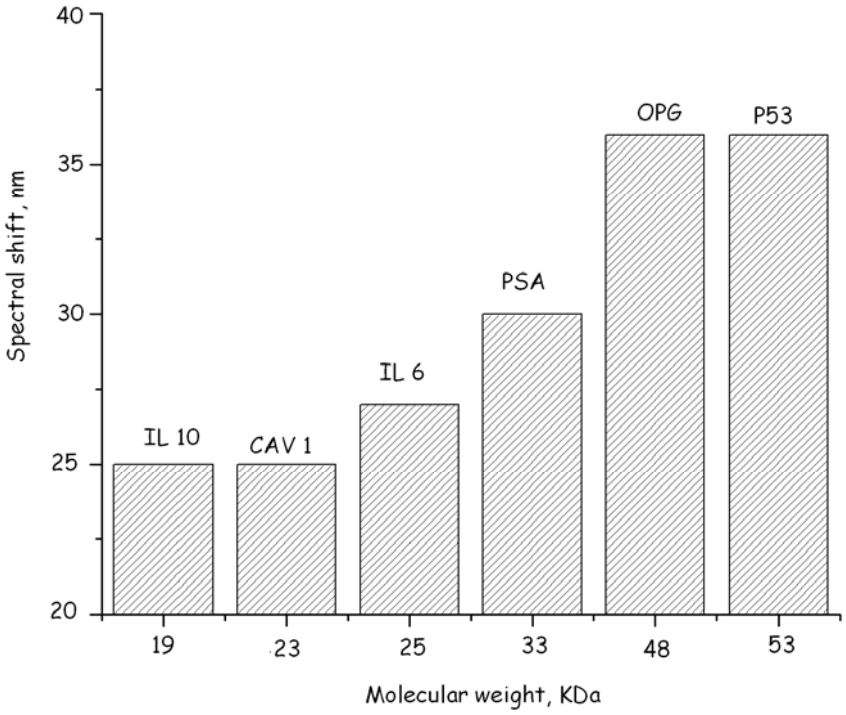

Figure 3.16 Dependence of the QD "blue" spectral shift on the molecular weight of the AB molecule, used for bioconjugation. The samples were deposited on silicon and dried at room temperatures for 11 days.

3.7.5. The influence of vacuum, argon, nitrogen and oxygen gases, increased moisture

In order to establish the possible influence of some environmental conditions on the shift, the two identical QD samples, pure and conjugated to CAV1 antibodies, were stored for 10-13 hours and measured hourly or every other hour. In order to speed up the shift development and shorten the experiment time to hours instead of days, the 50C storage temperature was applied (Figure 3.17). This temperature is not enough to denature the proteins [141-142], but it is good in elevating the shift development (Figure 3.14). The room controls were stored at room ambience, under constant 50C temperature, and the samples were maintained in the closed metallic boxes in constant gase/moisture/vacuum environments and under constant 50C temperature. The samples were taken out for the measurement which did not take longer than 10mins a day.

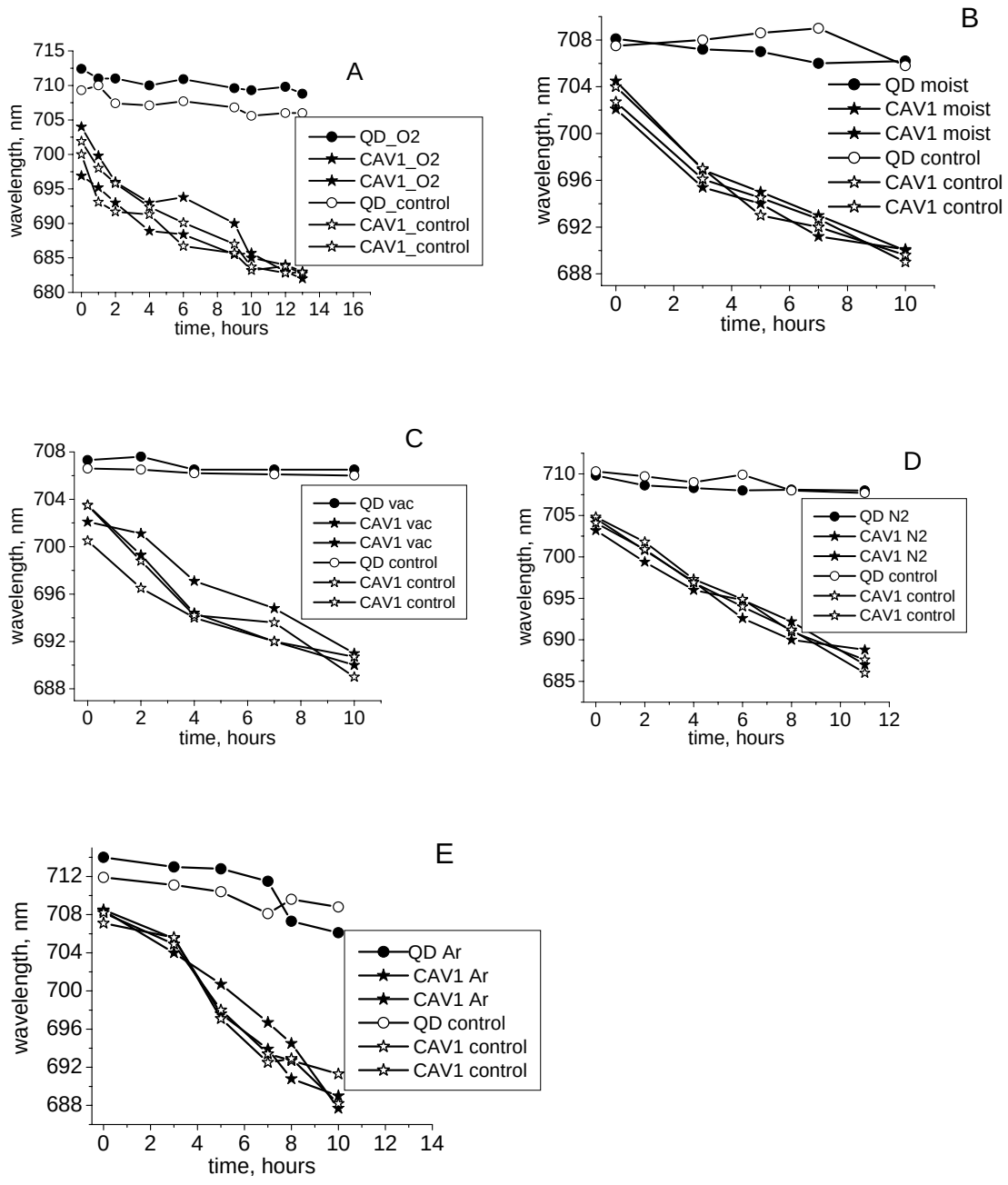

Figure 3.17 The blue shift of the conjugated to CAV1 sample (stars) in comparison to pure QD sample (rounds) after the 10-13 hours of storage under 50C. No noticeable influence of the following conditions (closed shapes) on the "blue" spectral shift was noticed in comparison to identical room ambience controls (open shapes): A – oxygen; B – increased moisture; C – vacuum; D – nitrogen; E – Argon.

The results are shown on Figure 3.17. It is clear, that no statistically important influence of the oxygen, moisture, argon, nitrogen and vacuum on the blue spectral shift was recorder. Nonconjugated, pure 705nm QDs don't seem to be affected as well. Based on these results, we conclude that chemical interaction of the QD-AB with gas molecules plays a negligible role in the observed effect. This will be further elaborated in the Discussion.

3.8. QD samples dried on the other substrates

Different substances were tried as substrates for drying of QD samples. In every case, the silicon sample served as a control. The initial hypothesis was such that more porous, less dense substrates may influence the spectral shift magnitude, as they influence the drying kinetics of the drops. The first experiment included four substrates – Si, SiC, Quartz and rubber. All samples were dried at room ambience for 12 days. The increased temperature was not used to enhance the shift, as rubber may melt. From the Figure 3.18 it is obvious that rubber sample had a very small (at most 4nm) blue shift in comparison to the three other substrates which developed a standard "blue" sift of the comparable magnitude.

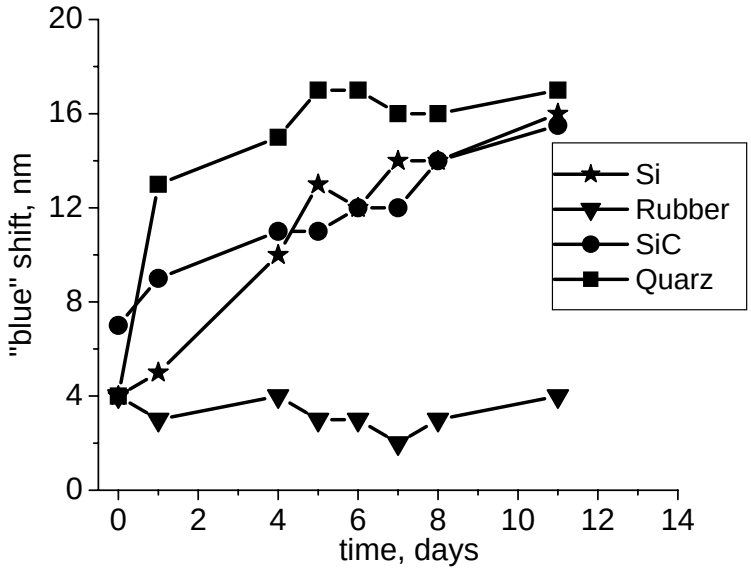

Figure 3.18. The relative "blue" shift of the 705nm QDs, bioconjugated to PSA antibodies, dried on the different substrates.

Similar results were obtained with the CMP pad which has a continuous porosity in its structure and is therefore similar to rubber (Figure 3.19). The conjugated to PSA 705nm QD sample, dried on silicon, developed approximately 28nm "blue" shift, while the CMP pad sample is just about 4-5nm in comparison to pure 705nm QD sample. The difference between the silicon and CMP samples is, therefore, about 23nm. These experiments allowed us to make a conclusion that the substrate's porosity, density and possibly other qualities have a noticeable effect on the shift magnitude. This data, along with the high and low temperature data, allows to draw a conclusion that the "blue" shift of bioconjugated QDs is probably caused by the particularities of the drying process. This will be further elaborated in the discussion section.

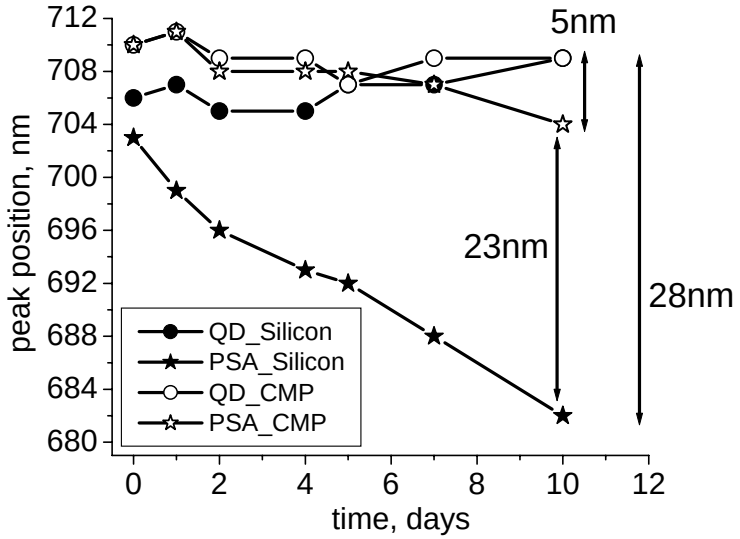

Figure 3.19. The blue shift of the conjugated to PSA sample (stars) in comparison to pure QD sample (rounds) after the 10 days of storage at room ambience. The silicon (closed shapes) conjugated sample performed a 23nm bigger "blue" shift in comparison to the rubber (open shapes) conjugated sample.

3.9. PL mapping measurements

In order to more carefully examine the "blue" shift pattern across the dried spot of QDs, the PL mapping technique was utilized. Silicon wafers with deposited QD spots were mounted on a computer controlled *X*-*Y* moving stage with a smallest step of 0.1 mm. The typical mapping area was 3 mm x 3 mm with a step of 0.25 mm. PL system, shown on the Figure 3.2, was employed to make the spectral maps.

PL spectral mapping technique has several important advantages over a "one spectra per spot" measurement, because it allows to:

1. track the spectral peak position inhomogenities across the dried spot;
2. obtain the lowest, the highest and the average peak positions for one spot;

3. compare the highest, the lowest and the average peak positions of bioconjugated spot vs the nonconjugated control, or the bioconjugated spot at a certain amount of time with the same spot at the different amount of time and/or after treatment;
4. helps to identify possible mechanism of the shift appearance, because of certain physical mechanisms (discussion);

The following advantages are illustrated in the Figure 3.20 and 3.21.

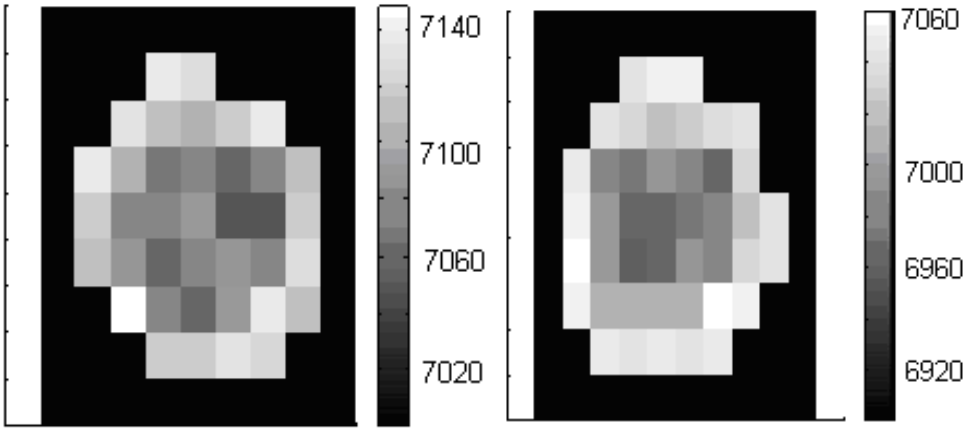

A B

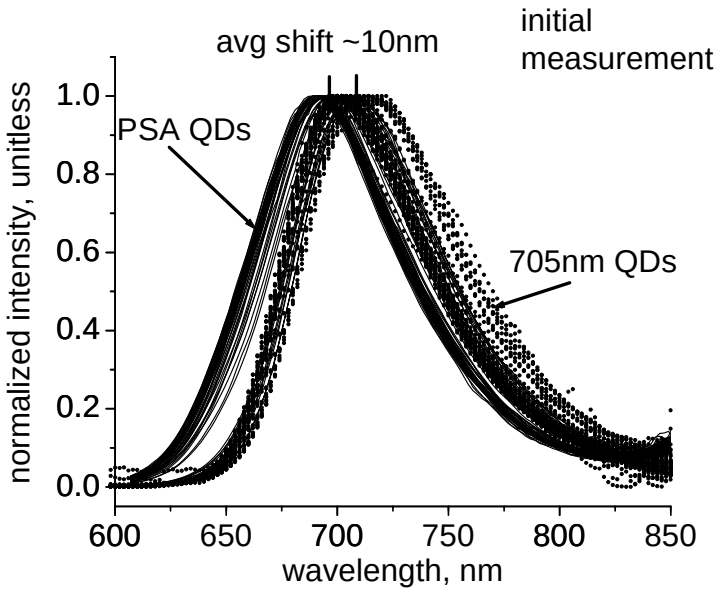

C

Figure 3.20. Initial spectral maps of the 705nm QDs, bioconjugated to PSA Antibody: A. peak position – pure QDs (in A); B. Peak position – bioconjugated QDs (in A); C. spectra of the maps, presented above. Each spectra corresponds to one spot on the spectral map.

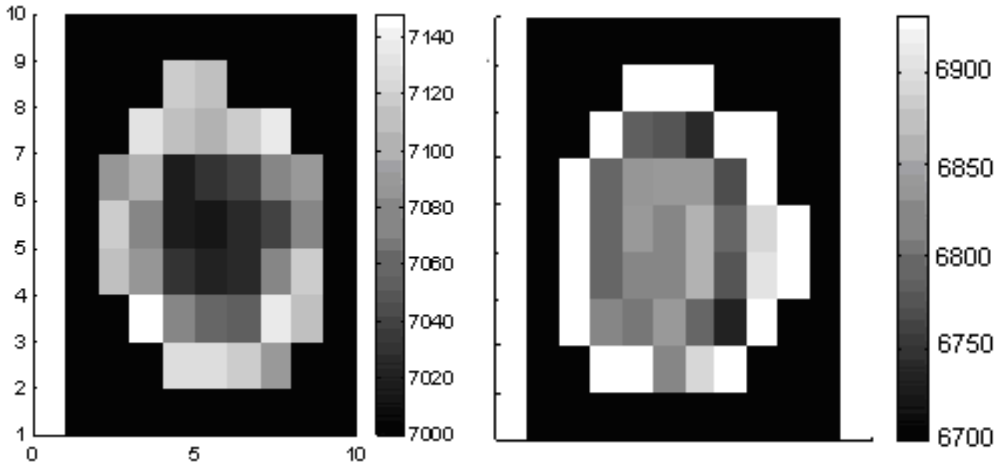

A B

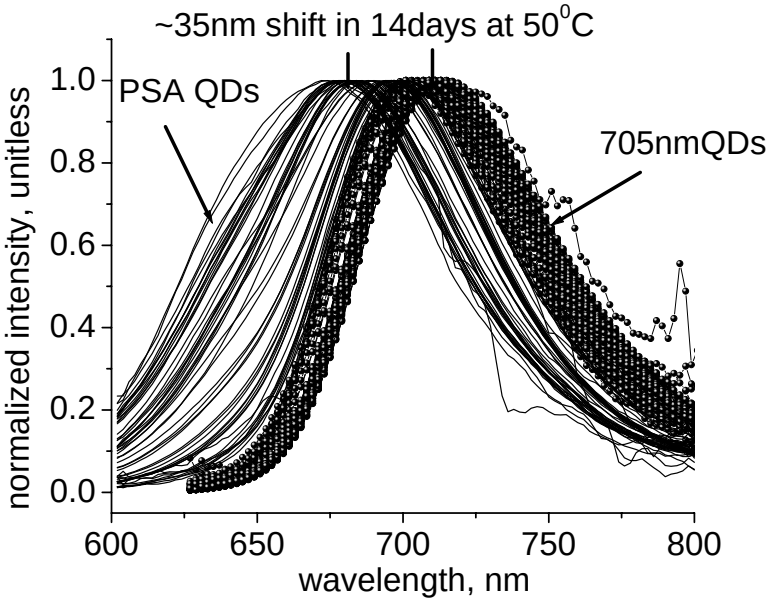

C

Figure 3.21. Spectral maps of the 705nm QDs, bioconjugated to PSA, stored for 14 days at 50C. : A. peak position – pure QDs (in A); B. Peak position – bioconjugated QDs (in A); C. spectra of the maps, presented above. Each spectra corresponds to one spot on the spectral map.

Figs 3.20 and 3.21 illustrate the spectral mapping of the same 705nm QD sample, bioconjugated to PSA Antibodies. As could be seen from the A and B parts of both

figures, the spectral peak positions differ from one spot to another even within the same sample (lighter spots correspond to higher PL intensity and more "red" PL peak positions). This spectral inhomogenity exists for both pure and conjugated QD, and the magnitude increases with time of storage. Having a spectral mapping data gives us an opportunity to calculate the average peak position for each spot, along with the spectral range. Therefore, such terms as an average spectral shift, or a maximum (minimum) spectral shift are becoming available. For instance, for the initial nonconjugated spot, the maximum high spectral position is 714nm, the lowest minimal is 702nm, therefore, the peak positions range for this spot is 702-714nm. The average peak position for the whole spot is calculated by simple summation of all peaks and dividing the sum on the number of spectra, which for this spot equals to 708nm. This number is in a good agreement with the one spectrum per spot measurement. The summary of the average spectral peak positions for each sample, along with their magnitudes, are shown in Table 3.3.

Table 3.3. The summary of the average spectral peak positions for each sample, along with their magnitudes.

	Minimal position, nm	Maximal position, nm	Average position, nm	The shift compared to pure QD sample, nm	The shift compared to initial conjugated sample, nm
Initial 705nm QD	702	714	708	N/A	N/A
Initial PSA QD	694	703	702	Max: 20 Average: 10	N/A
Stored 705nm QD	701	712	704	N/A	N/A
Stored PSA QD	673	700	681	Max: 40 Average: 35	Max:30 Average:25

From the Table 3.3 it is clear, that the spectroscopic peak position and the shift magnitudes may vary across the sample drastically, and the shift may almost double, depending on the site of measurement. This data is helpful in the spectral shift appearance explanation and may be used as an additional tool to enhance the spectral shift. This effect may be used in favor of early cancer detection, as will be showed in the next section.

3.9.1. The intensity measurements and the spectral mapping

It is possible to create the similar spectral maps for intensity, as it was shown for the spectral shift (Figures 3.20 and 3.21). Intensity, however, may vary up to 40%, depending on the optical set up, and it is very hard to conclude you have the same exact optical set up every time when you turn on the PL system. Therefore, after several preliminary experiments, it was decided to exclude the intensity from the spectral peak investigation. This is why all spectra shown before are normalized, i.e. divided on the highest peak position to convert the scale from actual intensity to 0-1. This technique also helps in visualizing and detecting the spectral shift, as it is hard to see any shift if for some spots the PL intensity is very low, and the other's – very high (Figure 3.22). For illustration purposes, in Figure 3.22 to the Figure 3.21 C the same spectra are shown, but the Figure 3.21 C they are normalized. It is much easier to compare and study the spectral shift when the plots are normalized, therefore, all figures in this work are shown in normalized format.

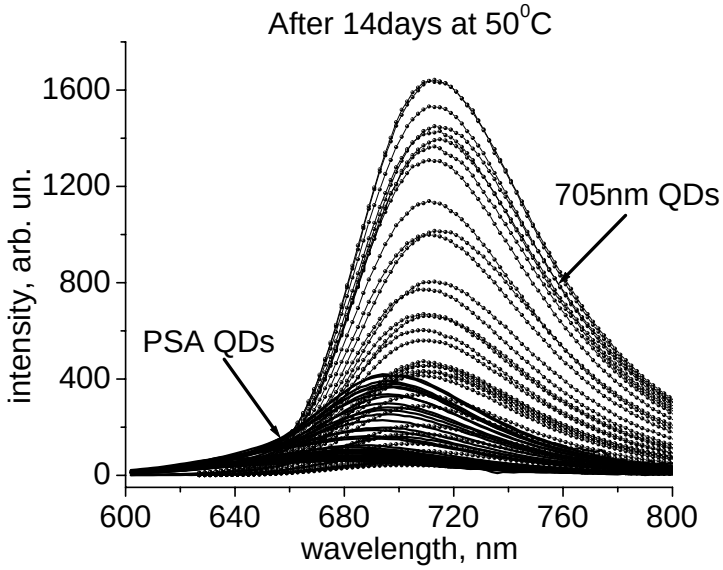

Figure 3.22. Non-normalized (raw) spectra of the 705nm QDs, conjugated to PSA Antibodies, stored for 14 days at 50C.

3.9.2. The "plate-shape" effect

As was mentioned in the previous section, both the peak position and the intensity are inhomogenious over a single dried QD spot. First we noticed that after sample deposition on the substrate and the initial 30 minutes of drying, the PL intensity shows a radial gradient profile with higher PL at the ring area at the spot periphery and reduced PL intensity in the central part. A similar PL intensity profile is maintained after 3 days of sample drying (fig 3.20A). Various regions, however, exhibit different rates of PL intensity reduction due to drying, as presented in figure 3.20C. Analysis of the PL spectra measured on different individual spots revealed a characteristic blue PL shift pattern across the sample which we assigned as a "plate-shape" pattern. This means that the blue spectral shift is more pronounced in the center of the spot and reduced in the periphery, as shown in figure 3.23B. Consistent with the data of the room temperature drying, we

also observed a strong enhancement of the PL shift which is quantified in figure 3.23D as two line scans of the PL peak position measured across the center of the sample. This effect is very pronounced on the conjugated dried samples and shows very small gradient from the center to periphery .

The observed "plate-shape" effect is important, because it provides a method to obtain a maximum blue spectral shift, concentrated in a central area of the deposited sample. Its origin and mechanism will be discussed below.

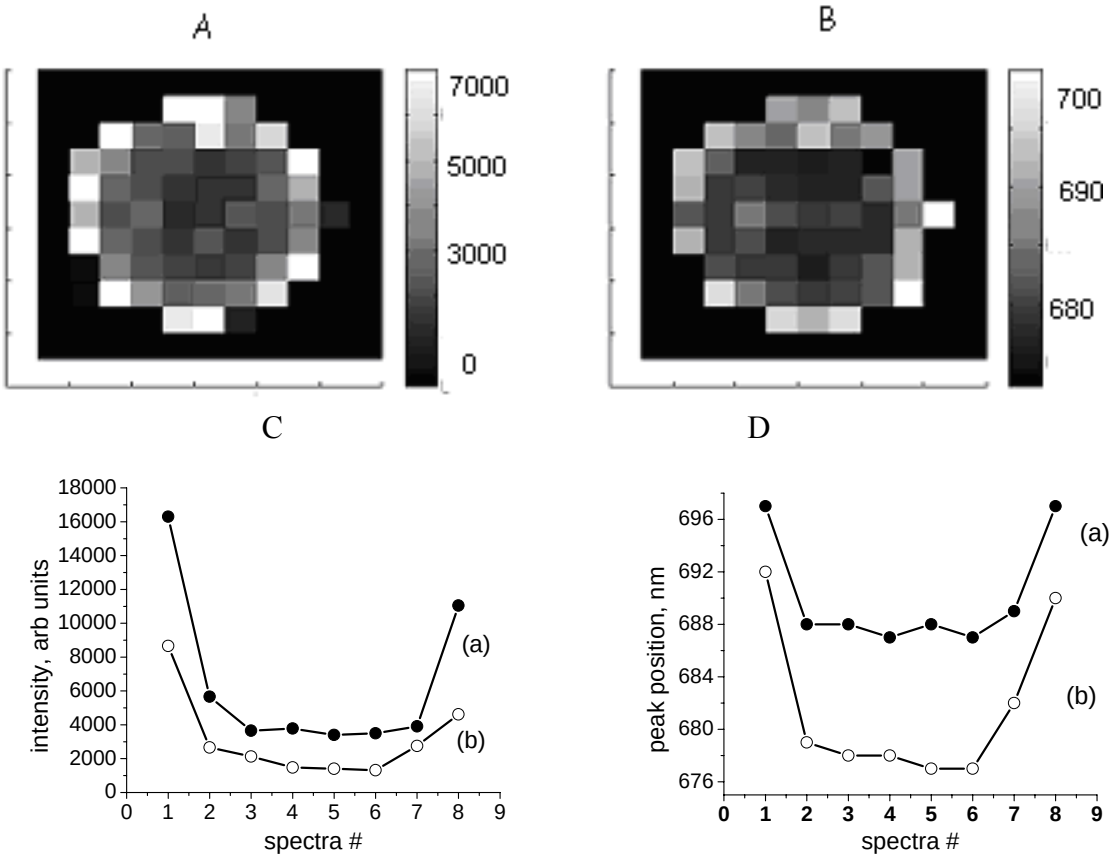

Figure 3.23. Photoluminescence (PL) maps of a conjugated to CAV1 antibodies sample stored for 3 days at 50^0C: A – PL intensity; B – PL peak position. The linescans of (a) 30 minuets dried and (b) stored for three days at 50C conjugated sample: C – PL intensity: D – PL peak position.

The non-conjugated control QD samples dried at identical conditions demonstrate the similar effect, however, it is less pronounced. Figure 3.24 illustrates the linescans of a

freshly dried (30mins at room ambience) and stored for 14days at 50C 705nm QD samples. The spectral maps of this exact sample is shown on the Figure 3.21.

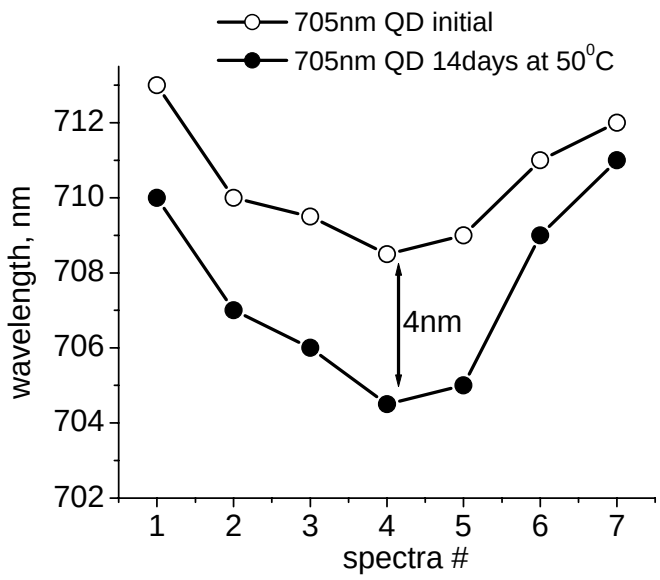

Figure 3.24. The linescans of 705nm pure QD sample, freshly dried (open shapes) and stored at 50C for 14 days (closed shapes).

The "blue" spectral shift of a pure QD sample shown in Figure 3.24, is in the range of 1 to 4nm and it takes a relatively long time to develop even such a small shift. In order to visually compare the linescans of pure 705nm QDs and bioconjugated QDs, they are shown together on one graph (Figure 3.25). Both samples were stored for 14days at 50C. Now it is obvious, that the blue shift of pure 705nm QDs is negligibly small in comparison to bioconjugated QDs.

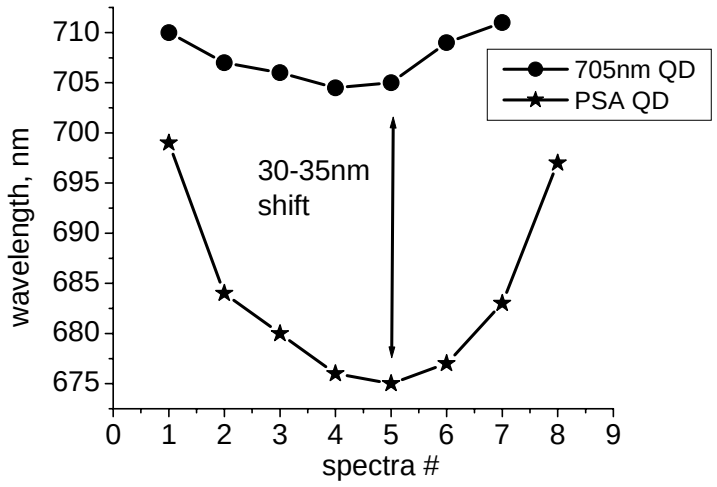

Figure 3.25. The linescans of pure 705nm QDs (rounds) and conjugated to PSA antibody 705nm QDs (stars) after 14 days of storage at 50C. The blue shift of a pure QD sample is negligibly small. The average blue shift is ~30-35nm.

The discovered "plate-shape" effect allows to maximize the measured "blue" spectral shift by selecting the central part of the dried sample. It also provides an understanding of a certain mechanisms of its appearance which will be discussed below. This effect is very repeatable and was observed on all the spectral maps, performed in the process of work. These samples included 705nm QDs, conjugated to mentioned above (table 3.2) antibodies, and dried on the silicon surfaces. The total number of spectral maps, analyzed in the scope of this work, is estimated to be at least 50 spectral mappings.

3.10. "Blue" spectral shift – discussion

In this section we address and discuss two major findings observed in the experimental part. The first is a blue PL spectral shift of the bio-conjugated QDs deposited on solid substrates compared to identical but non-conjugated QDs and the enhancement of this shift with drying time at elevated temperatures. The second is a

distribution of the blue shift across the dried spot as reveled by a spectroscopic PL mapping. It is obvious that various physical and chemical processes in the bulk, interface and surface of a quantum dot can modify the QD's excited states and exhibited in the PL band spectral shift. We will discuss two different mechanisms which can account for the blue PL shift in bio-conjugated QDs. The first mechanism is the elastic field applied to conjugated QDs caused by compressions that build up after drying the spot on a solid substrate. The second mechanism is a variation of the local electric field applied to the QD electronic levels caused by bioconjugation with charged or polar molecules that resulted in changes of the QD surface charge.

3.10.1 Compression stress

It is experimentally observed and theoretically explained that compression stress applied to II-VI compounds with embedded nano-scale objects having quantum confined wave functions provides a high-energy shift of the exciton transitions [143]. A typical example is represented by a super-lattice structure with quantum wells stressed due to lattice mismatch between the well and barrier materials, such as $ZnSeTe/ZnS_xSe_{1-x}$ quantum well/barrier structure. The objects in our study can be modeled as a similar system with stress originated at the interface between dried QD sample and a solid substrate, such as a silicon wafer. One can assume that stress is applied to the QDs caused by the change of the QD sample volume due to a slow drying process. Presumably the surface tension between the substrate and the drying sample is a driving force to generate this stress field.

Our experiments demonstrate a substantial role of elastic stress in the observed PL blue shift. One of critical results is a negligible PL shift in conjugated and non-conjugated QDs diluted in the buffer solution or immersed in the agarose gel. This must be compared to a substantial PL shift in identical bio-conjugated QDs dried on solid substrates at room or elevated temperatures. This mechanism is also consistent with the PL experiments on QDs dried on various substrates. The largest shift, up to 36 nm, is found on crystalline Si and SiC while a negligibly small shift on grids covered with amorphous carbon film, highly porous CMP pads and plain rubber substrate. These observations supply an evidence that the elastic properties of the substrate play an important role in determining the elastic stress applied to the QD. We suggest that compressive stress is applied to dried bio-conjugated QD samples at the interface between the substrate and a dried droplet (Figure 3.26 and 3.27). To support this hypothesis, TEM analysis of pure and conjugated 705nm QDs was conducted. It revealed an ellipsoid shape approximately 11x6 nm as illustrated in figures 3.3 and 3.4. Further TEM analyses of bioconjugated QDs are needed to confirm the absence of possible changes in the shape and/or size of bioconjugated QDs, caused by compression stress.

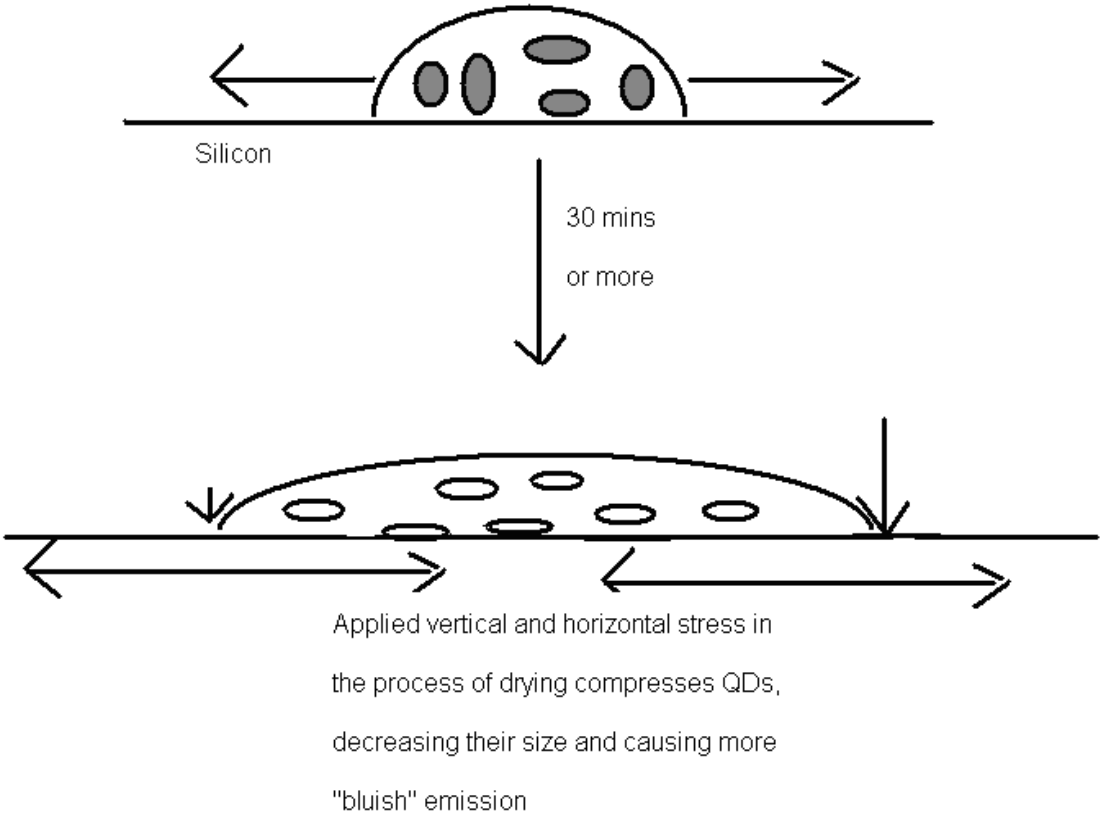

Figure 3.26. Schematic, explaining the rationale of a “blue” spectral shift.

A direct confirmation of the stress model was recently received using X-ray diffraction in similar QDs bioconjugated with IL-10 antigen and dried on silicon [122]. In this study a substantial increase of compression stress and corresponding compressive strain was directly measured. The increase of strain from 7.9 10^{-4} up to 9.6 10^{-3} was accompanied by 6 nm PL spectral shift. We conclude here that the stress effect is the most probable mechanism for the observed blue PL shift.

The second interesting feature we observed is a “plate-shape” profile of the PL shift in dried bioconjugated QDs (figures 3.23). According to our data, the largest PL shift is observed in the spot central part with gradual reduction toward the periphery. This

feature can be interpreted as a radial reduction of stress in dried sample from its center to the edge (Figure 3.27).

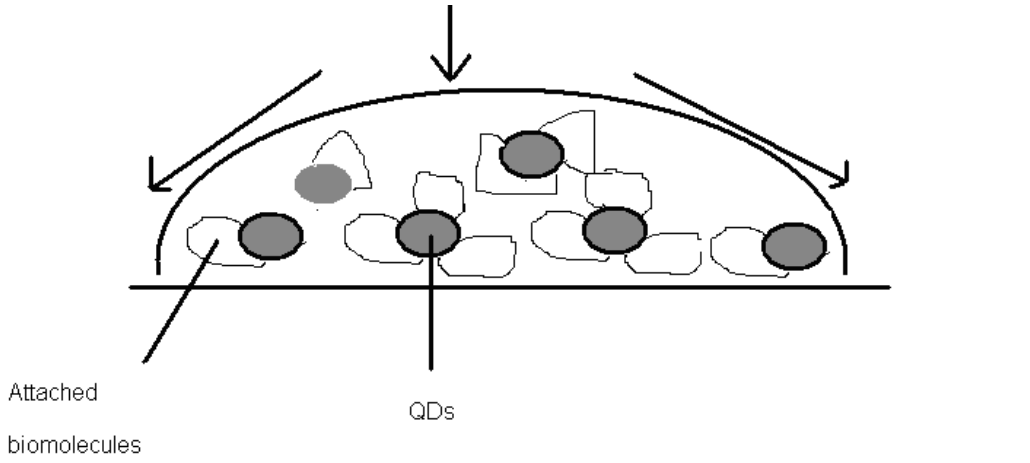

Figure 3.27. Schematic, explaining the “plate-shape” effect.

This would explain the similar but much smaller radial profile in a non-conjugated sample. On the other hand, another explanation is quite feasible. As we documented in figures 3.23A and 3.23C, the PL intensity also shows this type of non-homogeneity; the highest PL intensity is at the spot periphery and the smallest in the center. This intensity profile can be attributed to diffusion of the QDs to the sample periphery during drying. Taking into account that the bioconjugated sample contains some fraction of non-conjugated QDs we may suggest that the periphery region is enriched with non-conjugated QDs which is revealed as smaller blue PL shift at the

periphery. This process is explained by a higher mobility of non-conjugated QDs compared to bioconjugated, as confirmed by our gel electrophoreses study.

3.10.2. Electric field

We will also discuss a potential role of electric field variation on the observed PL shift. The influence of electric field was intensively studied and discussed in publications on quantum dots [144-145]. The following arguments, however, are generally in contradiction with the electric field model in our case, but we will discuss them as an alternative to the stress mechanism. We noticed that the appearance of the extra charge in the ensemble of non-oriented QDs is expected to lead to the "red" PL shift due to a quadratic Stark's effect [144]. At the same time, a compensation (reduction) of the initial charge which may be caused by bioconjugation and drying processes can explain that the PL shift will be in opposite, i.e. blue direction. Therefore, we would like to discuss this in more details. Electric field applied to the QDs can be changed due to conjugation with charged or polar biomolecules. We expect that this feature will be quite similar in the liquid and dried phase, which is in contrast with our data. Additionally, electric field should be affected by various gas environments due to photo-absorption of gas molecules [146]. However, our data on the sample drying in oxygen, nitrogen, argon and vacuum, are in a strong contrast with this process, i.e. PL spectral shift is independent of drying conditions performed at the same temperature. The PL shift is also not affected by light illumination and observed in a sample after storage in darkness. Finally, the electric field may be changed after drying due to evaporation of water molecules from the buffer solution and water ions attached directly to the bio-molecules. This, however, would

rather increase a net charge on the QD, and therefore lead to the "red" PL shift. All these considerations still can not rule out the electric field effect as an alternative to the stress mechanism.

3.10.3. Importance of the "blue" spectral shift phenomenon for early cancer detection

The described above "blue" spectral shift of bioconjugated QDs, is very interesting from the fundamental physics point of view, but also can be utilized in favor of the early cancer detection. In the scope of this research, four different QD types were analyzed, and six different types of Antibodies were used for bioconjugation. All of them performed a stable and repeatable "blue" spectral shift when dried on a solid substrate (silicon). The summary of QDs, antibodies, and the spectral shifts, along with the special remarks, are shown in the Table 3.4. As was already indicated earlier in this dissertation (Table 3.2), all the antibodies are important cancer biomarkers, and when bioconjugated, may be used in either in vitro detection assays (like ELISA), or for multiplexing analysis, as a part of the panel biomarkers. The last application is possible, because of the different magnitude of the spectral shift, conjugated to different antibodies (figures. 3.15 and 3.16).

As was already indicated, the author suggests to use the 705nm QDs, because after conjugation and drying they exhibit the largest "blue" spectral shift. This effect is attributed by the fact, that bigger QDs have more spaces for the antibody attachment, resulting in the increased elastic stress which is applied to such QDs. For instance, if the smaller ("blue") QDs with the size 3-6nm could attach 1-2 antibodies, the relatively big 705nm QDs with the size up to 12nm, could possibly attach 3 or more biomolecules. In

the scope of this research, about 80% of all effort was put into the 705nm QDs, conjugated to PSA antibodies. This is motivated by the fact, that PSA is an important (and the one reliable so far!) prostate cancer biomarker, which according to the recent data [33-39, 109-110] is present in a very small concentrations in a females body fluids, and such small amounts are on or below the standard method's of detection threshold. The final part of this work was dedicated to the utilization of the "blue" spectral shift effect for the early cancer detection via lowering the PSA ELISA threshold limit of detection.

Table 3.4. The summary of QDs, antibodies and spectral shifts of all experiments, performed in the scope of this work.

Antibodies	705 (CdTeSe)	655 (CdSe)	605 (CdSe)	580 (CdSe)
IL-10	Time-induced shift ~27nm during storage at room	Time-induced shift ~10nm during storage at room	Time-induced shift ~7nm during storage at room	~4nm initial shift; up to ~65nm T shift (190C, 12h); ~ 14nm room T aging shift (12 days)
PSA	Time-induced shift ~27nm during storage at room	No experiment	No experiment	No experiment
KLK19 (CAV1)	No experiment	~3nm initial shift; ~10nm T shift (190C, 12h); ~ 14nm room T aging shift (12 days)	No experiment	No experiment
P53	No experiment	~5nm initial shift; ~15nm temperature induced shift (190C, 12h); ~ 18nm room T aging shift (12 days)	No experiment	No experiment
IL-6	~4nm initial shift; ~20-25nm T induced shift (190C, 8h); ~21nm room T aging shift (12days);	No experiment	No experiment	No experiment
OPG	~10nm initial shift; ~36nm room T aging shift (12days); ~32-36nm temp induced shift (190C, 10h)	No experiment	No experiment	No experiment

3.11. Summary

Section 3 of this PhD dissertation describes and discuss the origin of a new "blue" or short-wavelength spectral shift of the photoluminescence spectrum in bioconjugated QDs, dried on the solid substrates. This shift starts to develop after the initial bioconjugated QD drop was dried on the solid substrate, and gradually increases with time, reaching the value of up to 40nm depending on the QD and biomolecule type after 12 days of room storage. Further storage causes a very slow increase and is therefore considered not effective. It must be pointed out that neither liquid, nor gel bioconjugated QD samples perform the "blue" spectral shift. It means, that the shift is most likely caused by the tensile and other forces, which influence the dried bioconjugated QDs.

The shift was found to be affected by the ambient temperature (high temperatures speed it up, low – slow down), and by the substrate type (more solid, crystal substrates, i.e. the Silicon chip, quartz cause bigger shifts than porous, more amorphous substrates, like rubber) , and it was not found to be influenced by different gases, vacuum and high moistures. This allows to conclude that the PL spectral shift is caused by elastic stress field applied to bio-conjugated QDs dried on solid substrates.

The inhomogenity of the spectral peak position and intensity across the dried spot was found with the PL spectroscopic mapping technique. This effect is called a "plate-shape effect" because more pronounced shifts and lower intensities are always located in the center of the dried spot. This effect was explained by the fact, that QDs, attaching more biomolecules, are heavier (bulkier) and therefore tend to settle in the center, causing increased stress forces and therefore increased spectral shift in that area. This effect is very interesting by itself, because it gives an opportunity to concentrate the biggest

spectral shift in the small area (or maximize it). The results, presented in this section, are useful from the fundamental science point of view, as well as may benefit the applied biomedical science. The last prospective is described in the next section of this work.

4. Modification of PSA ELISA technique with bioconjugated QDs for early cancer detection

4.1 Introduction

ELISA is a very sensitive molecular biology tool, allowing detection of most known biomarkers in nanomolar concentrations [97, 103]. However, as was shown in the section 2 of this work, the sensitivity of currently used PSA ELISA may not be low enough to detect it in women's biological fluids, presumably, because of this reason, for a long time it was not known, that female's organism also produces PSA and that this is not an exclusively "males" molecule [33-39]. PSA in female's organism was found to be elevated in may cancers, including breast, ovarian and uterine cancers, but even its elevated levels may be below 0.1-0.2 ng/ml, which makes this molecule virtually undetectable by standard PSA ELISA's. In effort to overcome this obstacle, standard "sandwich" PSA ELISA was modified with bioconjugated 705nm QDs as detection tags. This was expected to lower the method's limit of detection for the PSA molecule at least several times to allow the PSA detection in female's biological fluids. The results showed, that QD PSA ELISA may be much more sensitive than a standard "sandwich" PSA ELISA, employing optical density measurement. In this work, QD ELISA was able to detect 20 to 100 times smaller PSA concentrations, depending on the type of measurement. Despite the fact, that currently QD ELSIA is more labor and cost

consuming in comparison to a standard PSA ELISA, the author believes it may benefit both early cancer detection and forensic science.

4.2 ELISA QD procedure

Uncoated polystyrene ELISA wells were purchased from NUNC. All buffers in stock solutions (coating, stopping and washing) were purchased from Immunochemistry Technologies LLC. The scheme of the "sandwich"-ELISA method is shown in Fig. 4.1.

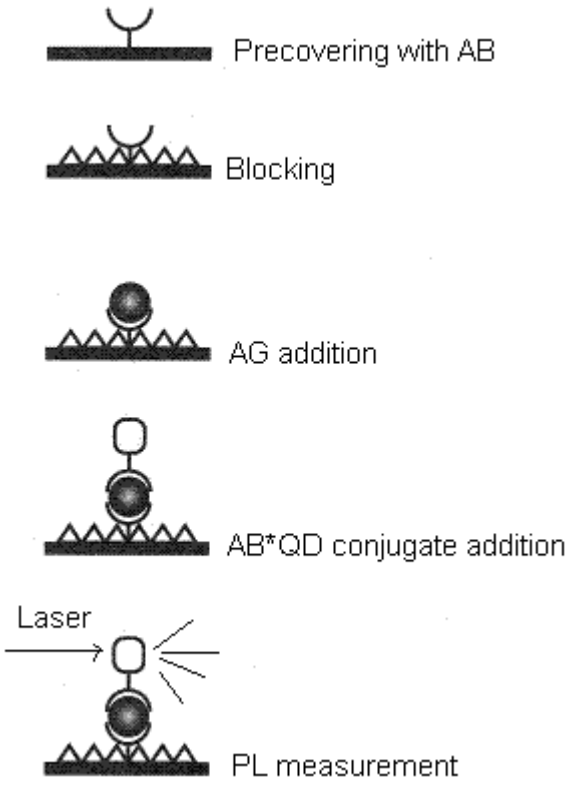

Figure 4.1. "Sandwich"-ELISA method schematic. Modified, original taken from [147]

Wells were coated with capture PSA AB by adding 50ul of 5X diluted coating buffer mixed with AB in concentration 7.5 µg/ml. The wells were then covered with

aluminum foil to prevent light exposure and incubated overnight at 4C. After that coated wells were washed 3 times with washing buffer and incubated with blocking buffer (300µl/well) at the same conditions to ensure blocking of all unused sites on the well, available for further protein bonding. This stage was also followed with 3-times washing, and immediately proceed to the AG solution/sera addition. 50 µl of PSA AG solution or sera was added to wells #2- 4 in the following concentrations: well #2 – 1.0ng/ml; well #3 – 0.1ng/ml; well #4 -0.01ng/ml; and well #5 was a control – pure PBS (pH 7.4) added, no AG. The wells were incubated in the same conditions for 12h, washed 3 times with washing buffer, and the 50 µl of 2X diluted AB*QD solution was added immediately, incubated for 12h at the same conditions, washed 3 times and let dry on air until the further spectroscopic analysis. The 2X dilution of a conjugate with QD incubation buffer was used in the effort to lower the expenses, associated with the experiment. QD*AB conjugated is very concentrated in ABs (the AB solution used for conjugation is 1mg/ml), therefore, they are taken in excess even if the conjugate is diluted 2 times. The 2X dilution of a conjugate with QD incubation buffer (obtained from Invitrogen Inc) was used in the effort to lower the expenses, associated with the experiment. QD*AB conjugated is very concentrated in ABs, therefore, they are taken in excess even if the conjugate is diluted 2 times (table 4.1):

Table 4.1: AB concentration estimate

Main stage of conjugation	Brief description	Estimated AB concentration and volume
Initial	Stock AB solution	1 mg/ml, 300µl [inv]
Mixed with QD	125ul of QD solution	0.7mg/ml, 425µl
Separation column	To get rid of unconjugated ABs; Assuming no AB losses	0.6mg/ml, 500µl
Final volume	Assuming 50% of AB losses	0.3mg/ml, 500µl
	Assuming 90% of AB losses	0.06mg/ml, 500µl, or 60ug/ml, 500µl
	Assuming 99% of AB losses	0.003mg/ml, 500µl or 3ug/ml, 500µl

Therefore, even assuming 99% of all AB losses we still have 3µg/ml AB solution, which diluted 2 times gives us 1.5µg/ml solution, which is 1000-100000 times more than target AG concentrations.

QD concentration could also be the limiting point in effort to use diluted conjugate for ELISA. The authors believe that it is possible to use even more diluted conjugate solution and the most suitable dilution should be determined empirically. The research in this direction is currently in progress.

4.3 ELISA standard procedure

In order to compare the QD PSA ELISA results with the established, commercially available ELISA, the regular ELISA was run with a tPSA detection kit supplied by CanAg (CanAg PSA EIA 340-10) [148]. The methods sensitivity, claimed by the vendor, is above 0.1 ng/ml. The detailed ELISA procedure could be found at the wendor's website [148]. The main stages are shown on Figure 4.2 . The method employs

a classic "sandwich" ELISA principle, where the optical detection is based on the Horseradish peroxidase (HRP) enzyme, cleaving the substrate, yields to the change of color [149]. An enzyme horseradish peroxidase (HRP), found in horseradish, is used extensively in molecular biology applications primarily for its ability to amplify a weak signal and increase detectability of a target molecule [150]. Commercial kit includes 96 precovered with the PSA coating Antibody wells, to which the samples (PSA antigens) are added, following with the addition of detecting PSA Antibody, conjugated to HRP. Next, the substrate is added, following with the stopping solution addition, and absorbance reading at 450nm (Figure 2.21). All samples were run in duplicates and the results are the averages of the two [148]. The reading was performed using a Synergy™ HT Multi-Mode Microplate Reader supplied by BioTek, at 450nm.

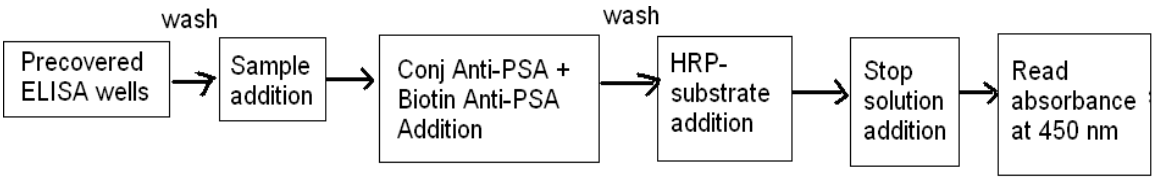

Figure 4.2. The brief schematic of the CanAg EIA procedure

After the final washing, ELISA wells were first filled with 50µl of PBS and the PL was measured on the Synergy™ HT Multi-Mode Microplate Reader (Biotek) with the 360 +/- 20nm excitation and 640 +/- 40nm emission filters. In order to ensure correct QD's PL reading by the microplate reader with the mentioned above filters, the pure QD dilutions were prepared and measured which resulted in a straight PL dependence on QD concentration [Fig 4.3A]. Because the working range is expected to be in the high QD

dilutions (0-10% of the original QD in the solution), this area is presented separately on the Figure 4.3B.

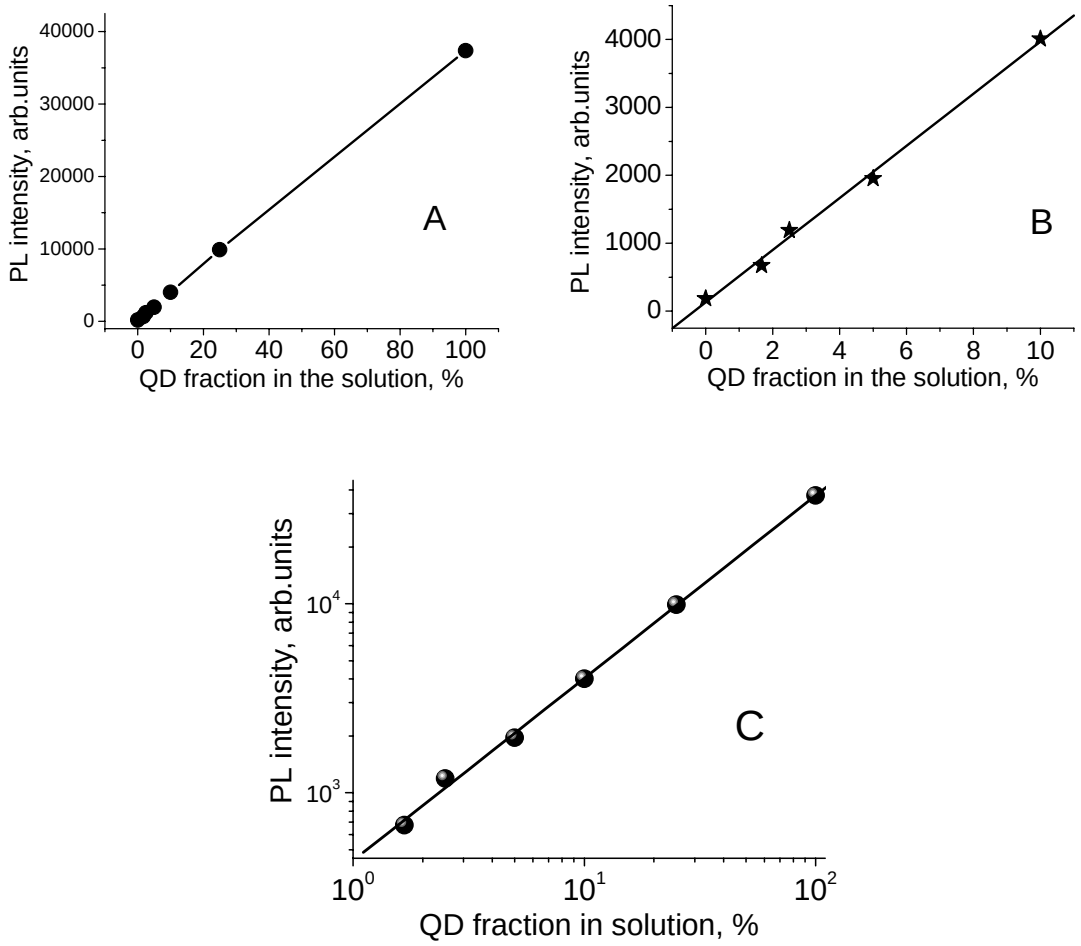

Figure 4.3. PL intensity dependence on the QD dilutions: A – the full range; B – high dilutions (QD portion is 0-10%); C – subfigure A in a double log scale.

After the mentioned above measurement, the PBS was disposed and the wells were dried in the room ambience for several hours, and ELISA wells were taken for the spectroscopic analysis.

4.4 Spectroscopic mappings of ELISA plates

After the final washing, ELISA wells were dried on air at room ambience for up to 120min, and then each well was stored in a clear plastic box in order to minimize contamination of the wells. In order to get rid of QDs which may occasionally stick to the walls of the well and have no relation to the "sandwich" formation, the bottom was separated from the walls with the clean heated blade which allowed a very accurate cut. Future spectroscopic measurements were conducted with ELISA bottoms only. We realize that this procedure is complicated and hardly to use as described in clinics, but we believe it is suitable for the main purposes of this work – to research a possibility to form a "sandwich" with conjugated QDs, using lower AG concentrations, and measure and research the spectral shift of bioconjugated QDs, involved into the "sandwich" formation. In order to accurately measure, record and analyze the PL signal across the samples, the spectroscopic mapping technique was employed.

Spectra, obtained from ELISA wells are shown in Figure 4.4. It is obvious that all wells, containing AG (B-D) provide the PL spectrum that matches to the QD luminescence. In contrast, the control well # 5 (E) without PSA AG shows negligible PL peak intensity in the range of 575-800nm, although was loaded with the same amount of conjugated QDs and undergone identical washing regime. Clearly, the AB*QD conjugate in the well # 5 did not form a "sandwich" because of the PSA AG absence, and was therefore washed out. We point out that a residual optical signal observed in the well #5, is a spectroscopic tail of 488nm laser line, scattered by the plastic well, and therefore has no relation to the QD luminescence. Well # 1 (A) was included in the experiment in order to compare the "blue" spectral shift of conjugated QDs in comparison to nonconjugated.

Well # 1 was precovered with primary AB in the same way all other wells were, but did not undergo any washing cycles, therefore, the PL spectral peak position of nonconjugated QDs, dried on the plastic ELISA well, could be taken from the well #1.

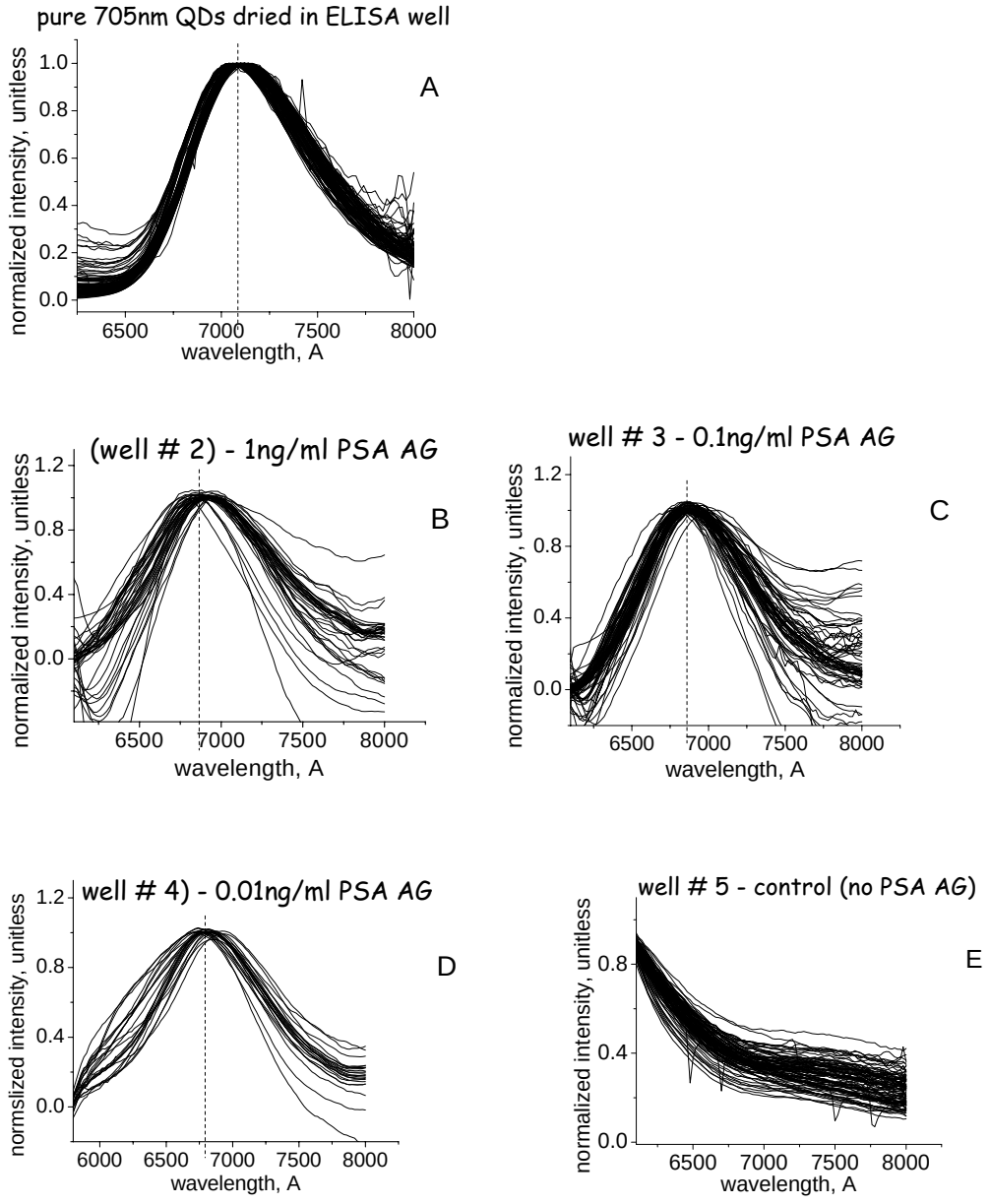

Figure 4.4. Normalized PL spectra measured on ELISA wells # 1-5 (A-E, respectively). Dashed lines correspond to the average PL peak positions.

PL spectra, obtained in the process of the spectral mapping of ELISA wells, were compared with the spectra, obtained from identical batch of nonconjugated and conjugated QDs, dried on the silicon substrate. The results are shown on Figure 4.5. From Figures 4.5 and 4.6 it is evident, that conjugated QDs show a "blue" spectral shift, and its numerical values (13-37nm) and standard deviations will be described below.

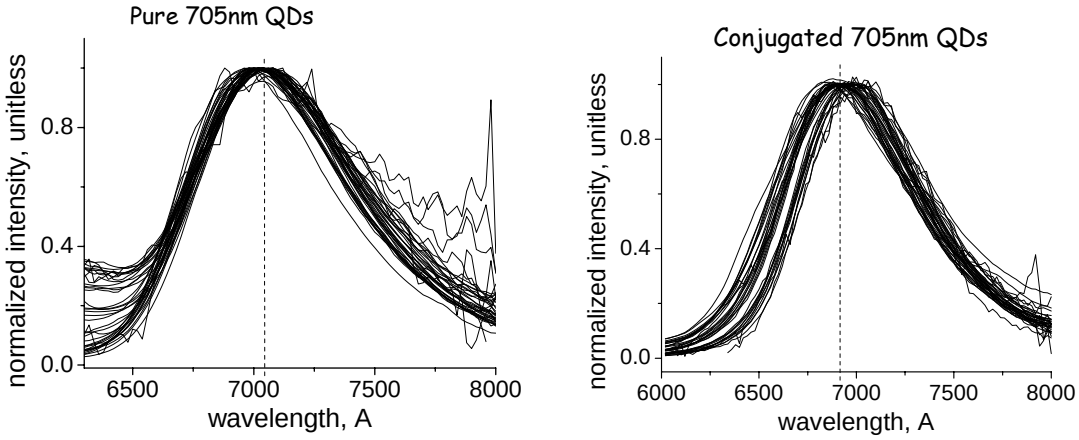

A B

Figure 4.5. Normalized PL spectra from the spectroscopic mapping on non-conjugated 705nm QDs (A) and bio-conjugated with PSA antibody 705nm QDs (B), dried on a silicon substrate. Dashed lines correspond to the PL peak positions averaged across the sample area**.**

4.5. Spectral mapping and "blue" spectral shifts

All ELISA wells, which contained PSA AG, have a PL signal from the conjugated QDs, involved into the "sandwich" formation. It was obvious that PL intensity and PL peak spectral position are not uniform across the well area, and this nonuniformity was tracked with the PL spectroscopic mapping procedure. The spectral maps of the #2-4 ELISA wells are shown in Figure 4.6. The spectral map of the well #1 is not informative (because nonconjugated QDs were simply dried in the well), while the

well #5 does not exhibit a measurable PL intensity from the 705nm QDs. The well #4 (with the smallest AG concentration of 0.01 ng/ml) shows the QD PL peaks mostly at the periphery area, the wells # 2 and #3 at the centers, and the well # 3 all over the sample. This inhomogeneity can be attributed to a non-uniform capture of the PSA AG molecules by the capturing antibodies, when forming a sandwich structure.

In this experiment using the PL spectral mapping technique we observed a new effect, as a dependence of the "blue" spectral shift versus the AG concentration. In Figure 4.7 the average peak positions, along with the PL shift are presented. The average PL peak position is shifted towards the "blue" (short wavelength) region for wells with decreased AG concentrations, and its standard deviations are also increasing for wells with decreased AG concentrations. The average peak positions, along with their standard deviations, are as follows in wells # 1-4: 7080 (+-10); 6900 (+-32); 6870 (+-40); 6810 (+-52). Additional research in the effort to confirm this interesting effect is currently in progress.

A

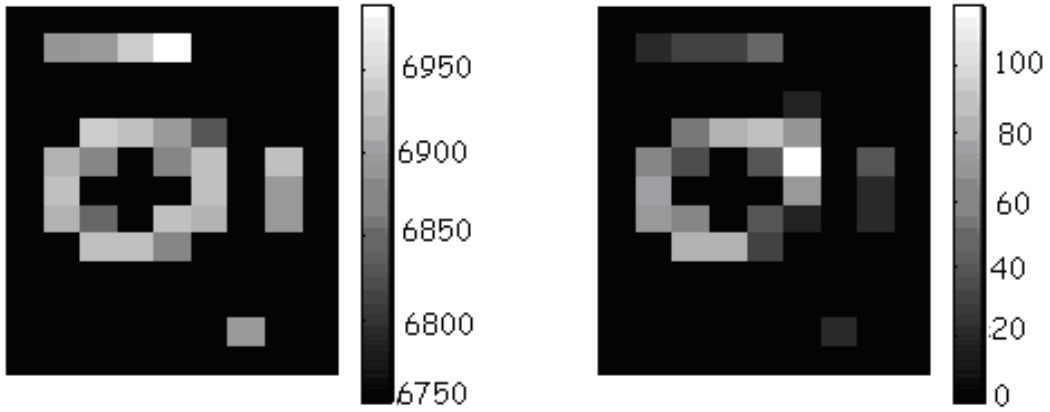

B

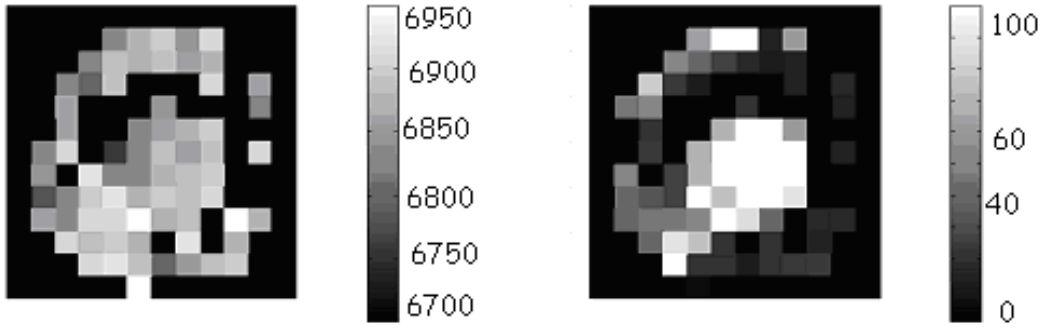

C

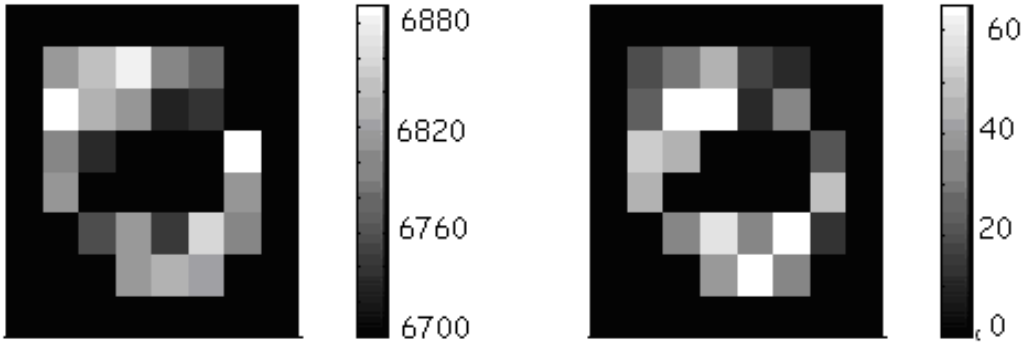

Figure 4.6 Spectral maps of the ELISA wells # 2-4 (A-C, respectively). Left column – peak positions [A], right column – corresponding intensities [arb units].

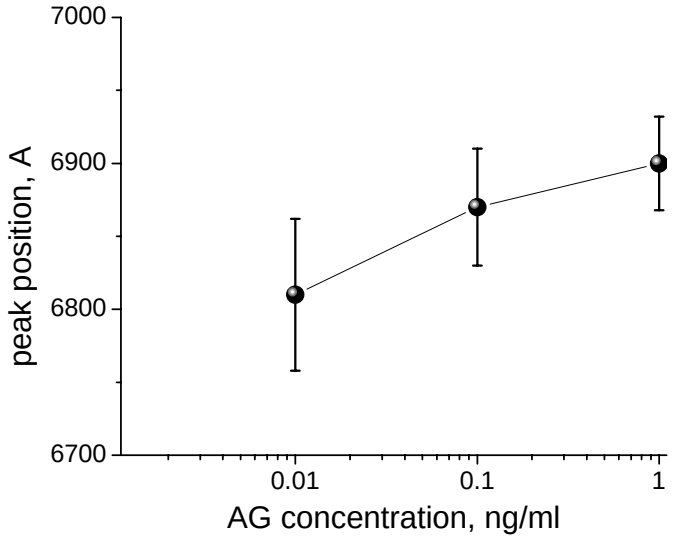

Figure 4.7. Average spectroscopic peak (close to 705nm) positions and their standard deviations of the ELISA wells with corresponding AG concentrations, used in the experiment.

To identify if the "blue" spectral shift vs the PSA dependence is statistically significant, the two-tailored t-test was performed with the following hypotheses:

H_0: The slope of the regression line is equal to zero.

H_a: The slope of the regression line is *not* equal to zero.

For this analysis, the significance level is 0.05. We get the slope (b_1) and the standard error (SE) from the simple excel calculations, for the following set of data:

$$b_1 = (-6.75676) \qquad SE = 0.3161$$

We compute the degrees of freedom and the t-score test statistic, using the following equations.

$$DF = n - 2 = 3 - 2 = 1$$

$$t = b_1/SE = 6.75676/0.3161 = 18.3315$$

Based on the t-score test statistic and the degrees of freedom, we determine the P-value. The P-value is the probability that a t-score having 1 degree of freedom is more extreme than 18.3315. Since this is a two-tailed test, "more extreme" means greater than 18.3315 or less than -18.3315. We use the t Distribution Calculator to find P(t > 18.3315) = 0.0173. Therefore, the P-value is 0.0173 + 0.0173 or 0.0347.

Interpret results**.**

Since the P-value (0.0347) is less than the significance level (0.05), we cannot accept the null hypothesis. It means that the slope of the regression line is NOT equal to zero, and the inverse relationship of the “blue” spectral shift VS the PSA concentration IS statistically significant.

4.6. “Plate-shape” effect and residual nonconjugated QDs

As was described in our works [119-123], the authors found a so-called “plate-shape” effect on the QD samples dried on the solid surface (silicon). This effect was especially pronounced for conjugated samples. It means the different intensity and peak profiles across the area of a dried sample, with both intensity and peak positions being elevated in the periphery region and decreased in the center. The typical “plate-shape” effect for 705nm QD, conjugated to PSA AB, dried on the clear silicon chip, is shown on the Figure 4.8.

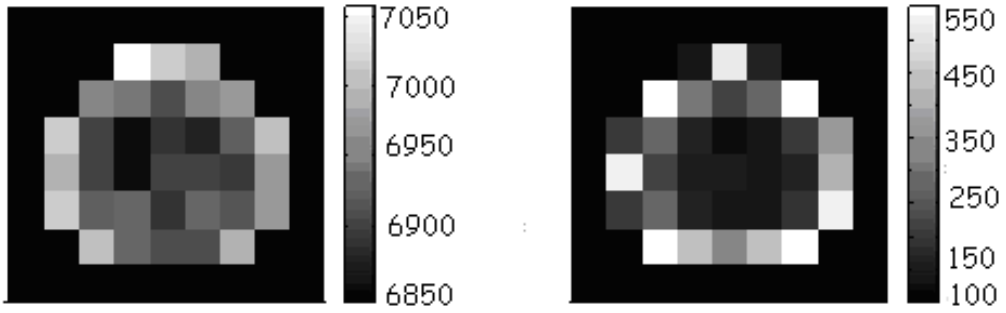

A B

Figure 4.8. Spectroscopic peak position (A) and PL intensity (B) maps of 705nm QD sample, conjugated to PSA AB, dried on a clear silicon chip. Lighter areas correspond to elevated intensity/peak position values. Peak positions in angstroms, intensity in arb. units.

The authors attributed this effect to either increased stress applied to QDs in the center, which may change their shape/size, or to the increased concentration of nonconjugated QDs in the periphery region, which is caused by their increased mobility because of their small size in comparison to heavy and bulky conjugated QDs. In the effort to approve one of this hypothesis, an average peak position values along with their ranges were analyzed for ELISA wells #2-4 and conjugated sample, presented in Figure 4.6. The results are shown in the Table 4.2.

Table 4.2. Average peak positions for different conjugated samples and their magnitudes.

Sample	Average PL peak position, nm	PL peak range, nm
Conj dried on Si	694	682-706
Well #2	690	687-693
Well#3	687	675-694
Well#4	681	671-691

From the Table 4.2 it is clear that the upper limit of the sample, dried on the silicon surface, is 11-13nm elevated in comparison to any of the ELISA wells. And what is even more important, is that the upper limit of the dried on Si chip conjugated sample

surely lies on the very periphery (Figure 4.8A) and corresponds to the wavelength of emission of pure, 705nm QD sample, deposited on the silicon surface [119-123]. This helps to draw a conclusion that because only conjugated QDs take part in the ELISA "sandwich" formation, nonconjugated QDs, small fraction of which is always present in a conjugate, are washed away and don't interfere with the PL from conjugated QDs. However, when a small droplet of conjugate is deposited on silicon, the nonconjugated fraction of QDs contributes to the PL signal. This observation is important, because allows to separate and eliminate the residual nonconjugation QDs, and their PL signal which may interfere with conjugated QDs and cause false positive results. It is also important, because serves as an additional proof that the PL, coming from ELISA wells, is the PL of conjugated 705nm QDs, involved into the "sandwich" formation, and not the residual QDs, got stuck into the plastic.

4.7. QD ELISA is more sensitive than the regular tPSA ELISA

The regular, commercially available and QD modified PSA ELISA's were performed on the same set of samples, which included four female serum samples with known tPSA concentrations (1.82, 0.66, 0.093 and 0.013 ng/ml) and four PSA AG solutions in PBS (0.1, 0.01, 0.005 and 0.001 ng/ml). As for the serum samples, the two lowest concentrations were prepared by dilutions of other samples with greater concentrations. The samples in commercially available ELISA were run in duplicates, and the samples in QD ELISA were run in just one sample each. This was done in order to minimize the cost of the experiment, which is at the moment high, especially for the

QD ELISA. The main goal of the experiment was to determine if the QD ELISA can go lower than the current threshold (0.1ng/ml), and if yes, how low can it possibly go.

On Fig.4.9, the results of commercial ELISA is shown. As expected, among the plasma samples 0.013 and 0.093 ng/ml were undetectable (Fig 4.9A), as well as the whole range of the AG dilutions in PBS (Fig 4.9B). According to our results, 0.1ng/ml and below were undetectable in both the serum and AG dilutions samples which is in a good agreement with the claimed method threshold [148].

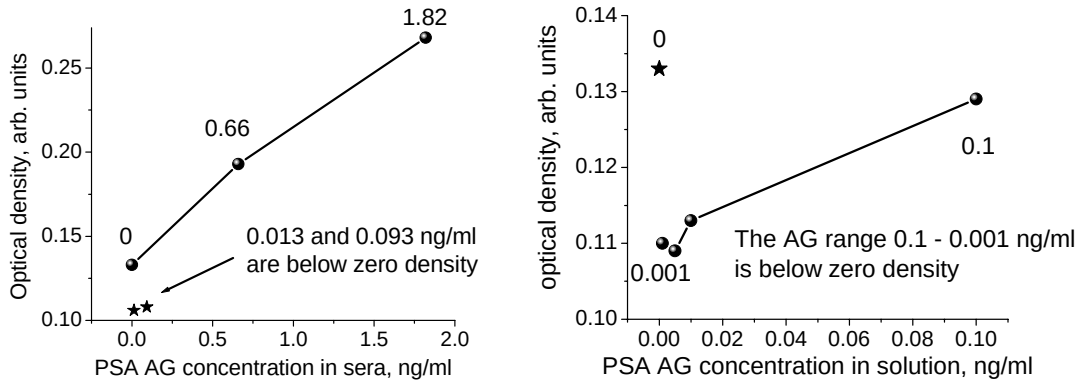

A B

Figure 4.9 CanAg PSA AG detection limits: A – in sera samples; B – in AG solution in PBS.

Different results, however, were obtained with the QD ELISA using same set of samples (Figure 4.10). As obvious from the Pic 4.10A, all plasma samples were successfully detected, including the 0.013 and 0.093 ng/ml dilutions. As for the AG in PBS solutions, the the lowest 0.001ng/ml concentration was almost at zero level (Figure 4.10C), so it is considered undetectable, however, the next dilution – 0.005ng/ml, was detected (Figure 4.10B) and therefore may be considered as a new threshold for the PSA AG detection with the QD ELISA method.

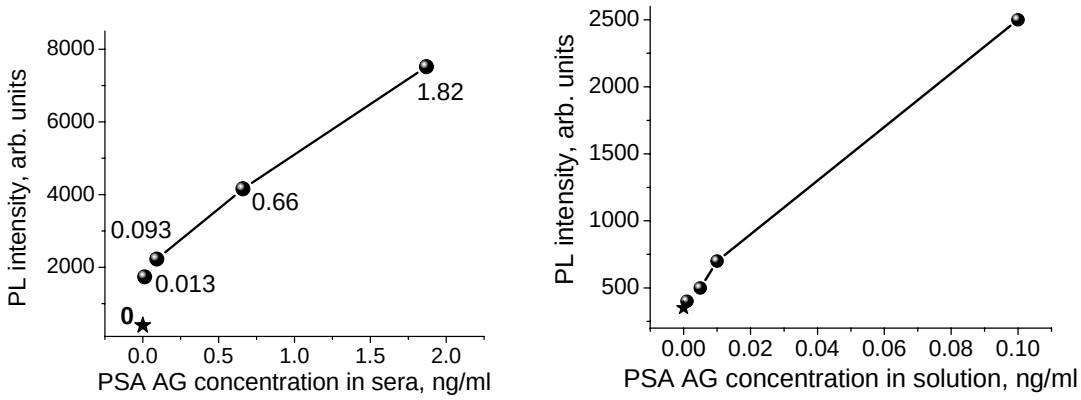

A B

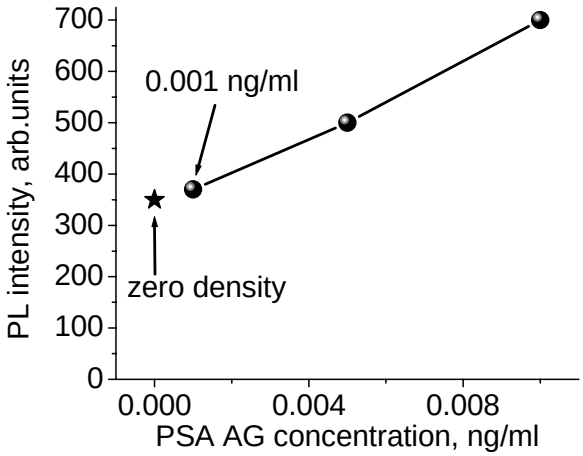

C

Figure 4.10. QD ELISA detection limits: A – in sera samples; B – in AG solution in PBS; C – the range 0 – 0.01 ng/ml for the AG solution in PBS, to better see the lowest (0.001 ng/ml) concentration.

So, based on the mentioned above results, the authors conclude that ELISA, which utilizes bioconjugated QDs as detection markers is at least 20 times more sensitive that the currently available commercial ELISA (0.005 vs 0.1 ng/ml). This is attributed to a very efficient mechanism of QD emission, so that just a relatively small amount of QDs, which are engaged into the sandwich formation, is enough to create detectable PL signal.

4.8. Spectroscopic measurements of ELISA wells – pure AG solution

After the liquid PL measurements on the microplate reader, the PBS was disposed, wells were dried and used for the spectroscopic analysis. Initial mapping was performed (next day), and it was repeated on the 5th day. Between the measurements, the wells were stored in a clear plastic boxes at the room temperature (RT). An attempt was made to map the wells later, but it was a substantial intensity drop, probably because of the sandwich gradual denaturation, and therefore, the further mappings of these wells was impossible.

The actual spectral PL maps at the lowest concentration of 0.001ng/ml for the antigen solution (subfigure A) and 0.013 ng/ml for serum sample (subfigure B,) after 5 days of storage are shown on Figure 4.11. These pictures show the distribution of the PL peak positions and intensities across the ELISA wells. The lowest concentrations are shown, because they generate the largest spectral shift. Note that non-conjugated samples exhibit the PL peak position in the range of 702 – 706 nm, therefore the samples dried in ELISA wells (Fig 4.11) show a substantial average spectral shift ~ 35 nm with the PL maximum in the range 655-687 nm.

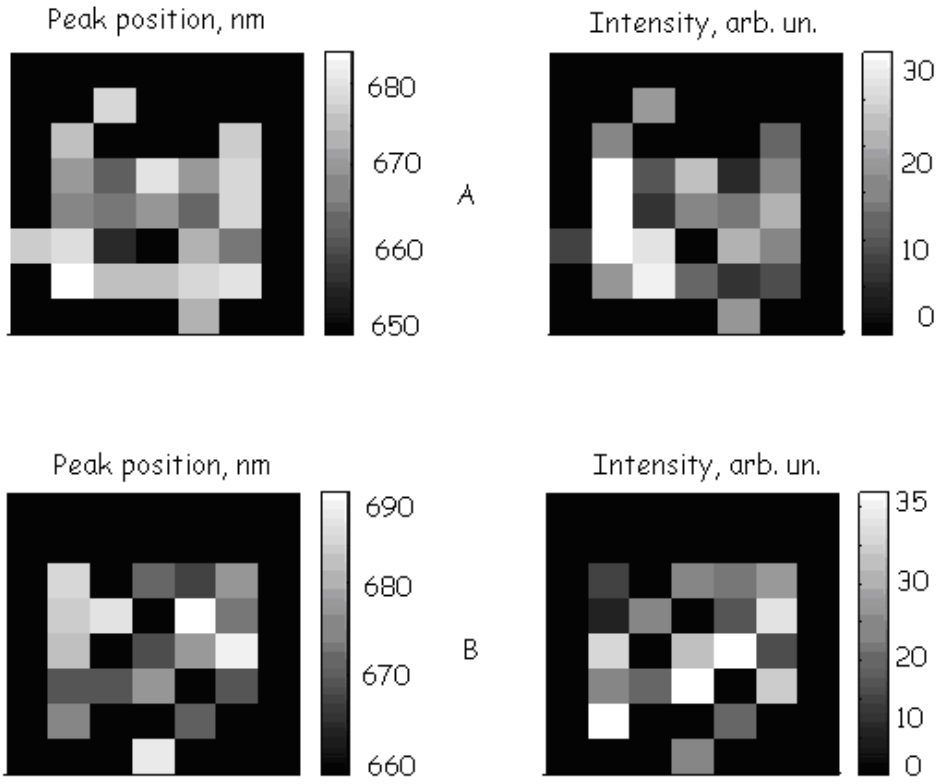

Figure 4.11. The actual spectral maps for the lowest concentrations of the pure Antigen solution (A, 0.001 ng/ml), and the serum sample (B, 0.013 ng/ml) after 5 days of room storage. Peak position (nm) – left column, intensity (arb. Un.) – right column.

The results of the spectral mappings are shown on figures 4.12 (pure PSA Ag solution) and 4.13 (female serum samples, analyzed for the presence of PSA Ag). Subfigures A show comparison of the average peak positions across the wells during the initial and after 5 days of storage treatment, while the subfigures B shows the same dynamics for the sample's intensity. Subfigures C depicts the difference between the highest and lowest concentrations of Antigen and its relation to the spectral shift – after 5 days of storage with the spectral peak position around 703nm. Initial data has the similar, just the less pronounced, trend, and therefore is not shown.

The standard deviation for Figures 4.12A and 4.13A (spectral peak position) did not exceed 1% (+/- 7nm) for the initial measurement, and did not exceed 2% (+/- 14nm) for the 5 days measurement.

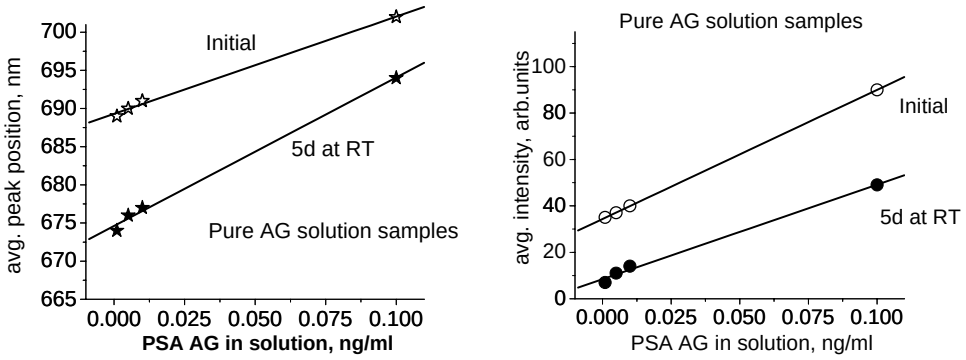

A B

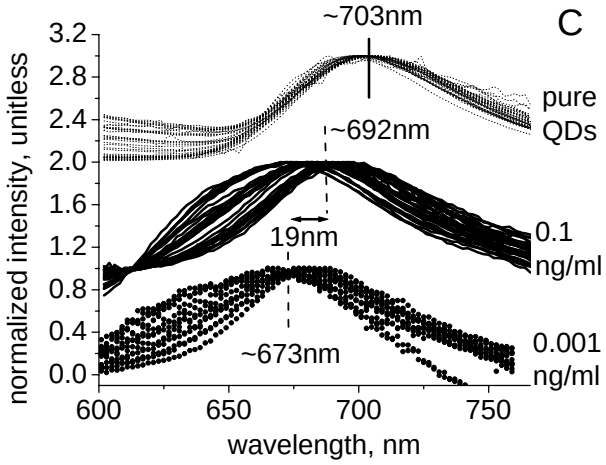

Figure 4.12. QD ELISA of the pure PSA Ag solution samples: A – comparison of the spectral peak positions (initial and after 5days of room storage); B - comparison of the intensities (initial and after 5days of room storage); C – spectra of the highest (0.1ng/ml) and lowest (0.001ng/ml) PSA Ag concentrations after 5 days of room storage, compared to pure 705nm QDs.

4.9. Spectroscopic measurements of ELISA wells – serum samples

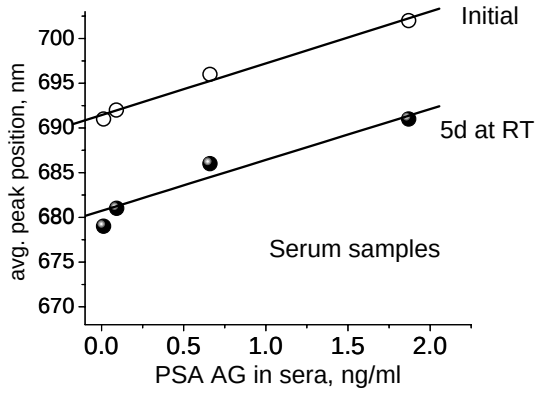

A

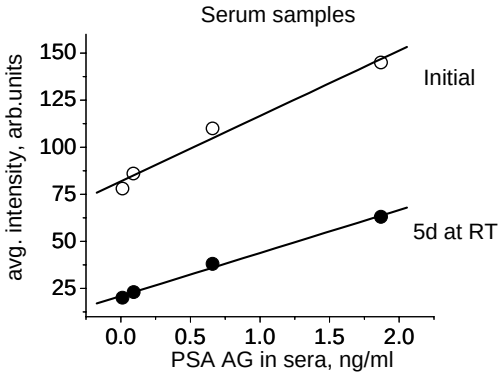

B

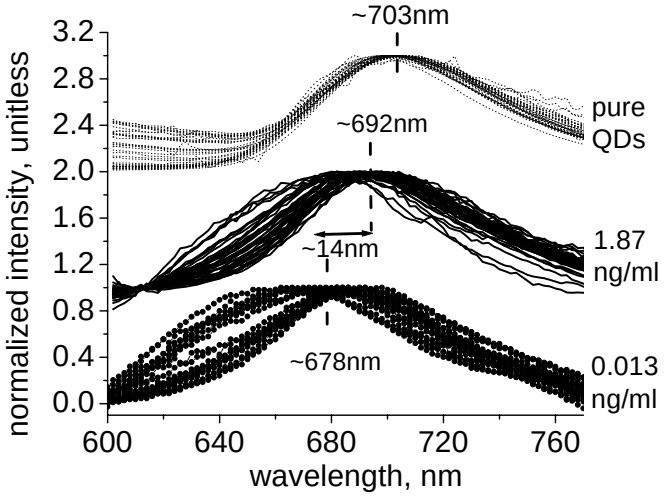

C

Figure 4.13. QD ELISA of female serum samples: A – comparison of the spectral peak positions (initial and after 5days of room storage); B - comparison of the intensities (initial and after 5days of room storage); C – spectra of the highest (1.87ng/ml) and lowest (0.013ng/ml) PSA Ag concentrations after 5 days of room storage.

Table 4.3 A and B summarizes the most important numbers for the spectral shift and intensity changes between the different samples, AG concentrations and the time of storage. The most important findings will be discussed below.

Table 4.3 The most important numbers for the spectral shift and intensity changes between the different samples, AG concentrations and the time of storage.
A

	Pure PSA AG solution INITIAL				Female serum samples INITIAL			
Conc AG, ng/ml	0.001	0.005	0.01	0.1	0.013	0.091	0.66	1.87
Avg init peak pos nm	689	690	691	702	691	692	696	702
Peak ranges	685-702	685-703	687-705	700-705	684-703	686-703	691-703	699-705
Avg init intens a.u.	35	37	40	90	78	86	110	145
Intens ranges	8-57	10-66	9-69	17-126	43-111	57-99	71-148	92-188

B

	Pure PSA AG solution 5 DAYS AT ROOM T				Female serum samples 5 DAYS AT ROOM T			
Conc AG, ng/ml	0.001	0.005	0.01	0.1	0.013	0.091	0.66	1.87
Avg init peak pos nm	674	676	677	694	678	681	686	692
Peak ranges	665-683	671-688	672-687	674-699	659-694	670-690	674-694	679-700
Avg init intens a.u.	7	11	14	49	20	23	38	63
Intens ranges	0-29	0-31	2-43	5-77	0-39	1-41	7-56	11-89

4.10. Pure PSA AG solution and female serum samples ELISA results discussion

When the described above experiment was planned, the two main goals or set of questions were asked:

This project targeted two main objectives

1. How sensitive is QD ELISA compared to the commercially available ELISA test used for PSA detection; and

2. what is a dependence between the “blue” spectral shift of bioconjugated QDs and the PSA AG concentration.

The results clearly show the following.

705nm QD ELISA can detect the PSA AG concentrations which are undetectable with commercial CanAg ELISA. The manifested and observed threshold of the commercial ELISA used was about 0.5ng/ml PSA AG, and QD ELISA was able to detect as low, as 0.001ng/ml of PSA AG in the solution, and this amount may not be the lowest possible. The sensitivity was even increased with the spectroscopic detection via the mapping technique in comparison to the microplate reader detection, as in the microplate reader the 0.001 ng/ml was very close to the zero photoluminescence intensity (Figure 4.10C), while the spectroscopic mapping technique was able to detect a pretty good red PL (Figure 4.12B). Based on this results, one may conclude that QD ELISA is ~100 more sensitive, than commercial ELISA, if the spectroscopic mapping technique was used. If the microplate reader was used, it is 20 more sensitive.

The "blue" spectra shift range is inversely dependent on the PSA AG (detection molecule) concentration. It means, that for the PSA AG ranges used (0.001-2 ng/ml) the "blue" shift was observed to be more pronounced for higher AG concentrations. This effect was observed for both serum and pure antigen solution samples. This effect was not checked on other Antigens or biomolecules, and if confirmed, may be the reliable additional (together with the intensity) feature, allowing the careful biomolecules detection/quantitation in extremely low concentrations. In future, two detection techniques – the PL intensity and the spectral shift assessment – may be used for ELISA, allowing generation of two separate standard curves and comparison of the results. This may potentially allow a better accuracy of detection, because two independent variables are used, instead of just one (intensity). This may even eliminate the need to run ELISA samples in duplicates. The observed effect is very interesting both by itself, and from the

diagnostics point of view, and requires additional research. The possible rationale for this effect will be proposed below.

4.11. Inverse "blue" spectral shift versus the PSA dependence - discussion

According to Figures 4.12A and 4.13A, decreased AG concentration causes an enhancement of the spectral shift up to maximum value of 35 nm at the lowest AG concentration of 0.001ng/ml. We will briefly discuss a mechanism which may contribute to this unusual spectroscopic effect. It is known that one AG molecule can attach several (usually up to three) AB molecules [151], and the blue shift magnitude may depend on the amount of AB*QD complexes, attached to one AG as well as on the special configuration of ELISA sandwiches. However, a preferable model to account for observed experimental results can be qualitatively described as following.

As was shown in [119-123], the blue shift is enhanced after a drop of conjugate is dried on a solid surface, and its magnitude is determined by elastic stress caused by the tensile forces at the sample-substrate interface. In the current project, the ELISA samples were also dried on the solid substrate (the bottom of the well), therefore it is conceivable that in this case the blue shift is caused by a similar elastic stress mechanism. The average blue shift magnitude of the AB-AG-AB*QD sandwich is larger than that of isolated AB*QD conjugate, which may be explained by the increased size/weight of the complex. This is in a good agreement with the previously published data on increased blue shift with increasing of the AB molecular weight [120]. This model is partially supported by the blue shift dynamics with the drying time of the sample (Figures 4.12A and 4.13A – compare the initial shift and the one after 5 days of storage).

Because the magnitude of the mechanical forces are maximized near the interface of the dried sample and the substrate, and it is gradually decreased in the perpendicular direction, it is obvious that the blue shift will depend particularly on orientation of the QD*Ab complex with respect to the interface. We suggest that at high Ag concentration the distance between the neighboring QD*Ab complexes, attached to the bottom of the well is decreased and complexes are oriented as illustrated in (Figure 4.14A). For such complexes the blue shift caused by interface stress is relatively small. If the Ag concentration is extremely low, then some QD*Ab pairs are reoriented in a manner that the QD is located near the interface and experience maximum elastic stress (Figure 4.14B). Therefore, with decreasing Ag concentration a fraction of complexes oriented along the interface will be high which leads to increasing blue spectral shift. In this case, the blue shift is maximized consistent with the experiment.

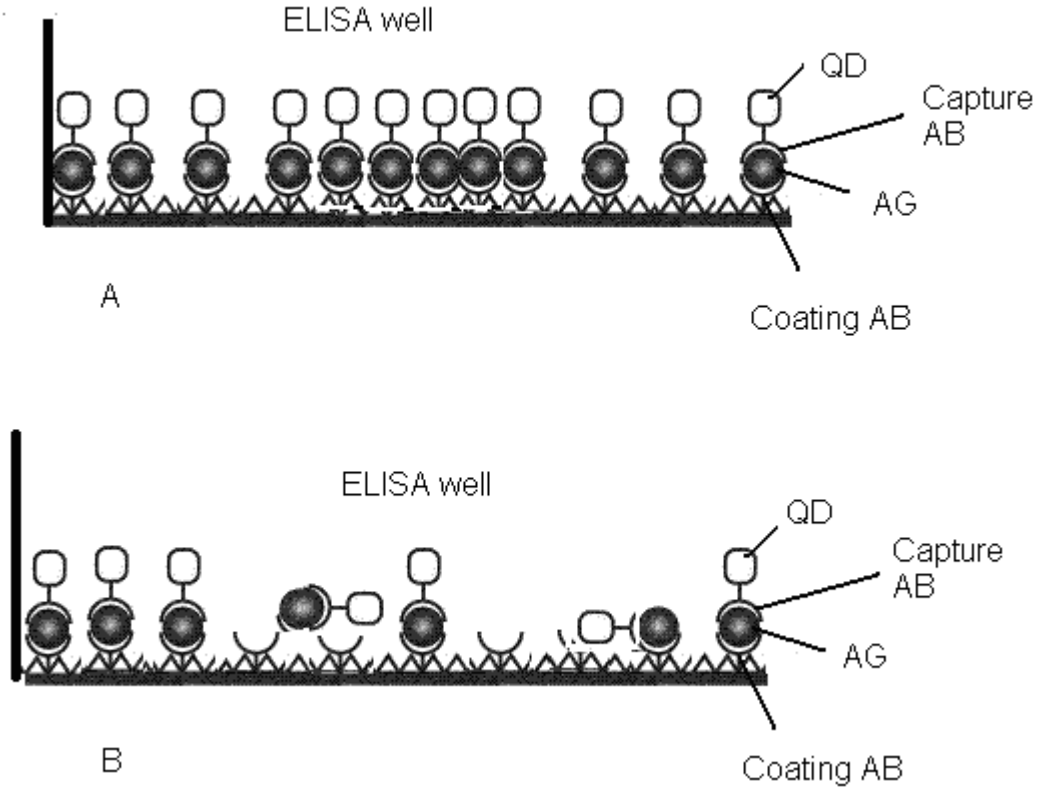

Figure 4.14. Possible orientation of the AG molecules, capturing AB and QDs in ELISA wells with different AG concentration: A - higher AG concentrations, most of the capturing ABs are occupied, the complexes are parallel to the bottom of the well and more or less uniformly distributed across the bottom area; B – lower AG concentrations, some of the capturing ABs are empty, one AG molecule may be attached by two capturing ABs. The "sandwiches" may be more concentrated near the interface with the well bottom.

4.12. QD ELISA vs regular ELISA, benefits

As was explained before, QD ELISA has several important benefits over the standard commercially available ELISA.

It allows to lower the PSA AG limit of detection up to 100 times, in comparison to standard techniques, based on the PL intensity measurements alone. This feature may be used for early detection of some female cancers, as well as in the forensic science.

The tracking of bioconjugated QDs spectral shift may provide additional evidence of the sandwich formation and add another variable to the detection parameters. Because of the negative "blue" shift magnitude vs PSA antigen concentration dependence, it may be possible to track the biomolecule's concentration, based on the spectral shift alone, or on the intensity combined with the spectral shift measurements separately. This may eliminate the need in the duplicates as well as improve the overall reliability and sensitivity of the method.

The samples of the QD ELISA retain their PL for days (at least for 5 days in the PSA experiment) in comparison to standard ELISAs which must be measured within minutes after the experiment ends. This feature is very convenient, because it's not always possible to perform the measurement immediately after the experiment ends. It also allows repeatedeasurement of the samples, if the results of the first one may cannot be used.

4.13. Possible limitations of QD ELISA

Although QD ELISA may look very promising from the research point of view, several limitations/disadvantages are currently needed to be overcame in order to implement it in clinics.

As for now, the reliable estimation of the number of biomolecules, attached to one QD, is not possible. For instance, the 705nm Invitrogen QDs may possible attach 1-3 biomolecules, however, the exact estimation of how much was attached is not available at the time. This is a serious limitation, which may lead to the wrong PL intensity and/or spectral shift assessment. For instance, if the majority of bioconjugated QDs in the

conjugate attached 1 biomolecule, the final intensity of the sample will be higher, than if the conjugate, containing mostly 1 QD+3 biomolecules, is used. This may lead to failure to discriminate between the samples with similar, but different, concentrations (especially when the low concentrations are used). This may also have an effect on the spectral shift magnitude. In future, if the reliable method of estimation the number of biomolecules, attached to one QD, is developed, this limitation may be successfully overcomed.

Possible toxicity of QDs. Although properly capped/shelled QDs are considered safe for living organisms, the growing body of publications are available on the possible QD toxicity to living organisms. It was published, that different types of QDs may cause the following effects in living objects: vascular thrombosis in the pulmonary circulation [87], could induce apoptosis and cell death [88], and may accumulate in the lungs, spleen, liver and kidneys [89]. It may happen, therefore, that it is not safe to work with QDs without the proper protection. Although this factor by itself is not the major obstacle in using QDs for in vitro studies, possible negative consequences for the lab personnel may be considered before starting the work with QDs. This may impose additional charges and/or other limitations of the QD ELISA in comparison to standard ELISAs, making it not as favorable as it may have been otherwise.

The time and labor efforts may also be a limiting factor in implementing QD ELISA. Although it is possible to order the bioconjugated QDs directly from the company, it is very expensive and may require additional excessive waiting times, and it is not very common. Performing the bioconjugation procedure in the lab requires additional time (about 5 hours) and the trained personnel, which clearly adds a new big, rather tedious step to the QD ELISA. Spectroscopic analysis of the samples is also time

consuming, and may take several days for the spectral shift to develop. The mapping itself also requires time, and depending on the step size (precision), may take as long as 8 hours per well (usually, at least 3 hours). Optimization of the QD ELISA procedure and implementation of the new equipment (i.e. PL system, capable of mapping several wells at the same time) may improve the timing, but as for now it was not done.

QD ELISA is more expensive than any of the current commercial ELISAs. The major limiting factor which makes QD ELISA not cost-effective, is the conjugate quantity. For the Invitrogen conjugation kit, which allows 2 conjugations, each conjugation produces approx 200µl of conjugate, which was determined, can be diluted twice (table 4.1). So, one conjugation kit produces up to 800µl of conjugate, accepting one sample needs at least 40µl of it, one kit is enough to analyze at most 20 samples.

Table 4.4 describes the average cost of one sample analysis for this work (the table excludes expenses associated with the microplate readers, as it is common for both ELISAs, and the laser/equipment charges, associated with the spectroscopic mapping, as it is hard to accurately estimate). It is obvious, that the cost of $52 per sample, compared to $7.80 per sample in a standard ELISA, is more than excessive. In future, however, if/when QDs become cheaper and more readily available, this technique may become very popular.

Table 4.4 Summary of the costs associated with the regular and QD PSA ELISAs.

Charge	QD PSA ELISA	Average regular PSA ELISA
Average ELISA kit cost	N/A	$350-400 (1 kit, 96 wells, 48 samples)
QD 705nm conjugation kit	$600	N/A
Coating and detection antibodies	$400	Included in the kit
Misc. ELISA supplies (buffers, plates etc)	$50	Included in the kit
Average sample amount	20	48
Average cost per sample, $	52	7.30-8.30 7.80 average

Table 4.5 summarizes the benefits and limitations of the QD ELISA in comparison to regular ELISA.

Table 4.5 The benefits and limitations of the QD ELISA in comparison to regular ELISA.

Feature	QD PSA ELISA	Commercial PSA ELISA
Sensitivity by intensity	+	-
Sensitivity by spectral shift	+	-
Samples PL shelf-life	+	-
Time, cost and overall effort to perform the experiment	-	+
Imperfections of the bioconjugation procedure	-	N/A
Possible QD toxicity	-	+

The author of this work believes, that if the increased sensitivity of ELISA is needed, QD ELISA will be used even regardless of the increased cost. However, if in future the cost and overall tediousness of the procedure is reduced, QD ELISA has all chances to successfully compete with the regular, commercially available ELISAs.

4.14. Conclusions

Several important conclusions may be drawn from this PhD dissertation.

Agarose gel electrophoresis technique, optimized with organic dye fluorescamine, could successfully be used to verify bioconjugation. The optimal parameters for 705nm PEGylated QDs, conjugated to different antibodies, were found. They are: 2% agarose gel, 1.5V working voltage, 0.5X TBE as a running buffer, and about 120 mins running time. We have achieved an obvious retardation in movement of bioconjugated QDs, in comparison to pure QDs, because of their increased weight and size. Pure antibodies, labeled with fluorescamine, have the fastest speed due to their small size and run out of the gel in approx. 30-40mins. The optimal parameters for different QDs may vary, and could be experimentally optimized further if necessary.

The shape and size of pure 705nm QDs was verified with the TEM technique. QDs were found to be oval shaped, approximately 11x6nm. Bioconjugated QDs were not found to have substantially changed shape and/or size, however, the TEM analysis should be performed on substrates, not covered with amorphous carbon film, to finalize this conclusion.

The “blue” spectral shift of bioconjugated QDs was described, conditions which may influence it were listed, and the possible mechanism of its appearance was proposed. It was found that the short-wavelength spectral shift of bioconjugated QDs is observed for all samples dried on the silicon substrates, in comparison to pure QDs of the same size/color, dried at the same conditions. The shift was increased with the time of storage at the room ambience for all samples, reaching 27-40nm in approx 14 days. Further storage caused a very slow increase and was considered not effective.

Larger size QDs generate spectral shifts of larger magnitudes, presumably because they have more sites for biomolecule attachment and can therefore attach more biomolecules. Six biomolecules, currently being considered cancer biomarkers (IL-6, IL-10, CAV1, OPG, p53, and PSA), were used for bioconjugation, and all of them performed a repeatable "blue" spectral shift, when dried on the silicon surface. The shift positively correlated with the biomolecule's size/weight. This effect can be explained by greater tensile forces which are generated at the bioconjugate-substrate interface in the process of drying for biomolecules with bigger molecular weights.

The shift was substantially accelerated at elevated temperatures of sample drying (50-250C) and slowed down at lower temperatures (2-4C). This effect was attributed to the slower drying of attached biomolecules at lower temperatures. Argon, nitrogen, oxygen, moisture and vacuum were not found to influence the rate of the spectral shift development, suggesting that it is caused mostly by physical (stress), rather than chemical (chemical reactions between the QD/biomolecule) factors.

Samples dried on porous and elastic substrates (CMP pad, rubber, grid) did not exhibited PL spectral shift, or the shift was mush smaller in comparison to crystalline silicon substrates. The PL shift was attributed to the elastic and compression stress due to nonhomogenious drying of the QD droplet and the reaction with the solid surface.

Dried bioconjugated QD drops were found to have an nonhomogenious profile across the spot (lower in the periphery and higher in the center). This effect was named a "plate-shape effect" and was observed for all conjugated samples. It is important, because gives a chance to concentrate the maximal spectral shift in the smaller area.

The final part of this study implements the spectral shift for improving the sensitivity of PSA ELISA. It was found that QD ELISA could be as much, as 100 times more sensitive than the regular commercial ELISA, based on the enzymatic detection. The cut off for commercial ELISA was about 0.1ng/ml, while QD ELISA was able to detect as low, as 0.001 ng/ml of the PSA Antigen when the spectroscopic mapping technique was used, or as low as 0.005 ng/ml when the standard microplate reader was used for the PL detection.

The magnitude of the spectral shift was found to be in a negative correlation with the PSA antigen concentration, suggesting a new variable, besides PL intensity, in the biomolecules detection process. As of now, QD PSA ELISA was found to be labor and cost expensive in comparison to a regular PSA ELISA, but if the cost of QDs drop in future, or if the urgent need for increased sensitivity arises, it may become a valuable alternative.

The further experiments following this work are described and proposed in the next chapter.

5. Recommendation for further research

Further experiments related to the revealing the mechanisms of the "blue" spectral shift appearance are recommended. More biomarkers should be involved into the study, as well as other QDs, possibly of a bigger size (deep red to near infrared emission). It may be useful to try the near infrared QDs, as they may generate the largest spectral shift. This may lead to the database of the spectral shift magnitudes for different QD-AB combinations, under certain environmental conditions/storage times. The combinations of environmental factors (for instance, increased temperature, higher moisture and oxygen environment) may be tested in order to reveal the conditions under which the spectral shift is maximal.

TEM analysis of bioconjugated QDs shall be conducted on the grits, which are not covered with the amorphous carbon grit, because the grit may diminish the tension forces and reduce the deformation of QDs, which appear on solid crystal substrates and is responsible for the spectral shift.

Further QD ELISA experiments shall be conducted with different antibodies, in order to establish the sensitivity of this method for other biomarkers. Substantial amount of samples must be generated in order to create a reliable database of both the sensitivity cutoff and the negative spectral shift dependence on the biomolecule's concentration. If confirmed for all or at least several biomolecules, this effect may be implemented as a detection parameter, along with the PL intensity, to increase the detection accuracy.

Spectral shifts of ELISA sandwiches for different antibodies may be compared under certain conditions, and the database of them created. This may serve as a future base for a simultaneous detection of several biomolecules in one probe, based on the detected wavelength and spectral shifts. As the overall goal, proposed research may lead to a substantial increase in the ELISA sensitivity and serve as a better tool for earlier cancer detection.

The results of this work were published in the following journals:

1. Chornokur G., Ostapenko S., Korsunska N., Oleynik E., Tanner R., Sellers T., Bhansali S. and Phelan C. Bioconjugated Quantum Dots as fluorescent biomarkers allow detecting lower concentrations of PSA by sandwich-ELISA. Submitted to the Journal of Biomedical Nanotechnology.

2. G. Chornokur, S. Ostapenko, E. Oleynik, C. Phelan, N. Korsunska, T. Kryshtab, J. Zhang, A. Wolcott and T. Sellers. Scanning Photoluminescent Spectroscopy of Bioconjugated Quantum Dots // Superlattices and Microstructures (in press) 2009

3. G Chornokur**,** S Ostapenko, Yu Emirov, N E Korsunska, T Sellers and C Phelan. Spectroscopic behavior of bioconjugated quantum dots// Semicond. Sci. Technol. 23 (2008)

4. Ganna Chornokur, Sergei Ostapenko, Yusuf Emirov, Nadezhda Korsunska, Abraham Wolcott, Jin Zhang, Catherine Phelan, Abhilasha Nagaram, Thomas Sellers. Biologically Engineered Quantum Dots for Biomedical Applications// MRS Proceedings Volume 1095E**,** 1095-EE08-05, 2008

5. Borkovska L, Korsunska N, Krystab T, Pecherska E, Germash L, Ostapenko Chornokur G The influence of bioconjugation on photoluminescence and structural characteristics of quantum dots CdSe/ZnS *Semiconductors* (in press) 2009

6. Dybiec M, Chornokur G, Ostapenko S, Wolcott A, Zhang JZ, Zajac A, Phelan and Sellers T 2007 Photoluminescence spectroscopy of bioconjugated CdSe/ZnS quantum Dots *Appl. Phys Lett* 90 263112

References

1. National Vital Statistics Report 2007 55 (19)

2. Colditz GA, Sellers TA and Trapido E 2006 Epidemiology – identifying the causes and preventability of Cancer *Nat Rev Cancer*, 6: p. 75

3. Smith S, Dave S, Nie L T and Gao X 2006 Multicolor quantum dots for molecular diagnostics of cancer *Expert Rev M. Diag,* 6(2): p. 231-44

4. So M-K, Hu C, Loening AM, Gambhir SS and Rao J 2006 Self illuminating quantum dot conjugates for in vivo imaging *Nat Biotechnol* 24(3): p. 339

5. Rhyner MN, Smith AM, Gao X. Mao H, Yang L and Nie S 2006 Quantum dots and multifunctional nanoparticles: new contrast agents for tumor imaging *Nanomedicine* 1(2): p. 1-9

6. Xing Y, Shaudry Q and Shen S 2007 Bioconjugated quantum dots for multiplexed and quantitative immunochemistry *Nature Protocols* 2(5): p.1152

7. Goldman ER, Medintz IL and Mattoussi H *2006* Luminescent quantum dots in immunoassays *Anal Bioanal Chem* 384(3): p. 560

8. Pathak S, Choi SK, Arnheim N and Thompson ME 2001 *J. Am. Chem. Soc.* 123: p. 4103.

9. Xiao Y and Barker PE 2004 *Nucleic Acids Res* 32**:** p. 28.

10. Crut A, Geron-Landre B, Bonnet I, Bonneau S, Desbiolles P and Escude C 2005 *Nucleic Acids Res* 33**:** p. 98.

11. Chan WCW and Nie S 1998 *Science* 281**:** p. 2016.

12. Bruchez Jr, Moronne M, Gin P, Weiss S and Alivisatos AP 1998 *Science* 281**:** p. 2013.

13. Lidke DS, Nagy P, Heintzmann R, Arndt-Jovin D-J, Post NJ, Grecco HE, Jares-Erijman EA and Jovin TM 2004 *Nat. Biotechnol*. 22**:** p. 198.

14. Dubertret B, Skourides P, Norris DJ, Noireaux V, Brivanlou AH and Libchaber A 2002 *Science* 298**:** p. 1759.

15. Han M, Gao X, Su JZ and Nie S 2001 *Nat. Biotechnol*. 19**:** p. 631.

16. Jaiswal JK, Mattoussi H, Mauro JM and Simon SM 2003 *Nat. Biotechnol*. 21 47.

17. Wu X, Liu H, Liu J, Haley KN, Treadway JA, Larson JP, Ge N, Peale F and Bruchez MP 2003 *Nat. Biotechnol*. 21 41.

18. Goodsell DS 2004 Bionanotechnology: lessons from nature New Jersey: Wiley-Liss, Inc.

19. 20. SYPRO® Orange Protein Gel Stain Instruction Manual: http://www.bio.indiana.edu/~ybelab/procedures/SyproOrange.pdf

20. Skelley AM and Mathies RA 2003 Chiral separation of fluorescamine-labeled amino acids using microfabricated capillary electrophoresis devices for extraterrestrial exploration *J Chromatography A* 1021 191–99

21. Udenfriend S, Stein S, Böhlen P, DairmanW, Leimgruber W and Weigele M 1972 Fluorescamine: a reagent for assay of amino acids, peptides, proteins, and primary amines in the picomole range *Science, New Series* 178(4063) 871-72.

22. Gerion D, Pinaud F, Williams SC, Parak WJ, Zanchet D, Weiss S and Alivisatos AP 2001 Synthesis and properties of biocompatible water-soluble silica-coated CdSe/ZnS semiconductor quantum dots *J Phys Chem B* 105 8861-71.

23. Warren C, Chan W and Nie S 1998 Quantum dot bioconjugates for ultrasensitive nonisotopic detection *Science* 281 2016-18.

24. Bruchez M., M. Moronne P. Gin S. Weiss, and Alivisatos A.P. 1998 Semiconductor Nanocrystals as Fluorescent Biological Labels *Science* 281: p. 2013-2016.

25. Leatherdale, C.A., Woo W.K., Mikulec F.V., and Bawendi M.G. 2002 On the Absorption Cross Section of CdSe Nanocrystal Quantum Dots *J. Phys. Chem. B*, 106: p. 7619-7622.

26. www.invitrogen.com

27. Michalet X., Pinaud F.F., Bentolila L.A., Tsay J.M., Doose S, Li J.J., Sundaresan G, Wu A.M., Gambhir S.S., Weiss S. 2005 Quantum dots for live cells, in vivo imaging, and diagnostics *Science*,307(5709): p. 538-544.

28. Dabbousi, B.O., Rodriquez-Viejo J., Mikulec F.V., Heine J.R., Mattoussi H., Ober R., Jensen K.F., and Bawendi M.G. 1997 (CdSe)ZnS Core-Shell Quantum Dots: Synthesis and Characterization of a Size Series of Higly Luminescent Nanocrystallites *Journal of Physical Chemistry B* (101): p. 9463-9475.

29. Kaul, Z., Yaguchi T., Kaul S.C., Hirano T., Wadhwa R., and Taira K. 2003 Mortalin imaging in normal and cancer cells with quantum dot immunoconjugates *Cell research* 13(6): p. 503-507.

30. Human PSA ELISA Kit from Abazyme: http://www.biocompare.com/itemdetails.asp?itemid=434262

31. Sato I., Sagi M., Ishiwari A., Nishijima H., Ito E., and Mukai T. 2002 Use of the ‘‘SMITEST’’ PSA card to identify the presence of prostate-specific antigen in semen and male urine *Forensic Science International* 127: 71–74

32. Levine B.,Titus J., Moore K., and Fowler D. 2004 Use of Prostate Specific Antigen in the Identification of Semen in Postmortem Cases The American *Journal of Forensic Medicine and Pathology* 25(4): 288-290

33. Sauter E.R., Babb J., Daly M., Engstrom P.F., Ehya H., Malick J., and Diamandis E. 1998 Prostate-specific Antigen Production in the Female Breast: Association with Progesterone *Cancer Epidemiology, Biomarkers & Prevention 7*(3/5): 315

34. Ulutin H.C. and Pak Y. 2000 Prostate Specific Antigen in the Female Body: Its Role in Breast Cancer Prognosis *Radiation Medicine*18(5): 273–276

35. Schmidt S., Franke M., Lehmann J., Loch T., Stockle M., and Weichert-Jacobsen K. 2001 Prostate-specific antigen in female urine: a prospective study involving 217 women *Urology* 57 (4)

36. Fieler E.L., Coleman D.E., and Baselt R.C. 1998 Is Prostate-Specific Antigen Present in Female Serum? *Clinical Chemistry* 44(3)

37. Negri C., Tosi F., Dorizzi R., Fortunato A., Spiazzi G.G., Muggeo M., Castello R., and Moghetti P. 2000 Antiandrogen Drugs Lower Serum Prostate-Specific Antigen (PSA) Levels in Hirsute Subjects: Evidence That Serum PSA Is a Marker of Androgen Action in Women *The Journal of Clinical Endocrinology & Metabolism* 85(1)

38. Diamandis EP, and Yu H. 1997 Nonprostatic sources of prostate-specific antigen. *Urol Clin North Am*. 24:275–282.

39. Melegos DN, Yu H, Ashok M, Wang C, Stanczyk F, and Diamandis EP. 1997 Prostate-specific antigen in female serum, a potential new marker of androgen excess. *J Clin Endocrinol Metab*. 82:777–780.

40. www.apha.org

41. Sutherland A.J. 2002 Quantum dots as luminescent probes in biological systems *Current Opinion in Solid State and Materials Science* 6:365–370

42. Peng X.J., 2003 *Adv. Mater*. 15: 459.

43. Roederer M. *et al*. 1997 *Cytometry* 29, 328

44. Schrock E. *et al*. 1996 *Science* 273, 494

45. Graybeal, J.D., *Molecular spectroscopy*. 1993: Mcgraw-Hill College.

46. Borovitskaya E., and Shur M. *Quantum Dots (Selected Topics in Electronics and Systems, Vol. 25)*. 2002: World Scientific Publishing Company; 1st edition, ISBN: 9810249187.

47. Hines, M.A., and Guyot-Sionnest P. 1998 Bright UV-Blue Luminescent Colloidal ZnSe Nanocrystals *Physical Chemistry B*102(19): p. 3655.

48. Chen, F.Q., Gerion, D. 2004 Fluorescent CdSe/ZnS nanocrystal-peptide conjugates for long-term, nontoxic imaging and nuclear targeting in living cells. *Nano Lett.* 4:1827–1832.

49. Colvin V.L. 2003 The potential environmental impact of engineered nanomaterials. *Nat Biotechnol*.21:1166–1170.

50. Springer Zh. *Progress in Transmission Electron Microscopy: Concepts and Techniques*. 2001, ISBN 3540676805

51. www.nobelprize.org

52. Williams D.B., and Carter C.B. *Transmission Electron Microscopy: A Textbook for Materials Science*.1996: Pienum Press

53. Galian R.E., Guardia M. 2008 The use of quantum dots in organic chemistry *Trends in Analytical Chemistry* (in press)

54. Hezinger A.F.E., Teßmar J., and Gopferich A. 2008 Polymer coating of quantum dots – A powerful tool toward diagnostics and sensorics *European Journal of Pharmaceutics and Biopharmaceutics* 68:138–152

55. Jaiswal J.K. and Simon S.M. 2004 Potentials and pitfalls of fluorescent quantum dots for biological imaging *Trends in Cell Biology*14(9): p. 497-504.

56. Didenko V.V., Ngo H., and Baskin D.S. 2005 Polyethyleneimine as a transmembrane carrier of fluorescently labeled proteins and antibodies *Anal Biochem*. 344(2): 168–173.

57. Mason J.N., Farmer H., Tomlinson I.D., Schwartz J.W., Savchenko V., DeFelice L.J., Rosenthal S.J., Blakely R.D. 2005 Novel fluorescence-based approaches for the study of biogenic amine transporter localization, activity, and regulation *Journal of Neuroscience Methods* 143: 3–25

58. Parak W.J., Gerion D., Zanchet D.,Woerz A.S., Pellegrino T., Micheel, Williams S.C.,Seitz M., Bruehl R.E., Bryant Z., Bustamante C., Bertozzi C.R., and Alivisatos A.P. 2002 Conjugation of DNA to Silanized Colloidal Semiconductor Nanocrystalline Quantum Dots *Chem. Mater*. 14: 2113-2119

59. Shingyoji M., Gerion D., Pinkel D., Gray J.W., and Chen F. 2005 Quantum dots-based reverse phase protein microarray *Talanta* 67: 472–478

60. Nehilla B.J., Vu T.Q., andDesai T.A. 2005 Stoichiometry-Dependent Formation of Quantum Dot-Antibody Bioconjugates: A Complementary Atomic Force Microscopy and Agarose Gel Electrophoresis Study *J. Phys. Chem.* 109: 20724-20730

61. Huang X., Weng J., Sang F., Song X., Cao C., and Ren J. 2006 Characterization of quantum dot bioconjugates by capillary electrophoresis with laser-induced fluorescent detection *Journal of Chromatography A* 1113: 251–254

62. Schena M. *Protein Microarrays*. 2005, Sudbury: Jones and Bartlett Publisers

63. Geho D., Lahar N., Gurnani P., Huebschman M., Herrmann P., Espina V., Shi A., Wulfkuhle J., Garner H., Petricoin E., Liotta L.A., and Rosenblatt K.P. 2005 Pegylated, Steptavidin-Conjugated Quantum Dots Are Effective Detection Elements for Reverse-Phase Protein Microarrays *Bioconjugate Chem*.16: 559-566

64. Maciej Dybiec Doctoral Dissertation, 2006

65. Udenfriend S., Stein S., Böhlen P., Dairman W., Leimgruber W., and Weigele M. 1972 Fluorescamine: a reagent for assay of amino acids, peptides, proteins, and primary amines in the picomole range *Science, New Series* 178(4063) : 871-72.

66. Skelley A.M., and Mathies R.A. 2003 Chiral separation of fluorescamine-labeled amino acids using microfabricated capillary electrophoresis devices for extraterrestrial exploration *Journal of Chromatography* A1021:191–199

67. CHENG L.K., LEVITT M., and FUNG H-L. 1975 Fluorescence Reactions of Fluorescamine with Levodopa and Its Derivatives: Fluorescence Assay of 3 - Methoxy -4 - hy droxyphenylalanine in Levodopa Dosage Forms *PHARMACEUTICAL ANAL YSIS* 64(5): I839

68. www.sigmaaldrich.com

69. www.biotek.com

70. Vashist S.K., Tewari R., Bajpai R.P., Bharadwaj L.M., and Raiteri R. 2006 Review of Quantum Dot Technologies for Cancer Detection and Treatment *Journal of nanotechnology online* 2: p 1-14

71. Ballou B., Lagerholm B.C., Ernst L.A., Bruchez M.P. and Waggoner A.S. 2004 Noninvasive imaging of quantum dots in mice. *Bioconjug. Chem.* 15: 79–86

72. Kim, S. *et al* .2004 Near-infrared fluorescent type II quantum dots for sentinel lymph node mapping. *Nat. Biotechnol.* 22: 93–95

73. Gao X., Cui Y., Levenson R.M., Chung L.W.K. and Nie S. 2004 *In vivo* cancer targeting and imaging with semiconductor quantum dots *NATURE BIOTECHNOLOGY* 22(8)

74. Smith A.M., Gao X. and Nie S. 2004 Quantum Dot Nanocrystals for In Vivo Molecular and Cellular Imaging *Photochemistry and Photobiology* 80: 377–385

75. Nidaa D.L., Rahmana M.S., Carlsona K.D., Richards-Kortuma R, and Follen M. 2005 Fluorescent nanocrystals for use in early cervical cancer detection Gynecologic *Oncology* 99: S89 – S94

76. Sukhanova A., Devy J., Venteo L., Kaplan H., Artemyev M., Oleinikov V., Klinov D., Pluot M., Cohen J.H.M. and Nabiev I. 2004 Biocompatible fluorescent nanocrystals for immunolabeling of membrane proteins and cells *Analytical Biochemistry* 324:60–67

77. Rahman M., Abd-El-Barr M., Mack V., Tkaczyk T., Sokolov K., Richards-Kortum R., and Descour M. 2005 Optical imaging of cervical pre-cancers with structured illumination: An integrated approach *Gynecologic Oncology* 99: S112 – S115

78. Templin M.F., Stoll D., Schrenk M., Traub P.C., Vohringer C.F., and Joos T.O. 2002 *Trends Biotechnol*. 20:160.

79. Phizicky E., Bastiaens P.I., Zhu H., Snyder M., and Fields S. 2003 *Nature* 422: 208.

80. Bronzino J.D. *Tissue Engineering and Artificial Organs.* 2006 3rd edition, CRC Press, ISBN 0849321239

81. Zhang B., Liang X., Hao L., Cheng J., Gong X., Liu X., Ma G. and Chang J. 2009 Quantum dots/particle-based immunofluorescence assay: Synthesis, characterization and application *Journal of Photochemistry and Photobiology B: Biology* 94(1**):** 45-50

82. Liu T., Liu B., Zhang H. and Wang Y. 2005 The Fluorescence Bioassay Platforms on Quantum Dots Nanoparticles *Journal of Fluorescence* 15(5)

83. McNeil SE. 2005 Nanotechnology for the biologist. *J Leukoc Biol* 78: 585–94.

84. Cordero S.R., Carson P.J., Estabrook R.A., Strouse G.F., and Buratto S.K. 2000 Photo-Activated Luminescence of CdSe Quantum Dot Monolayers *J. Phys. Chem. B* 104: 12137-12142

85. Azzazy H.M.E., and Mansour M.M.H. 2009 In vitro diagnostic prospects of nanoparticles *Clinica Chimica Acta* (in press)

86. Bailey R.E., Smith A.M., Nie S. 2004 Quantum dots in biology and medicine *Physica E* 25:1–12

87. Geys J., Nemmar A., Verbeken E., Smolders E., Ratoi M., Hoylaerts M.F., Nemery B., and Hoet P.H.M. 2008 Acute Toxicity and Prothrombotic Effects of Quantum Dots: Impact of Surface Charge *Environmental Health Perspectives*116(12)

88. Hardman R. 2006 A Toxicologic Review of Quantum Dots: Toxicity Depends on Physicochemical and Environmental Factors *Environmental Health Perspectives*114(2)

89. Yang R.S.H., Chang L.W., Wu J-P.,Tsai M-H.,Wang H-J.,Kuo Y-C., Yeh T-K.,Yang C.S., and Lin P. 2007 Persistent Tissue Kinetics and Redistribution of Nanoparticles, Quantum Dot 705, in Mice: ICP-MS Quantitative Assessment *Environmental Health Perspectives* 115(9)

90. Derfus A.M., Chan W.C.W., and Bhatia S.N. 2004 Probing the Cytotoxicity of Semiconductor Quantum Dots *Nano Letters* 4(1):11-18.

91. Soltesz E.G., Kim S., Laurence R.G., DeGrand A.M., Parungo C.P., Dor D.M., Cohn L.H., Bawendi M.G., Frangioni J.V., and Mihaljevic T 2005 Intraoperative Sentinal Lymph Node Mapping of the Lung Using Near-Infrared Fluorescent Quantum Dots *Ann Thorac Surg* 79(1):269-277.

92. Ballou B., Ernst L.A., Andreko S., Harper T., Fitzpatrick J.A.J., Waggoner A.S., and Bruchez M.P. 2007 Sentinal Lymph Node Imaging Using Quantum Dots in Mouse Tumor Models *Bioconjugate Chem* 18**:**389-396

93. Anuradha K., Ponamgi S.P.D., Lakshmi V. 2002 Evaluation of two commercially available anti human immunodeficiency virus antibody Elisa Kits using clinical samples *Indian Journal of Medical Microbiology* 20(2): 102-104

94. www.pishtazteb.com

95. Van Dyk A. *HIV/AIDS Care and Counseling* 4th edition, Pearson Education, 497p.

96. KUUN E., BRASHAW M., HEYNS A. and DU P. 1997 Sensitivity and specificity of standard and rapid HIV-antibody tests evaluated by seroconversion and non-seroconversion low-titre panels *Vox sanguinis* 72(1): 11-15

97. Crowther J.R. Elisa: *Theory and Practice, Vol. 42* 1995 Springer-Verlag, ISBN-13: 9780896032798, 223p.

98. Kemeny D.M. *A Practical Guide to Elisa:* Pergamon press, New York 1991

99. Walker J.M., and Rapley R. *Molecular Biomethods Handbook* : Humana Press, 2nd edition, 2008, ISBN 1603273743, 1124p.

100. www.blueleaf.ca

101. www.abcam.com

102. Noedl H., Yingyuen K., Laoboonchai A., Fukuda M., Sirichaisinthop J., and Miller R.S. 2006 Sensitivity and specificity of antigen detection ELISA for malaria diagnosis *Am. J. Trop. Med. Hyg*. 75(6):1205-1208

103. Jones J.B., Somodi G.C. and Scott J.W. 1997 Increased ELISA sensitivity using a modified extraction buffer for detection of *Xanthomonas campestris* pv. *vesicatoria* in leaf tissue *Journal of Applied Microbiology* 83: 397–401

104. www.interferonsource.com

105. Belanger A.,Van Halbeek H., Graves H.C.B., Grandbios K., Stamey T.A., Huang L., Poppe I., and Labrie F. 1995 Molecular mass and carbohydrate structure of prostate specific antigen : studies for establishment of an international PSA standard *The Prostate* 27(4):187-197

106. Hilz H., Noldus J., Hammerer P., Buck F., Lück M., and Huland H. 1999 Molecular Heterogeneity of Free PSA in Sera of Patients with Benign and Malignant Prostate Tumors *Prostate Cancer* 36(4)

107. www.cancer.org

108. Laux, M.S., and Custis S.E. Forensic Detection of Semen III. Detection of PSA Using Membrane Based Tests: Sensitivity Issues with Regards to the Presence of PSA in Other Body Fluids**.** Midwestern Association of Forensic Scientists. http://mafs.net/pdf/forensicdetectionsemen3.pdf**.** Retrieved on 2008-05-11.

109. Mannello F., and Gazzanelli G. 2001 Prostate-specific antigen (PSA/hK3): a further player in the field of breast cancer diagnostics? *Breast Cancer Res* 3:238-243

110. Foekens J.A., Diamandis E.P., Yu H., Look M.P., Meijer-van Gelder M.E., van Putten W.L., and Klijn J.G. 1999 Expression of prostate-specific antigen (PSA) correlates with poor response to tamoxifen therapy in recurrent breast cancer. *Br J Cancer. 79*(5-6):888-94

111. Bangma C. 2006 PSA level changes over time in men with an initial PSA level of 4 ng/ml *Nature Clinical Practice Urology* 3:520-521

112. WATCH T. 2006 *Stratifying risk in prostate and cervical cancer* Nature Reviews Cancer *6: 902*

113. Clery J.M. 2001 Stability of prostate specific antigen (PSA), and subsequent Y-STR typing, of Lucilia (Phaenicia) sericata (Meigen) (Diptera: Calliphoridae) maggots reared from a simulated postmortem sexual assault. *Forensic Sci Int.* 120(1-2): 72-6

114. Medintz I.L., Uyeda H.T., Goldman E.R., and Mattoussi H. 2005 Quantum dot bioconjugates for imaging, labelling and sensing Nature Materials *4: 435 - 446*

115. Xu G., Yong K-T., Roy I., Mahajan S.D., Ding H., Schwartz S.A. and Prasad P.N. 2008 Bioconjugated Quantum Rods as Targeted Probes for Efficient Transmigration Across an in Vitro Blood−Brain Barrier *Bioconjugate Chem.*19(6):1179–1185

116. Pereira M. and Lai E.P.C. 2008 Capillary electrophoresis for the characterization of quantum dots after non-selective or selective bioconjugation with antibodies for immunoassay *Journal of Nanobiotechnology* 6**:**10

117. Pattani V.P., Li C., Desai T.A. and Vu T.Q. 2008 Microcontact printing of quantum dot bioconjugate arrays for localized capture and detection of biomolecules Biomedical Microdevices *10(3)*

118. Smith A.M., Duan H., Mohs A.M. and Nie S. 2008 Bioconjugated quantum dots for in vivo molecular and cellular imaging *Advanced Drug Delivery Reviews* 60(11**)**: 1226-1240

119. Chornokur G., Ostapenko S., Oleynik E., Phelan C., Korsunska N., Kryshtab T., Zhang J., Wolcott A. and Sellers T. 2009 Scanning Photoluminescent Spectroscopy of Bioconjugated Quantum Dots *Superlattices and Microstructures* (in press)

120. Chornokur G., Ostapenko S., Emirov Yu., Korsunska N.E., Sellers T and Phelan C. 2008 Spectroscopic behavior of bioconjugated quantum dots *Semicond. Sci. Technol.* 23

121. Chornokur G., Ostapenko S., Emirov Yu., Korsunska N., Wolcott A., Zhang J., Phelan C., Nagaram A., and Sellers T. 2008 Biologically Engineered Quantum Dots for Biomedical Applications *MRS Proceedings*1095E**,** 1095-EE08-05

122. Borkovska L., Korsunska N., Krystab T., Pecherska E., Germash L., Ostapenko S. and Chornokur G. 2009 The influence of bioconjugation on photoluminescence and structural characteristics of quantum dots CdSe/ZnS *Semiconductors* (in press)

123. Dybiec M., Chornokur G., Ostapenko S., Wolcott A., Zhang JZ., Zajac A., Phelan C. and Sellers T. 2007 Photoluminescence spectroscopy of bioconjugated CdSe/ZnS quantum Dots *Appl. Phys Lett* 90: 263112

124. Dybiec M., Ostapenko S., Torchynska T.V. and Velasquez Losada E. 2004 Scanning photoluminescence spectroscopy in InAs/InGaAs quantum-dot s tructures *Applied Physics Letters* 84(25): 5165-5167.

125. Dybiec M**.**, Ostapenko S., Torchynska T.V., Velasquez Lozada E., Eliseev P.G., Stintz A., and Malloy K.J. 2005 *Photoluminescence mapping on InAs/InGaAs quantum dot structures* Physica Status Solidi 2(8): 2951-2954.

126. http://www.tedpella.com/grids_html/grids.htm

127. Xie H-Y., Liang J-G., Zhang Z-L., Liu Y., He Z-K., and Pang P-W. 2004 Luminescent CdSe-ZnS quantum dots as selective Cu2+ probe *Spectrochimica Acta Part A* 60:2527–2530

128. Chen Y. and Rosenzweig Z. 2002 Luminescent CdS Quantum Dots as Selective Ion Probes *Anal. Chem.*74:5132-5138

129. http://www.aacr.org/

130. Gotlieb W.H., Abrams J.S., and Watson J.M. 1992 Presence of Interleukin-10 (IL-10) in the ascites of patients with ovarian and other intra-abdominal cancers. *Cytokine* 4: 385-390.

131. Fortis C., Foppoli M., and Gianotti L. 1996 Increased Interleukin-10 serum levels in patients with solid tumors. *Cancer Lett* 104: 1-5

132. Klein B., Lu Z.Y., and Gu Z.J. 1999 Interleukin-10 and Gp130 cytokines in human multiple myeloma. *Leuk Lymphoma* 34: 63-70

133. Holen I., and Shipman C.M. 2006 Role of osteoprotegerin (OPG) in cancer. *Clin Sci (Lond)*.110(3):279-91

134. Alberts D.A., and Srivastava S. *Cancer Biomarkers*: IOS Press, 2004

135. Fritzsche F., Gansukh T., and Borgono C.A. 2006 Expression of human Kallikrein 14 (KLKI4) in breast cancer is associated with higher tumour grades and positive nodal status *British journal of cancer* 94(4):540-547

136. Haeusler J., Hoegel J., Bachmann N., Herkommer K., Paiss T., Vogel W., and Maier C. 2005 Association of a CAV-1 haplotype to familial aggressive prostate cancer *Prostate* 65(2):171-7.

137. Coleman W.B., and Tsongalis G.J. *Molecular Diagnostics: For the Clinical Laboratorian* :Humana Press, 2nd edition, 2005, ISBN 1588293564

138. Sarvestani E.K., Khezri A., Vessal M. and Ghaderi A. 1999 A Simplified and Reproducible Two-Step Method for the Purification of Prostate-Specific Antigen *Iran. Biomed. J.* 3 87-91

139. www.labcorp.com

140. www.genwaybio.com

141. Dolk E., van Vliet C., Perez J.M., Vriend G., Darbon H., Ferrat G., Cambillau C., Frenken L.G., and Verrips T. 2005 Induced refolding of a temperature denatured llama heavy-chain antibody fragment by its antigen. *Proteins* 59(3):555-64

142. Scopes R.K. *Protein purification : priciples and practice*: Springer-Verlag, 3rd edition, ISBN 0387940723

143. Shahzad K., Olego D.J. and Van de Walle C.J.1988 Optical characterization and band offsets in ZnSe-ZnSxSe1-x strained-layer superlattices *Phys.Rev.B* 38: 1417

144. Empedocles S.A. and Bawendi M.G. 1997 *Science* 278: 2114 – 39

145. Empedocles S.A., Neuhauser R., Shimizu K. and Bawendi M.J. 1999 *Adv.Mater*. 11: 1243

146. Oda M., Tsukamoto J., Hasegawa A., Iwami N., Nishiura K., Hagiwara I., Ando N., Horiuchi H. and Tani T. 2006 Photoluminescence of CdSe/ZnS/TOPO nanocrystals expanded on silica glass substrates: adsorption and desorption effects of polar molecules on nanocrystal surfaces *J.Lumin*. 570 110-20

147. Suzuki C., Ueda H., Tsumoto K., Mahoney W.C., Kumagai I., and Nagamune T. 1999 Open sandwich ELISA with Vh/Vl -alkaline phosphatase fusion proteins *Journal of Immunological Methods* 224:171–184

148. www.canag.se

149. Steinman R.M. and Cohn Z.A. 1972 The interaction of particulate horseradish peroxidase (HRP)-anti HRP immune complexes with mouse peritoneal macrophages in vitro *J Cell Bio*l 55(3)

150. Cans A-S., Dean S-L., Reyes F.E., and Keating C.D. 2007 Synthesis and characterization of enzyme-Au bioconjugates: HRP and fluorescein-labeled HRP *NanoBioTechnology* 3(1)

151. Giaever I. 1973 The Antibody-Antigen Reaction: A Visual Observation *The Journal of Immunology*110: 1424-1426

About the Author

Ganna Chornokur received her bachelor degree in Biology at the National University of 'Kiev-Mohyla Academy", (NAUKMA) Kiev, Ukraine. Her bachelor diploma work was dedicated to the investigation of the genetics for the hereditary disease of human eye. In September 2003, Ganna joined the Master's program in the Environmental Sciences at NAUKMA, and she successfully defended her thesis "Waste- and Groundwater Treatment from Cu(II) Ions by Means of Ultrafiltration, Enhanced by Chitosan " in June 2005. In January of 2006 she joined the research group of Prof. Sergei Ostapenko at the University of South Florida (USF) to study the photoluminescence properties of bioconjugated quantum dots as a Ph.D. candidate. Starting November 2007, she worked as an Intern at Moffitt Cancer Center at USF, researching the possibility to use quantum dots for cancer detection. Her Ph.D. work was accomplished in February 2009 and in March 2009 Ganna defended her dissertation.